2018-12

WASTE HEAT RECOVERY SYSTEM FOR A GAS TURBINE ENGINE AND CARBON DIOXIDE COMPRESSION SIMULATION

Buck, Coria

Monterey, CA; Naval Postgraduate School

NAVAL POSTGRADUATE SCHOOL

MONTEREY, CALIFORNIA

THESIS

WASTE HEAT RECOVERY SYSTEM FOR A GAS TURBINE ENGINE AND CARBON DIOXIDE COMPRESSION SIMULATION

by

Coria Buck

December 2018

Thesis Advisor: Garth V. Hobson
Co-Advisor: Douglas L. Seivwright

THIS PAGE INTENTIONALLY LEFT BLANK

REPORT DOCUMENTATION PAGE	*Form Approved OMB No. 0704-0188*

1. AGENCY USE ONLY *(Leave blank)*	**2. REPORT DATE** December 2018	**3. REPORT TYPE AND DATES COVERED** Master's thesis

4. TITLE AND SUBTITLE WASTE HEAT RECOVERY SYSTEM FOR A GAS TURBINE ENGINE AND CARBON DIOXIDE COMPRESSION SIMULATION	**5. FUNDING NUMBERS** ONR ESTEP
6. AUTHOR(S) Coria Buck	
7. PERFORMING ORGANIZATION NAME(S) AND ADDRESS(ES) Naval Postgraduate School Monterey, CA 93943-5000	**8. PERFORMING ORGANIZATION REPORT NUMBER**
9. SPONSORING / MONITORING AGENCY NAME(S) AND ADDRESS(ES) N/A	**10. SPONSORING / MONITORING AGENCY REPORT NUMBER**

11. SUPPLEMENTARY NOTES The views expressed in this thesis are those of the author and do not reflect the official policy or position of the Department of Defense or the U.S. Government.

12a. DISTRIBUTION / AVAILABILITY STATEMENT Approved for public release. Distribution is unlimited.	**12b. DISTRIBUTION CODE** A

13. ABSTRACT (maximum 200 words)

The U.S. Department of Defense has implemented an initiative to become more energy efficient across all services. The Naval Postgraduate School supported development toward this goal by studying the possibility of energy generation using waste heat recovery within shipboard engine exhaust. This research included the development of a heat exchanger ultimately to use compressed CO_2 as the working fluid to run a Brayton cycle. In support of this research, this thesis details the baselining and instrumentation of a Rolls Royce M250 helicopter engine in the Marine Propulsion test cell, which was used as the platform for this development. Additionally, a model of the heat exchanger design was fabricated and installed in the engine exhaust.

The effects the installed heat exchanger has on engine performance was measured and analyzed.

This thesis also examined the compressor to be used in the CO_2 loop design. An ANSYS CFD model was developed and tested to create a compressor map of CO_2 performance through a centrifugal compressor. The sheath and casing for the compressor were designed in SolidWorks and fabricated using a 3D printer. This thesis is critical in the continuing development of a shipboard waste heat recovery system.

14. SUBJECT TERMS heat exchanger, CFD, CFX, T-63 installation, helical coil heat exchanger, waste heat recovery, carbon dioxide, gas turbine engine instrumentation, compressor analysis	**15. NUMBER OF PAGES** 127
	16. PRICE CODE

17. SECURITY CLASSIFICATION OF REPORT	**18. SECURITY CLASSIFICATION OF THIS PAGE**	**19. SECURITY CLASSIFICATION OF ABSTRACT**	**20. LIMITATION OF ABSTRACT**
Unclassified	Unclassified	Unclassified	UU

NSN 7540-01-280-5500 Standard Form 298 (Rev. 2-89) Prescribed by ANSI Std. 239-18

THIS PAGE INTENTIONALLY LEFT BLANK

Approved for public release. Distribution is unlimited.

WASTE HEAT RECOVERY SYSTEM FOR A GAS TURBINE ENGINE AND CARBON DIOXIDE COMPRESSION SIMULATION

Coria Buck
Lieutenant, United States Navy
BS, U.S. Naval Academy, 2012

Submitted in partial fulfillment of the
requirements for the degree of

MASTER OF SCIENCE IN MECHANICAL ENGINEERING

from the

NAVAL POSTGRADUATE SCHOOL
December 2018

Approved by: Garth V. Hobson
Advisor

Douglas L. Seivwright
Co-Advisor

Garth V. Hobson
Chair, Department of Mechanical and Aerospace Engineering

THIS PAGE INTENTIONALLY LEFT BLANK

ABSTRACT

The U.S. Department of Defense has implemented an initiative to become more energy efficient across all services. The Naval Postgraduate School supported development toward this goal by studying the possibility of energy generation using waste heat recovery within shipboard engine exhaust. This research included the development of a heat exchanger ultimately to use compressed CO_2 as the working fluid to run a Brayton cycle. In support of this research, this thesis details the baselining and instrumentation of a Rolls Royce M250 helicopter engine in the Marine Propulsion test cell, which was used as the platform for this development. Additionally, a model of the heat exchanger design was fabricated and installed in the engine exhaust.

The effects the installed heat exchanger has on engine performance was measured and analyzed.

This thesis also examined the compressor to be used in the CO_2 loop design. An ANSYS CFD model was developed and tested to create a compressor map of CO_2 performance through a centrifugal compressor. The sheath and casing for the compressor were designed in SolidWorks and fabricated using a 3D printer. This thesis is critical in the continuing development of a shipboard waste heat recovery system.

THIS PAGE INTENTIONALLY LEFT BLANK

TABLE OF CONTENTS

LIST OF FIGURES

LIST OF TABLES

THIS PAGE INTENTIONALLY LEFT BLANK

LIST OF ACRONYMS AND ABBREVIATIONS

atm	atmospheres
CCS	Carbon Dioxide Capture and Storage
CFD	computational fluid dynamics
CO_2	Carbon Dioxide
DoD	Department of Defense
DoN	Department of the Navy
ESTEP	Energy System Technology Evaluation Program
FOD	foreign object debris
GE	General Electric
GHG	greenhouse gas
GTG	gas turbine generator
LOH	Light Observation Helicopter
NPS	Naval Postgraduate School
ONR	Office of Naval Research
RPM	revolutions per minute
SFC	specific fuel consumption
SHP	shaft horse power
WHR	waste heat recovery

THIS PAGE INTENTIONALLY LEFT BLANK

ACKNOWLEDGMENTS

I would like to thank Dr. Hobson and Mr. Seivwright for their continued support, guidance, and encouragement. Their patience and dedication to this project were the cornerstone of its success. I would also like to thank Mr. John Gibson for his help and guidance with machine fabrication. His guidance, patience, and generosity of time allowed me to learn about metal work and fabrication. Finally, I would like to thank my husband for all of his love and support though my time at NPS and especially while working on my thesis.

THIS PAGE INTENTIONALLY LEFT BLANK

I. BACKGROUND

A. ENERGY NEEDS IN THE US NAVY

The operation, sustainment, and success of the U.S. military is intimately intertwined with the force's proper and effective use of all forms of energy. The U.S. Department of Defense (DoD) is the country's largest consumer of energy [1]. This leads to the DoD's high interest in maintaining and improving energy efficiency. Effective use of energy increases the range and endurance of assets and decreases the need of fleet forces to be occupied in protecting energy supply lines. This will, overall, decrease the long-term energy costs and greenhouse gas (GHG) emissions [1].

Among the services, the Department of the Navy (DoN) consumes 28% of the DoD's total petroleum use. Within the Navy's operations, 59% of its overall energy needs were met using petroleum [2]. By the year 2020 the DoD aspires to have 50% of energy produced by renewable methods [1]. Ship design and need for combat stealth and efficiency makes the installation of alternate fuel sources difficult. Solar panels and wind turbines will not logistically fit onboard. Therefore, waste heat recovery is the best fit for increasing effective energy usage on a ship. The main propulsion and exhaust systems are already installed and in use; by harnessing the waste heat expelled, useful energy can be recovered and used at little cost.

The Office of Naval Research (ONR) has created the Energy System Technology Evaluation Program (ESTEP) to continue the development of energy efficient technologies and cultivate their application to the fleet. The Naval Postgraduate School (NPS) participates in the ESTEP program by dedicating research and thesis work to these developments. This thesis supports the ESTEP initiative by examining and developing a new waste heat recovery (WHR) device to generate electricity that can be installed in shipboard exhausts.

B. HISTORY OF WASTE HEAT RECOVERY ON U.S. NAVY SHIPS

The U.S. Navy has implemented the use of WHR systems before. The CG-47 Ticonderoga-class AEGIS guided missile cruisers were each equipped with waste heat boilers. This system installed a steam boiler within the gas turbine electric generator (GTG) exhaust and piped the steam throughout the ship to provide hotel services and assist in fresh water distillation. However, the use of "wet steam" as the working fluid caused maintenance and corrosion problems. The burden of this system's problems was determined by the Navy to outweigh the benefits, and the waste heat boilers were removed from all of the ships within the class [3].

This project improved upon this design by using compressed CO_2 as the working fluid instead of wet steam, which will avoid internal corrosion issues. Additionally, this loop is to be used to generate electrical power locally at the heat exchanger, removing the need of intricate piping systems running the working fluid throughout the ship.

C. PROCEEDING NPS THESIS WORK

NPS students and faculty have spent several years investigating the problem of extracting the energy expelled by waste heat from a gas turbine. The progression of this work to date has been documented in the following:

1. "Turning Vanes in Exhaust Duct Flow" by Beale

Beale [4] studied the placement of turning vanes within the 90-degree bend of the exhaust duct to assist the flow. Using computational fluid dynamics (CFD) models, he varied the placement of a single turning vane to optimize the exhaust flow without inducing too much back-pressure on the engine. He then studied the effects of using multiple vanes within the exhaust duct. Beale concluded that a single turning vane in the center of the exhaust duct or three equally spaced turning vanes created a reduction in back-pressure by approximately 50–60% [4]. This work provided the basis for the initial design study of the WHR heat exchanger in an exhaust stream of a gas turbine.

2. "Optimal Placement of Non-Intrusive Waste Heat Recovery Devices in Exhaust Ducts" by Bohning

Bohning's [5] work considered a WHR system that places flat, heat absorbing plates on the outside of the duct. This approach avoids the introduction of any hardware within the exhaust duct, eliminating any potential effects of back pressure on the engine. Bohning determined the optimal placement of these plates was just past the bend, where a large recirculation zone formed. The recirculation zone slows the flow and allows for more contact time with the WHR plates [5].

3. "Energy Efficient Waste Heat Recovery from an Engine Exhaust System" by VanDenBerg

VanDenBerg [6] developed a series of 34 heat exchanger tubes that would be placed within the bend of the exhaust ducting. This thesis used these tubes to replicate the turning vane design in Beale's thesis to minimize the back-pressure placed on the engine as shown in Figure 1 [6].

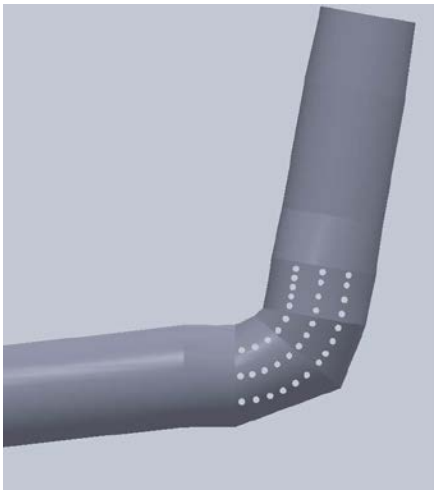

Figure 1. VanDenBerg Heat Exchanger Design. Source: [6].

VanDenBerg also analyzed the use of the Rankine cycle versus the Brayton cycle in the heat exchanger using Carbon Dioxide (CO_2) as the working fluid. CO_2 was chosen

because of its non-corrosive nature, efficiency, and gaseous operation. Through his analysis he found that the Brayton cycle to be the most effective method of WHR [6].

4. "Waste Heat Recovery Carbon Dioxide Heat Exchanger for Gas Turbine Engines" by Polsinelli

Polsinelli [7] modified the design of VanDenBerg's heat exchanger to contain four coils installed in the exhaust ducting instead of straight pipes. This allows for more exposure of the heat exchanger tubing to the engine exhaust. These four coils were designed to have flow run through the coils in series or in parallel [7]. This design is shown in Figure 2.

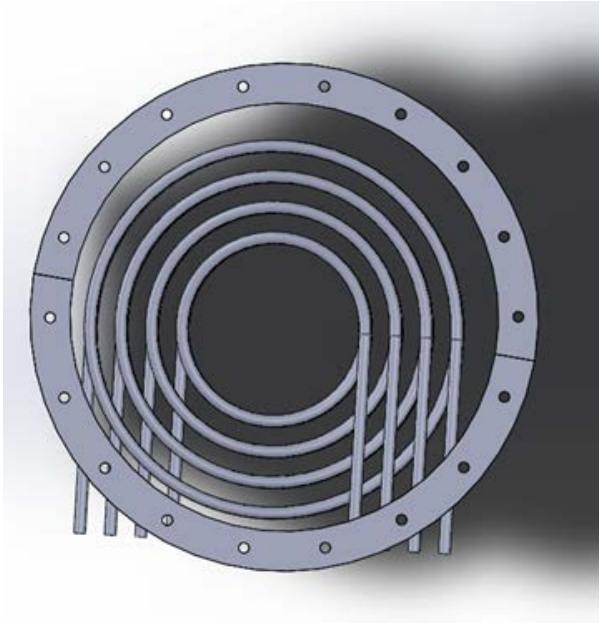

Figure 2. Axial View of Polsinelli's Heat Exchanger Design. Source: [7].

Polsinelli used CFD to examine the effects of this heat exchanger insert on the back pressure exerted onto the engine. He concluded that this design would, for the given exhaust mass flow rate, maximize the recovery of heat energy while minimizing any impact on the performance of the engine [7].

Polsinelli also assisted with the installation and baseline of the zero-hour Rolls Royce M250 T63-A-720 gas turbine engine into the NPS Marine Propulsion Laboratory's

gas turbine test cell. This included shaft alignment, creation and installation of a new bell mouth, and modified duct design to fit the heat exchanger [7].

D. OBJECTIVES AND GOALS

This thesis research contained three main objectives. The first was to establish an engine performance baseline for future data comparisons. This involved the setup of a new data acquisition system to gather temperature and pressure data from the engine using Labview hardware and MATLAB data acquisition based software, as well as the proper installation and calibration of the existing SuperFlow Dyno system used to record power output, engine torque, fuel flow, etc. A vibration monitoring system was also installed to monitor long term engine health. The second goal was to fabricate a prototype of Polsinelli's heat exchanger, and experimentally measure the back-pressure effects on the engine. Finally, an engineering analysis on the compressor to be used in the WHR CO_2 loop would be conducted using computational fluid dynamics (CFD) to predict performance.

THIS PAGE INTENTIONALLY LEFT BLANK

II. BASELINING THE ENGINE

A. BACKGROUND: THE ROLLS ROYCE M250 T63 GAS TURBINE ENGINE

The engine installed in NPS's Marine Propulsion Lab was a Rolls Royce M250, or T63-A-720 gas turbine engine, formally known as the Allison 250. The Detroit Diesel Allison Division of General Motors developed the original Model 250 in the late 1950s to meet Army needs for a Light Observation Helicopter (LOH) 250 shaft horse power (SHP) engine. In 1961, the first Allison 250 engine flew in a HUL-1M helicopter. Previous helicopter engine designs had the exhaust exit downward from the aircraft. Allison was asked to turn the exhaust ports in the 250 model upward to minimize infrared signature of the aircraft and to avoid accidental grass fires. In 1965, the Allison 250 was selected for use in the Army's LOH and until recently was still used by the U.S. Army [8]. A schematic of the engine design is shown in Figure 3.

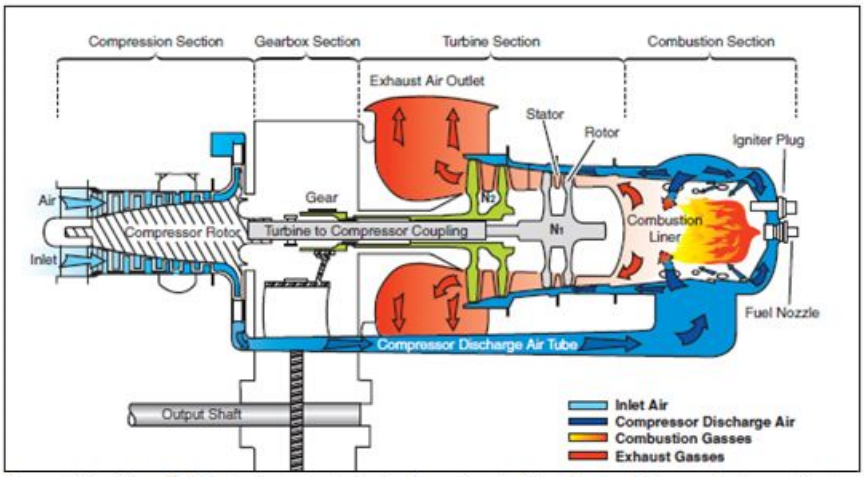

Figure 3. Schematic Diagram of Allison 250 Engine. Source: [6].

The innovative exhaust design of this engine provided an ideal setup for the study of a WHR system in the exhaust ducting. The dual exhaust configuration and upward orientation allowed for the installation of a test setup in one duct, and comparing this to the flow in the unmodified duct. SolidWorks drawings of the two ducts were developed by

VanDenBerg in his thesis. The engine with the unmodified exhaust duct configuration is shown in Figure 4.

Figure 4. NPS Gas Turbine Test Cell Exhaust Duct Setup. Source: [6].

The Rolls Royce M250 engine installed in the test cell was procured from the U.S. Army and overhauled by AeroMaritime America. Before any modifications were made to the engine, to include the heat exchanger and measurement instrumentation, the baseline power output and fuel consumption measurements were to be recorded.

B. ENGINE BASELINE MEASUREMENTS

Baseline performance parameters were measured at the engine operating points outlined in Table 1. N_1 represents the speed of the gas turbine compressor, N_2 is the power turbine spool speed, and N_d represents the speed of the dynamometer. The dynamometer provided the simulated load to the engine and measured torque and power outputs of the engine. The raw data collected by the SuperFlow data acquisition software at each operating point is included in Appendix A.

Table 1. Operating Points for Engine Testing

N_1	N_d	N_d	N_d	N_d	N_d
RPM	**RPM**	**RPM**	**RPM**	**RPM**	**RPM**
Idle	No load				
40,890	3,600	4,200	4,800	5,400	6,000
46,000	3,600	4,200	4,800	5,400	6,000
51,000	3,600	4,200	4,800	5,400	6,000

The engine was operated for baseline measurements on October 12, and October 15, 2018. The results of these tests are compared to the quoted measurements provided from the manufacturer and shown in Table 2.

Table 2. Comparison of Quoted Specifications against Baseline Measurements

	Quoted Specifications	Measured Results 10/12/2018	Measured Results 10/15/2018
N1	50,970 RPM	51,000 RPM	51,000 RPM
N2	33,290 RPM	34,980 RPM	34,980 RPM
Nd	6,016 RPM	6,000 RPM	6,000 RPM
$\dot{m}_f$	0.03 kg/sec (238.099 lbm/hr)	0.031 kg/sec (242.4 lmb/hr)	0.032 kg/sec (252 lbm/hr)
$\dot{m}_a$	1.420 kg/sec (11270.03 lbm/hr)	1.889 kg/sec (14992.32 lbm/kg)	1.9141781 kg/sec (15192.145 lbm/hr)
Shaft Power	313kW (420 SHP)	269.95 kW (362 SHP)	281.36 kW (377 SHP)

Figure 5 shows the power turbine speed versus engine power for the two baseline tests. The results sow the data to be repeatable and reproducible demonstrating a sufficient level of reliability regarding future measurements.

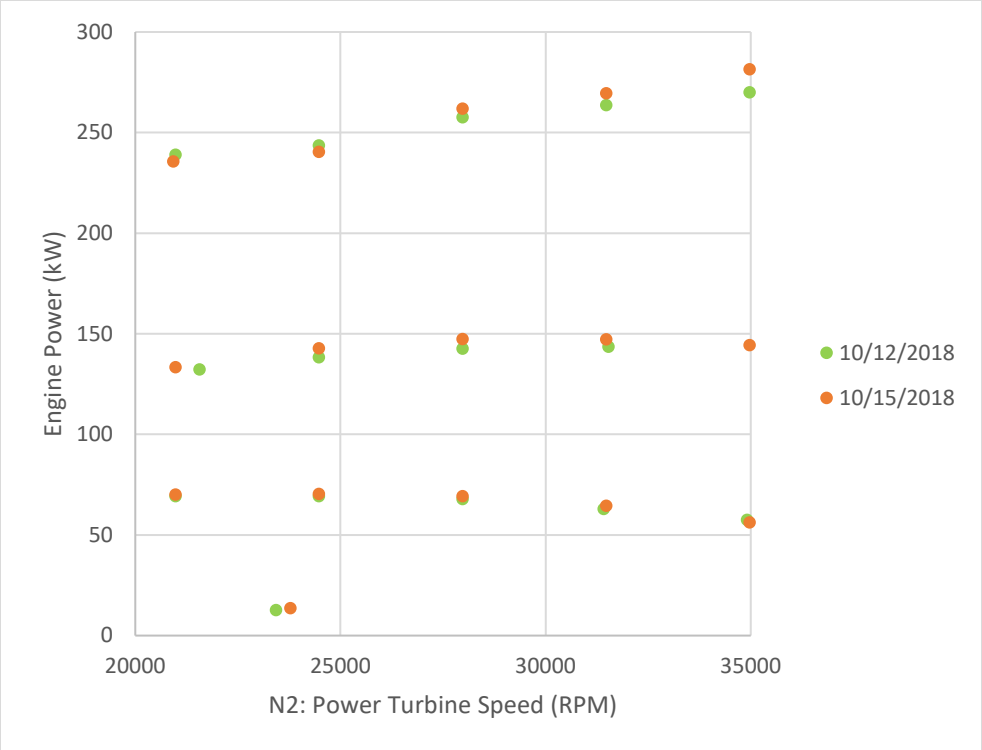

Figure 5. Measured Engine Performance of Baseline Tests

Performance measurements gathered by the SuperFlow data acquisition system are listed in Appendix A and are representative of the baseline performance of the engine. This data will be used to monitor and assess future modifications to the engine and their effectiveness in its performance as well as a measure of long term engine health.

1. Vibrations Measurements

Two accelerometers were attached to the engine support structure to measure axial and radial vibrations. The locations of the accelerometers are shown in Figure 6. The two feeds were linked to an oscilloscope and at each operating point listed in Table 1 three sets of data were collected. From each feed, the axial and the radial, the Peak-to-Peak voltage, the DC RMS voltage, and the DC RMS mean voltage were all recorded. Initial data collected for the unmodified configuration of the engine is included in Appendix B and is part of its baseline database.

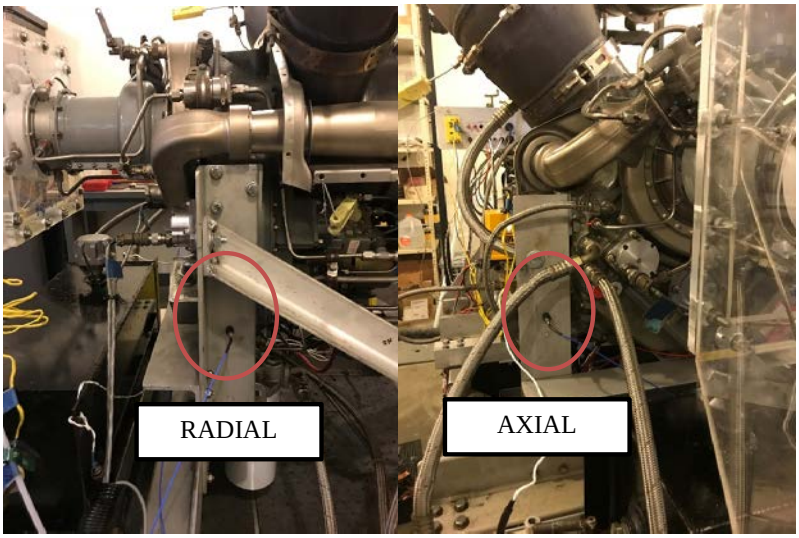

Figure 6. Accelerometer Locations on Engine Support Structure

This data was be crucial in evaluating the effects of the exhaust flow on heat exchanger when it was installed. Vibrations magnitudes greater than those of the recorded baseline would be cause for ending the test run and an analysis conducted to determine the exact cause A comparison of baseline vibrations data collected for each run is shown in Figure 7.

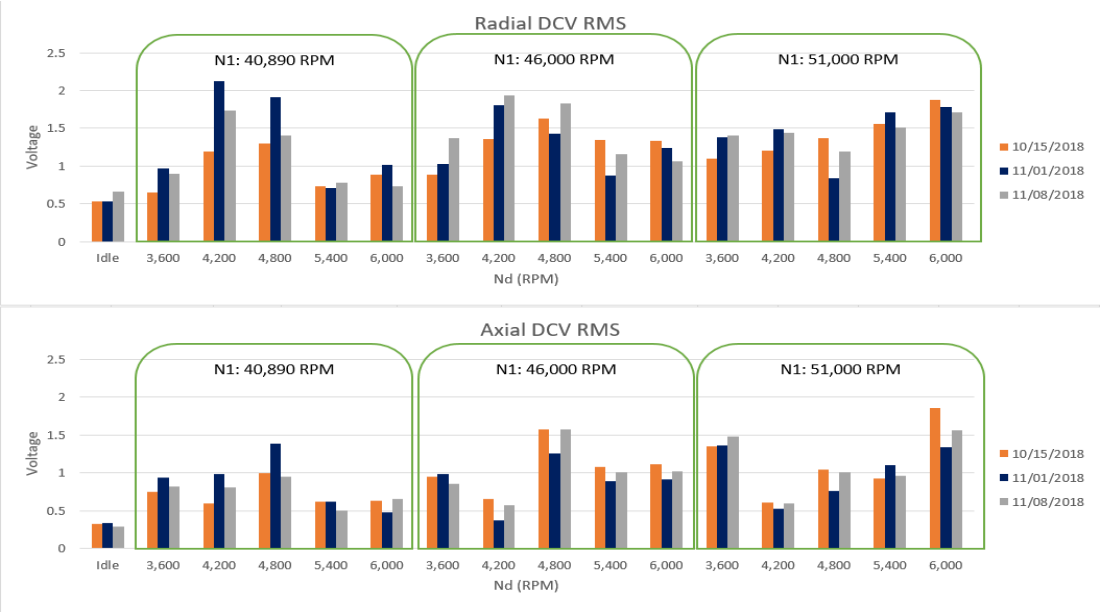

Figure 7. Comparison of Vibrations Measurements

2. Comparison to Refurbishment Results

Before the engine was installed into NPS's Marine Propulsion Lab, it was refurbished by Aero Maritime. The baseline measurements conducted at the repair facility are included in Appendix C. The results of the baseline runs conducted at NPS were plotted against these values; the comparison of the results is shown in Figure 8.

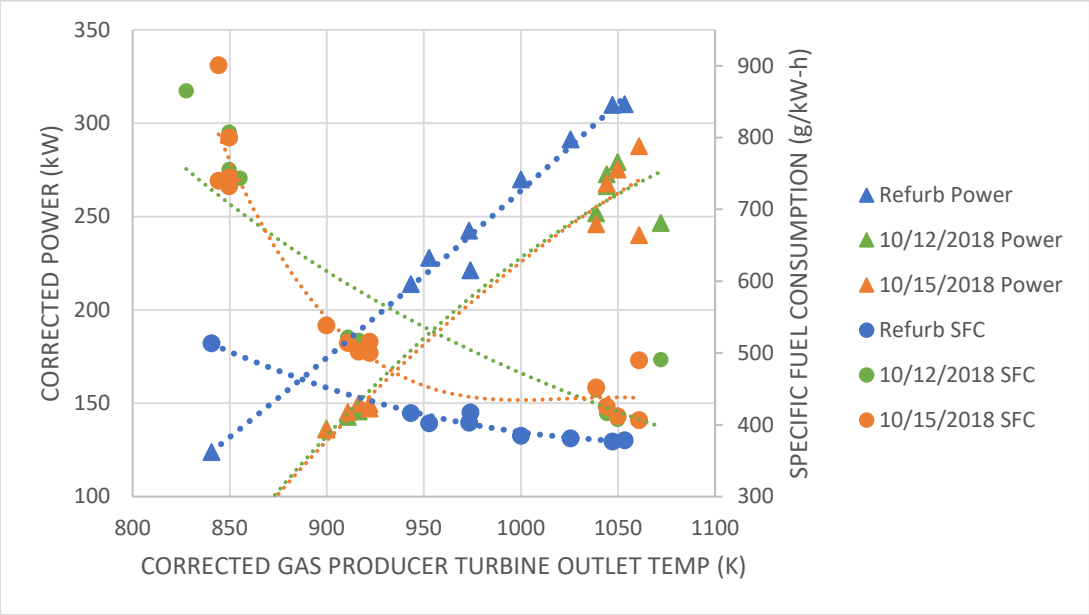

Figure 8. Comparison of Refurbishment Facility Data to NPS Baseline

The data for the runs between the two facilities shows a strong level of correlation.

C. INSTRUMENTATION INSTALLATION

With the baseline measurements of the engine complete, the engine was then equipped with additional temperature and pressure probes. These probes were installed in two phases: 1.) instrumentation installed along the engine and 2.) installed along the exhaust ducts. The instrumentation located on the engine would be used to gather data to determine both engine component performance as well as overall engine output for comparison with ideal cycle calculations. The instrumentation located along the exhaust ducts was used to gather data pertaining to backpressure as well as developing a

temperature profile. This data, in conjunction with the performance data, would be used to determine if a degradation in performance of the engine occurred as a result of the installed heat exchanger. Once the additional instrumentation was installed, the engine was operated on November 1, 8, and 19, 2018 to verify the effects these modifications had on the engine and to calculate additional engine parameters. The readings collected by the additional sensors were recorded using a MATLAB data acquisition system, the raw data of these readings are shown in Appendix D.

1. Pressure Sensors

Pressure sensors were added on the engine and exhaust ducting to acquire measurements at different locations of the fluid path. The locations are listed in Table 3. The pressure lines were connected to three Scanivalve Digital Sensor Arrays, each with a different maximum pressure, 10" H_2O, 2.5 PSID, and 100 PSID to ensure adequate resolution of the given pressure signal. The pressure probes installed during the first phase were located at the Compressor Inlet Static Pressure, Compressor Inlet Total Pressure, Compressor Outlet Left, Compressor Outlet Right, Left Stack Static Pressure, and Right Stack Static Pressure. The second phase of installation included four additional pressure probes along the stack, as shown in Figure 9. These locations were Left Stack 2, Left Stack 3, Left Stack 4, Left Stack 5, Right Stack 2, Right Stack 3, Right Stack 4, and Right Stack 5. Figure 10 shows the locations of the pressure inputs to the pressure devices and their respective IP addresses.

Table 3. Pressure Sensor Locations

	Port Number	Location
Phase 1	1	Compressor Inlet Static Pressure
	2	Compressor Inlet Total Pressure
	3	Compressor Outlet Left
	4	Compressor Outlet Right
Phase 2	7	Right Stack Pressure 2
	8	Right Stack Pressure 3
Phase 1	9	Left Stack Static Pressure
	10	Right Stack Static Pressure
Phase 2	11	Right Stack Pressure 4
	12	Right Stack Pressure 5
	13	Left Stack Pressure 2
	14	Left Stack Pressure 3
	15	Left Stack Pressure 4
	16	Left Stack Pressure 5

Figure 9. Locations of Pressure and Temperature Probes Along Stacks

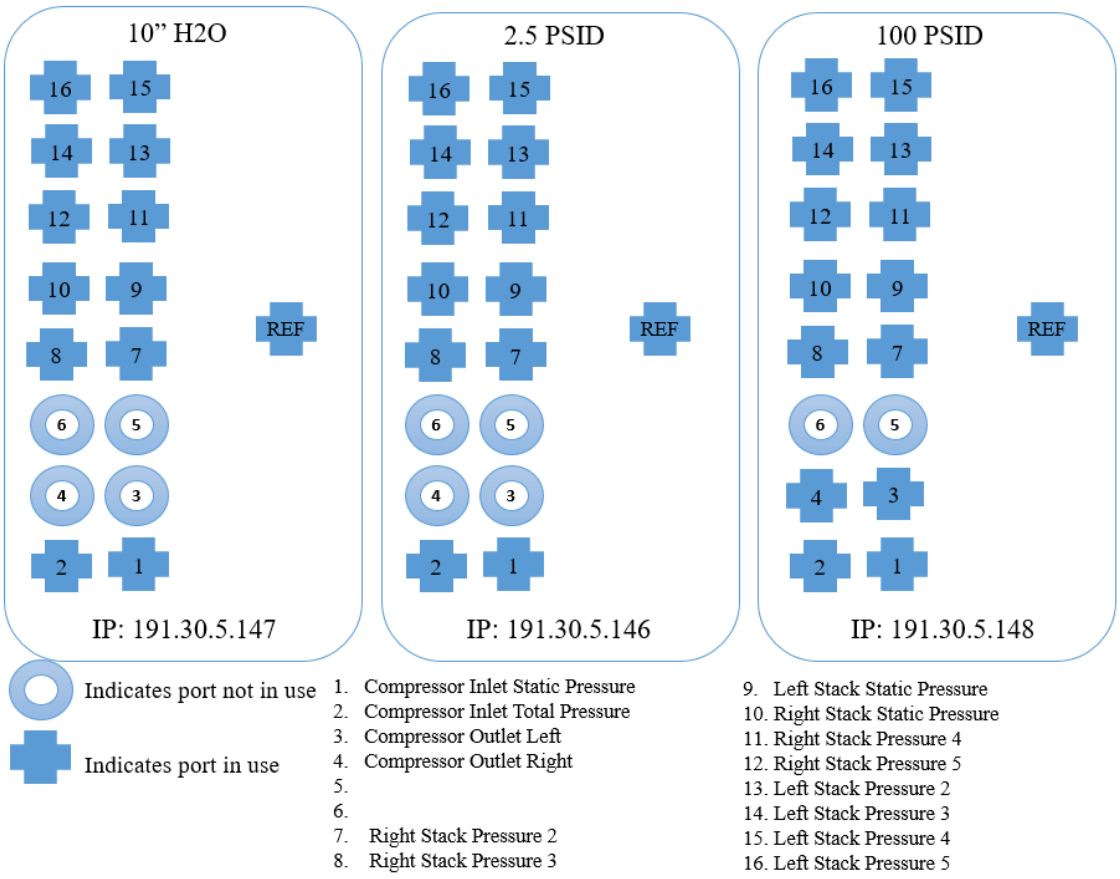

Figure 10. Pressure Measurement Diagram

2. Temperature Sensors

Fifteen additional K-type thermocouple sensors were installed on the engine, their locations listed in Table 4. These additional temperatures were used to determine engine performance as well as developing a temperature profile along the exhaust ducting. The temperature measurements installed in the first phase included the Compressor Inlet 1, Compressor Inlet 2, Compressor Outlet Left, Compressor Outlet Right, T5, Left Stack 1, Left Stack 2, Right Stack 1, and Right Stack 2. The temperature sensors installed in the second phase included Left Stack 3, Left Stack 4, Left Stack 5, Right Stack 3, Right Stack 4, and Right Stack 5. These second phase temperature probes are shown in Figure 9.

Table 4. Temperature Sensor Locations

	Probe Number	Measurement Location
Phase 1	1	Compressor Inlet 1
	2	Compressor Inlet 2
	3	Compressor Outlet Left
	4	Compressor Outlet Right
	5	T5
	6	Left Stack 1
	7	Left Stack 2
	8	Right Stack 1
	9	Right Stack 2
Phase 2	10	Left Stack 3
	11	Left Stack 4
	12	Left Stack 5
	13	Right Stack 3
	14	Right Stack 4
	15	Right Stack 5

3. Calculating Mass Flow Rate of Air

The data collected by the additional temperature and pressure sensors was used to calculate the mass flow rate of air, $\dot{m}_a$, into the engine and compare it to the mass flow rate of air obtained from the installed SuperFlow data acquisition system. The calculated $\dot{m}_a$ was found using the equation below were the C_D is the coefficient of drag, 0.98, P_T is the total pressure at the bell mouth, P is the static pressure at the bell mouth, A is the cross sectional area of the bell mouth, R is the universal gas constant, 287 J/kg-K, and T_T is the total temperature at the bell mouth.

$$\dot{m}_a = C_D \rho A V = \frac{C_D P_T A}{\sqrt{R T_T}} \left(\frac{P}{P_T}\right)^{\frac{1}{\gamma}} \sqrt{\frac{2\gamma}{\gamma - 1}\left[1 - \left(\frac{P}{P_T}\right)^{\frac{\gamma-1}{\gamma}}\right]} \text{ (kg/s)}$$

Once the $\dot{m}_a$ was calculated, it must be corrected for the environmental effects of the barometric pressure and air temperature for the day of testing. These corrections were made using the following equations.

$$\delta = \frac{P_{in}}{P_{STD}} \qquad \theta = \frac{T_{in}}{T_{STD}} \qquad \dot{m}_c = \frac{\dot{m}\sqrt{\theta}}{\delta}$$

The $\dot{m}_a$ obtained by this calculation for each test operation of the engine is compared to the $\dot{m}_a$ measured by the SuperFlow data acquisition system. A comparison both mass flow rates for each testing date are shown in Table 5.

Table 5. Comparison of $\dot{m}_a$ Results from SuperFlow vs. MATLAB

11/01/2018			11/08/2018			11/19/2018		
SuperFlow		MATLAB	SuperFlow		MATLAB	SuperFlow		MATLAB
N2 RPM	$\dot{m}_a$ Corrected kg/s	$\dot{m}_a$ Corrected kg/s	N2 RPM	$\dot{m}_a$ Corrected kg/s	$\dot{m}_a$ Corrected kg/s	N2 RPM	$\dot{m}_a$ Corrected kg/s	$\dot{m}_a$ Corrected kg/s
23728	0.887	0.853	24136	0.902	0.880	23845	0.897	0.867
20930	1.312	1.214	20988	1.291	1.194	20988	1.301	1.209
24486	1.294	1.198	24486	1.288	1.189	24544	1.301	1.203
27984	1.317	1.129	27984	1.287	1.181	27984	1.303	1.204
31482	1.300	1.186	31482	1.290	1.180	31540	1.306	1.203
35038	1.327	1.106	34980	1.296	1.182	34980	1.307	1.203
34980	1.489	1.299	34980	1.510	1.342	34921	1.524	1.357
31482	1.482	1.262	31482	1.517	1.344	31482	1.528	1.357
27984	1.499	1.272	27925	1.516	1.341	27984	1.530	1.356
24544	1.488	1.279	24486	1.521	1.335	24544	1.529	1.351
20988	1.539	1.223	20988	1.522	1.339	20988	1.530	1.352
20988	1.871	1.492	20988	1.920	1.591	20988	1.910	1.599
24486	1.914	1.425	24486	1.909	1.563	24486	1.923	1.572
27984	1.953	1.468	27984	1.928	1.558	27984	1.933	1.573
31540	2.023	1.432	31482	1.926	1.552	31482	1.930	1.565
34980	2.040	1.499	34980	1.930	1.553	34921	1.932	1.563

The mass flow rates calculated using the MATLAB measurements are lower than the SuperFlow measurements and closer to the expected values for this engine. A possible explanation of this discrepancy may be due to the SuperFlow air turbine intake meters lacking a recent calibration.

4. Sensor Effect on Engine Performance

The engine was operated on November 1st and 8th, 2018 with the additional pressure and temperature sensors installed in the first phase, and again on November 19, 2018 after the installation of the second phase. These testing runs were used to verify the newly installed equipment was taking accurate readings and to ensure the additional instrumentation did not have any negative effects on the engine performance. The SuperFlow raw data from these runs is included in Appendix A. The raw data collected from the MATLAB system is included in Appendix D. The vibrations levels were monitored and shown in Figure 11 at each operating point, the raw data is included in

Appendix B. The vibrations levels indicate that the additional instrumentation did not have any adverse effects on the vibration of the engine during operation. The engine performance data for the runs is shown in Figure 12. This chart shows that the additional instrumentation had no adverse effect on the performance of the engine.

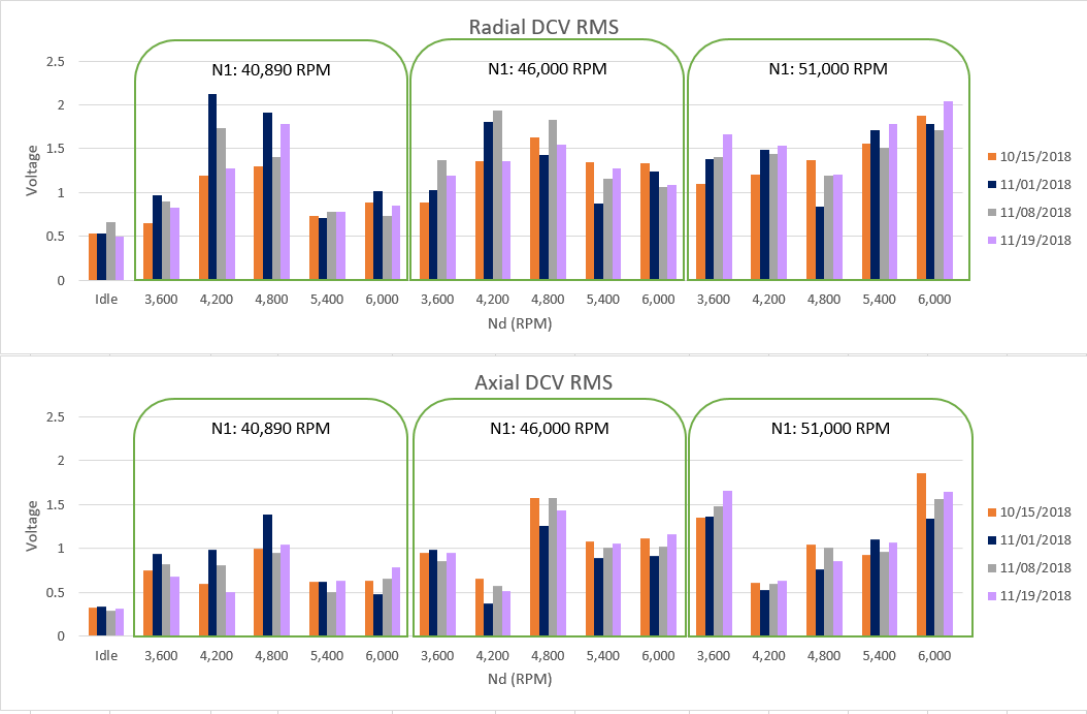

Figure 11. Vibrations of Engine Structure with Installed Instrumentation

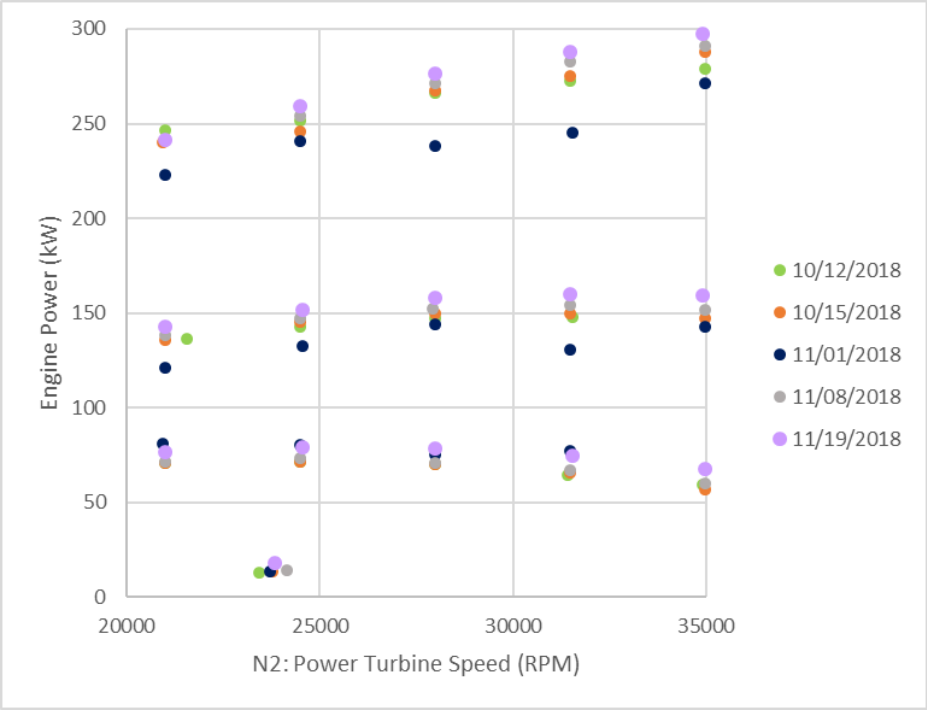

Figure 12. Measured Engine Performance with Instrumentation

The results show no significant changes on the performance of the engine due to the addition of instrumentation as compared to the baseline readings.

5. Exhaust Readings

The sensors installed in the second phase allowed insight into the flow inside the exhausts. Figure 13 shows the distribution of the pressures through the left and right exhausts. These readings were essential to establish the unaltered exhaust flow characteristics, to which the effects of the heat exchanger were compared.

Figure 13 shows the pressure decreases along the exhaust at probe locations 1-4, and then increases at probe location 5. The increase in pressure at probe 5 was expected as this probe is located after the upward bend in the exhaust where separation of flow occurs at the bend resulting in a highly turbulent flow causing a resulting increase of backpressure to develop.

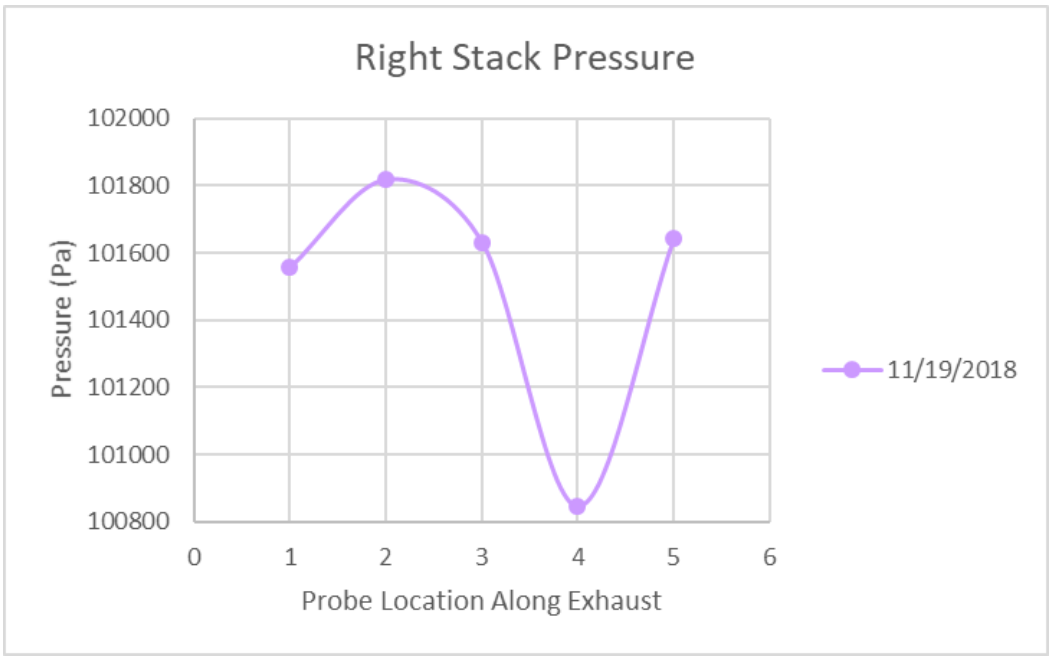

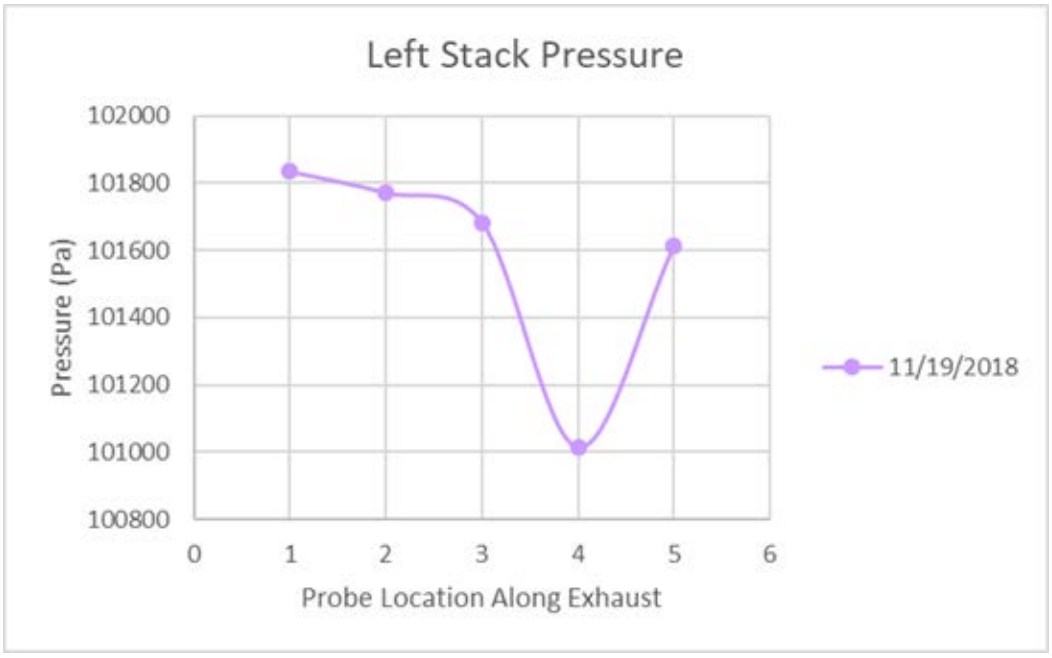

Figure 13. Pressure throughout each Exhaust with No Heat Exchanger

D. GASTURB MODEL OF ENGINE

The engine performance data gathered using SuperFlow and MATLAB data acquisition systems provided the parameters required to develop a model of the engine using GasTurb software. GasTurb was used to create a model of the T-63 engine. Three parametric studies were conducted, one at each N_1 speed used for experimentation, 100%, 90.2%, and 80.2%. The parametric study held the N_1 speed constant and varied the N_d speed, similar to the testing operation of the engine. A comparison of the results gathered in GasTurb and the engine performance observed on November 19th, are shown in Figure 14.

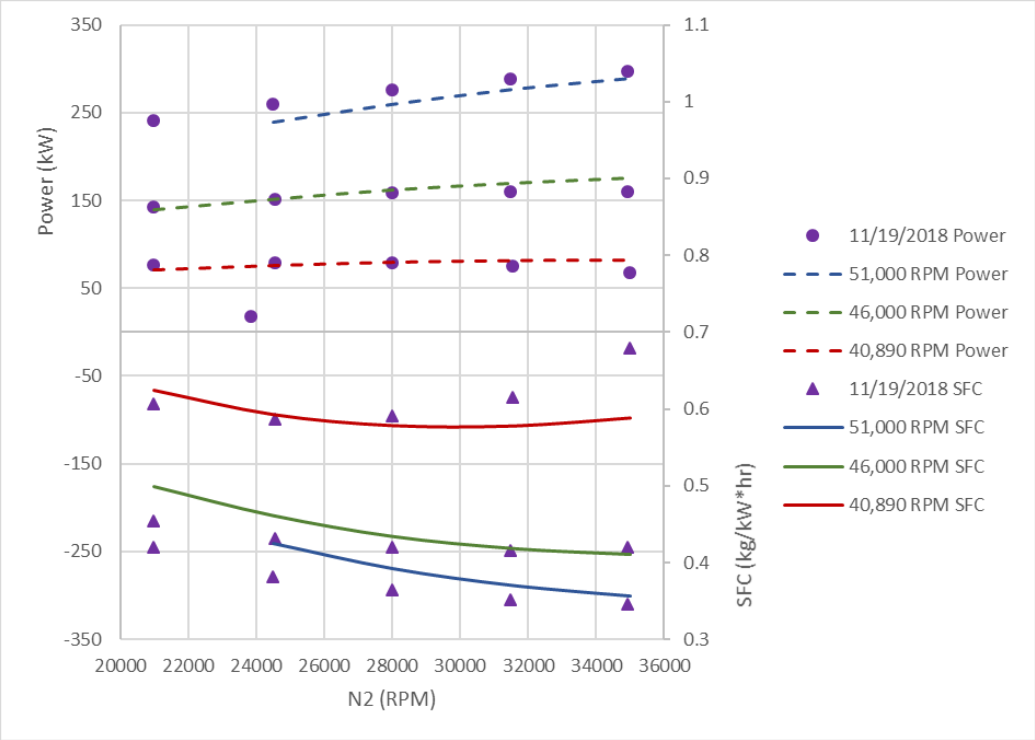

Figure 14. Comparison of GasTurb Results to Engine Run on 11/19/2018

These results demonstrate the GasTurb model accurately predicts the engine performance. The power output predictions match closely with the experimental observations. The experimental power values are observed directly. The specific fuel

consumption (SFC) predictions have more variance from what was observed because these were derived values from fuel flow rate and power.

III. IMPLEMENTING THE HEAT EXCHANGER

A. HEAT EXCHANGER FABRICATION

The heat exchanger exhaust insert prototype, designed by Polsinelli, was fabricated at NPS's Turbopropulsion Laboratory. The heat exchanger design consisted of two clamshell halves that encompassed four coils. Each coil had a different diameter, 15.24 cm (6 inches), 20.32 cm (8 inches), 25.40 cm (10 inches), and 30.48 cm (12 inches). These coils consisted of 8 loops and stood approximately two feet in height to fit within the clamshell. These individual coils are shown in Figure 15.

Figure 15. Heat Exchanger Coils

Each coil exits the heat exchanger at both the top and the bottom of the same clamshell piece, as shown in Figure 16. Having each coil enter and exit the exhaust allowed for the flow of the CO_2 to be manipulated into a series or parallel configuration. This allowed for variations in mass flow rate and exposure time in the flow.

Figure 16. Heat Exchanger Clamshell Half

The coils exited the clamshell through a plate at the top and bottom of the clamshell. Each coil exit contained a brass bushing to hold the coil in place and that bushing was held in place with a spring pin. The plate is held to the clamshell with screws that have been threaded into the clamshell. This allows for the plate to be held in place without the need for additional hardware on the inside of the clamshell. This prevented the possibility of loose hardware falling down the exhaust and causing foreign object debris (FOD) in the engine. The exit plate is shown in Figure 17.

Figure 17. Exit Plate of Coils

The coils were held in place with braces to reduce vibrations within the exhaust pipe. These braces clamp over a row of the four coils to hold them in place. The ends are riveted together and the brace is bolted to the inside of the clamshell. These bolts are welded to the brace. Welded bolts and rivets were used to reduce the potential of FOD that would be present with loose hardware. Three braces were installed around the coils, approximately 60 degrees apart, one at the top, middle, and bottom of coil stack, shown in Figure 18 and Figure 19.

Figure 18. Brace around Heat Exchanger Coils 1

Figure 19. Brace around Heat Exchanger Coils 2

The completed heat exchanger is shown in Figure 20 and Figure 21.

Figure 20. Assembled Heat Exchanger 1

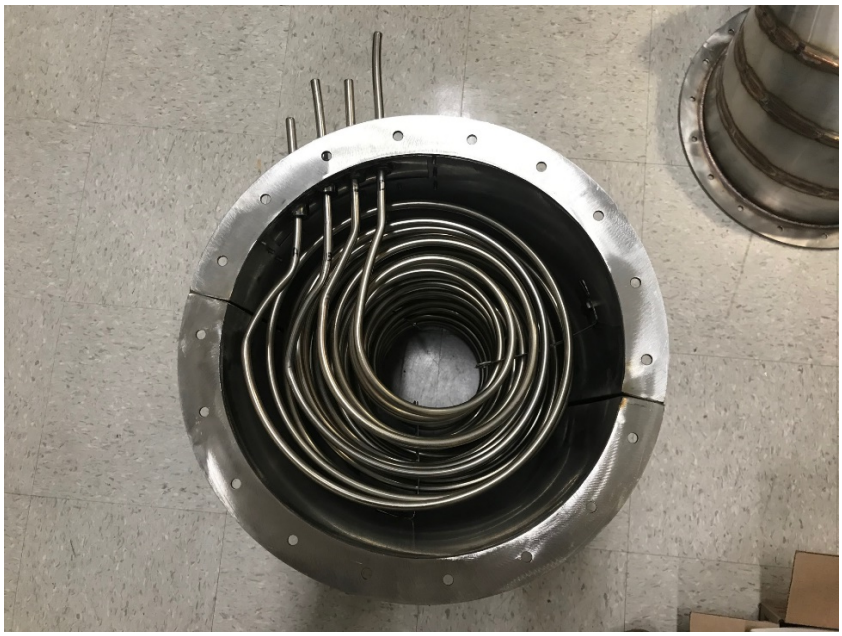

Figure 21. Assembled Heat Exchanger 2

Once the prototype was ready, the assembly was installed on the vertical run of the right exhaust duct as shown in Figure 22 and 23. Two pressure probes were installed, one above and one below the heat exchanger and shown on Figure 23.

Figure 22. Installed Heat Exchanger 1

Figure 23. Installed Heat Exchanger 2

B. THE EFFECTS OF THE HEAT EXCHANGER ON ENGINE PERFORMANCE

After the heat exchanger prototype was installed the engine was operated on November 20, 2018, at the operating points listed in Table 1. The vibrations were closely monitored to ensure the addition of the heat exchanger did not cause excessive vibrations to the test rig. A comparison of the vibration levels is shown in Figure 24. The observed vibration levels showed the heat exchanger did not have a significant adverse effect on the test rig.

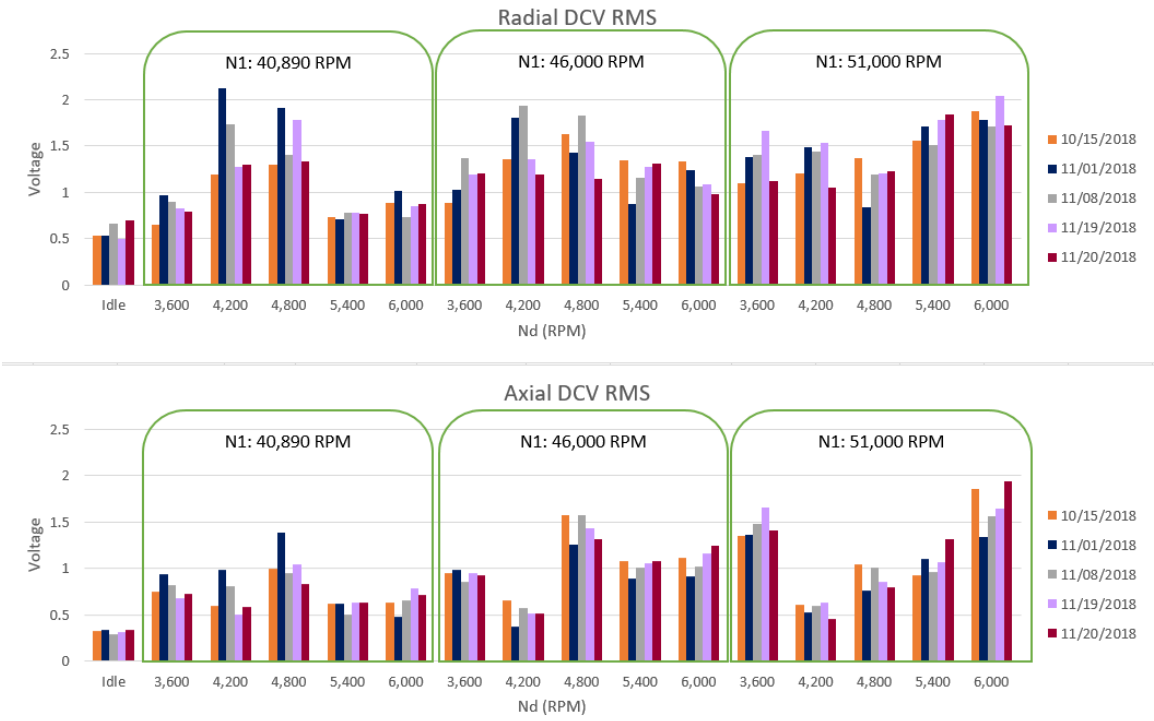

Figure 24. Vibration of Engine Structure with Installed Heat Exchanger

A decrease in engine horsepower output especially at high N_2 settings was noted. A comparison of the engine performance for each run is show in Figure 25. The top row of engine power performance shows the runs for November 20th produced lower power outputs than previously obtained.

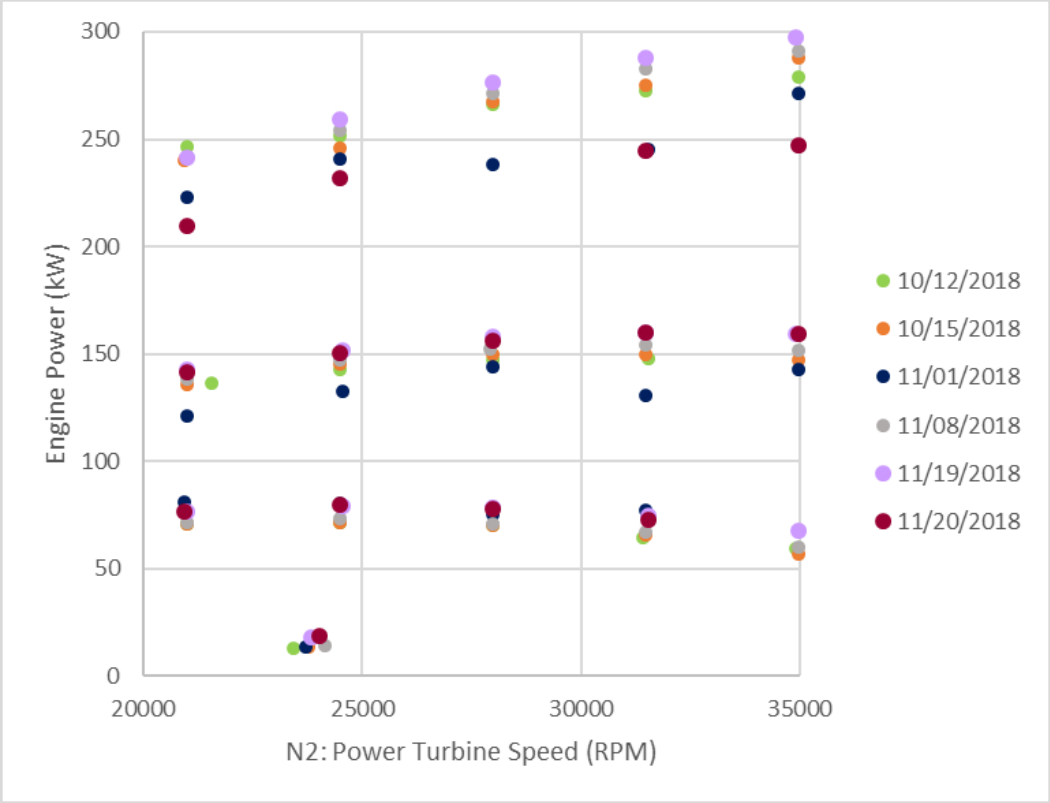

Figure 25. Measured Engine Performance with Heat Exchanger

A comparison of the pressures within the exhausts before and after the heat exchanger are shown in Figure 26. The right exhaust experienced higher pressures along the duct with the heat exchanger installed. The left exhaust experienced a higher pressure and the location of probe 1, closest to the engine, and then experienced pressures similar to before the heat exchanger was added. The increase in pressure in the right duct suggests that the area ratio of the tubing to duct cross-sectional area may require modification or that the duct exhaust nozzle geometry could require modification as well.

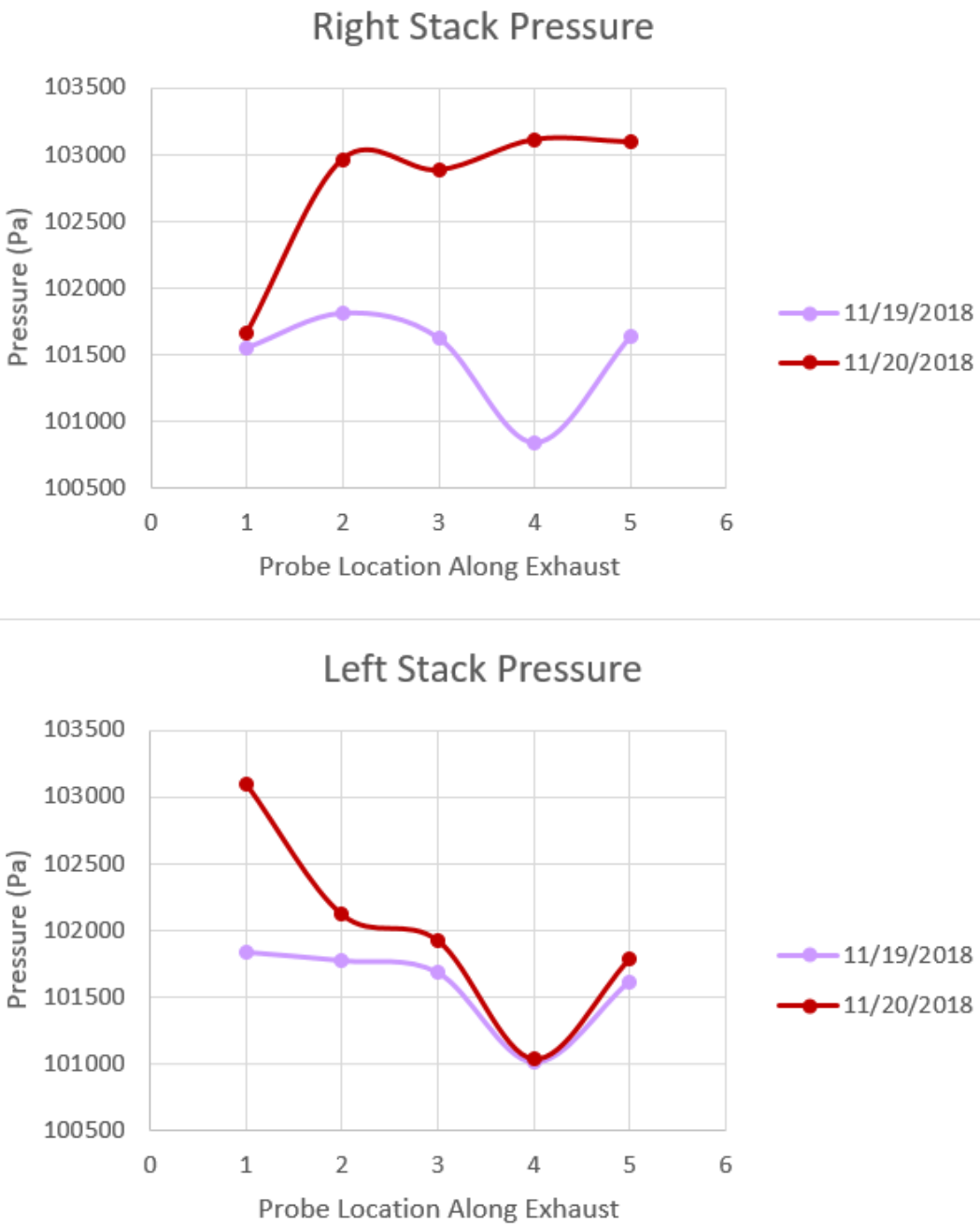

Figure 26. Pressure throughout each Exhaust with Heat Exchanger

IV. CO_2 COMPRESSOR ANALYSIS AND DESIGN

In tandem to the engine installation and study of the effects of the heat exchanger on the engine, an analysis was conducted on the design of the CO_2 loop based on the Brayton cycle. Specifically, efforts were focused on the design of the compressor and its casing. A diagram of the engine and the heat exchanger are shown in Figure 27.

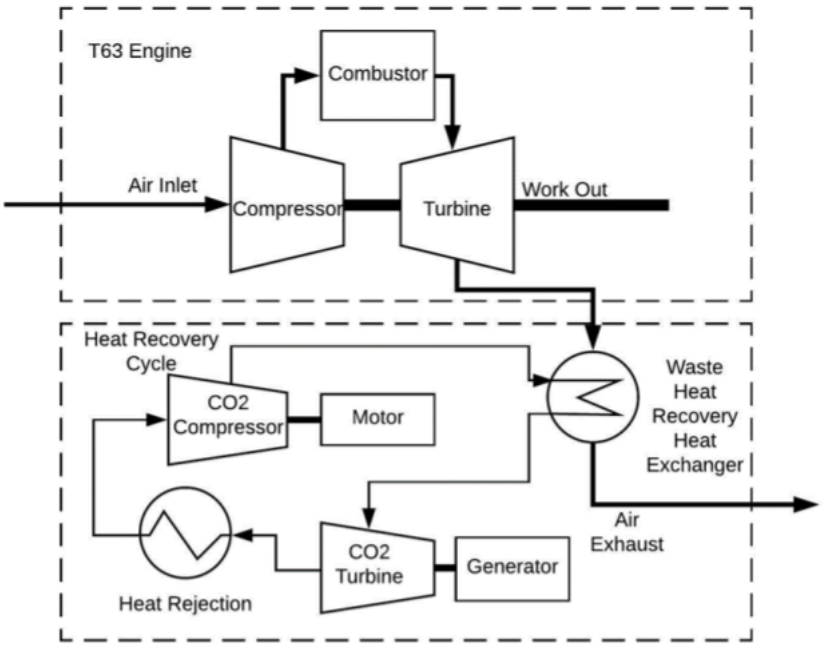

Figure 27. Waste Heat Recovery Schematic. Source: [7].

A. BACKGROUND: CURRENT USE OF CO_2 COMPRESSION

In efforts to combat global climate change, the technique of Carbon Dioxide Capture and Storage (CCS) has been developed and implemented. The process of CCS requires capturing CO_2 from the waste products of facilities, transporting it through pipelines, and pumping it underground to be stored. For this research, the technologies used to compress the CO_2 for transport and storage are of interest.

Industries developing CCS technologies have found that centrifugal compressors are preferred because of their ability to handle large flow rates [9]. The discharge pressure versus the inlet volume for varies types of General Electric (GE) compressors using CO_2 are shown in Figure28. Figure 28 demonstrates that a centrifugal compressor provides the widest variations of inlet mass flow rate, and can provide a comparable range of discharge pressures. For the heat exchanger used in this WHR system, a centrifugal compressor will be used. This type of compressor was chosen because of the wide use in industrial CCS and from its versatile range compared to other options.

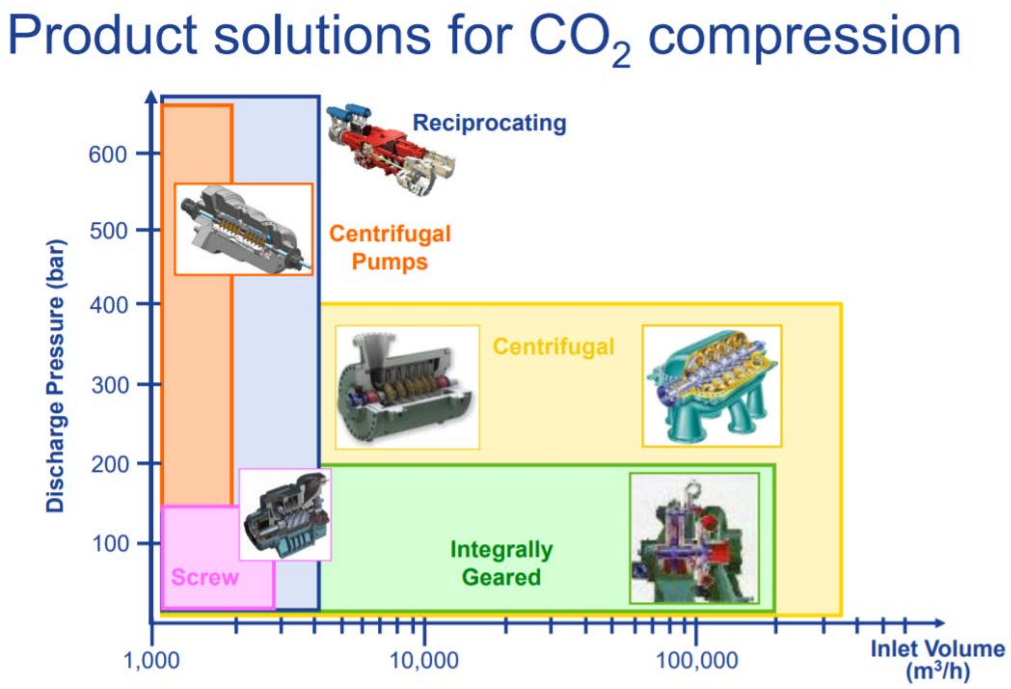

Figure 28. CO_2 Performance of Various GE Compressors. Source: [10].

B. ANSYS MODELING OF THE COMPRESSOR

For the impeller of the CO_2 compressor the Garrett T2 Turbocharger Compressor impeller was chosen. This impeller was then scanned using a 3D scanner and loaded into the SolidWorks software to create the model shown in Figure 29. Around this impeller a

flow field was designed in SolidWorks to generate a simulated flow from onto the impeller and out radially, as shown in Figure 30.

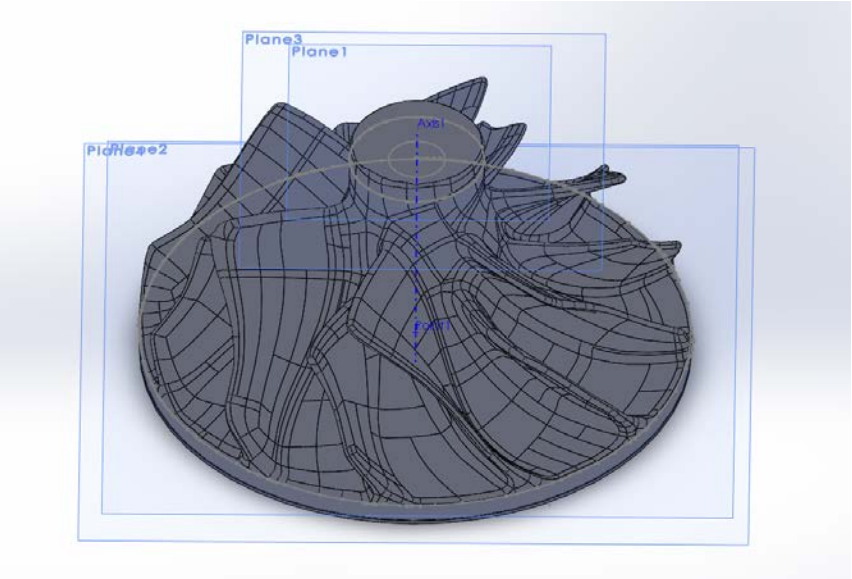

Figure 29. SolidWorks Model of Impeller

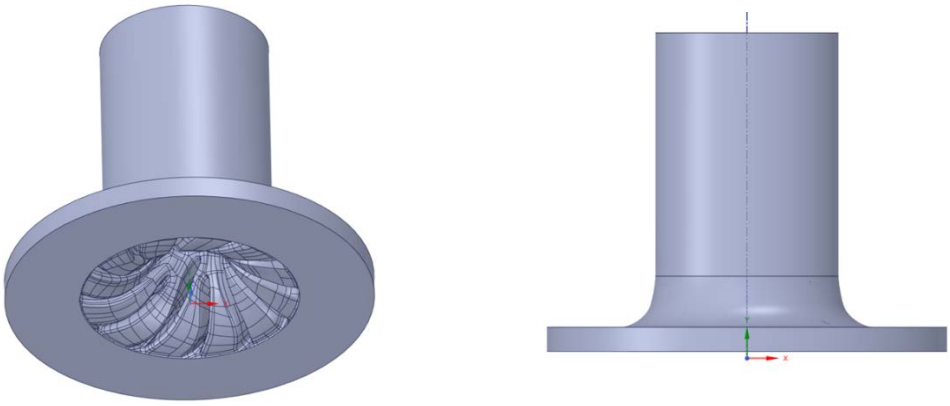

Figure 30. SolidWorks Model of Fluid Flow

Using this SolidWorks model, the ANSYS Workbench software was used to create a Fluid Flow (CFX) simulation of the impeller. Screenshots of the complete input settings for each module can be found in Appendix E.

1. Meshing the Model

Once the SolidWorks Geometry was imported, a mesh of the model was created using the Mesh element of the ANSYS Workbench. Due to the complex geometry of the impeller piece of the fluid flow model, the impeller was selected as the face to build the inflation layer from. Once the mesh of the fluid flow region was complete, the resulting model had 845,683 nodes and 2,096,576 elements. The visual representation of the meshed flow model is shown in Figure 31.

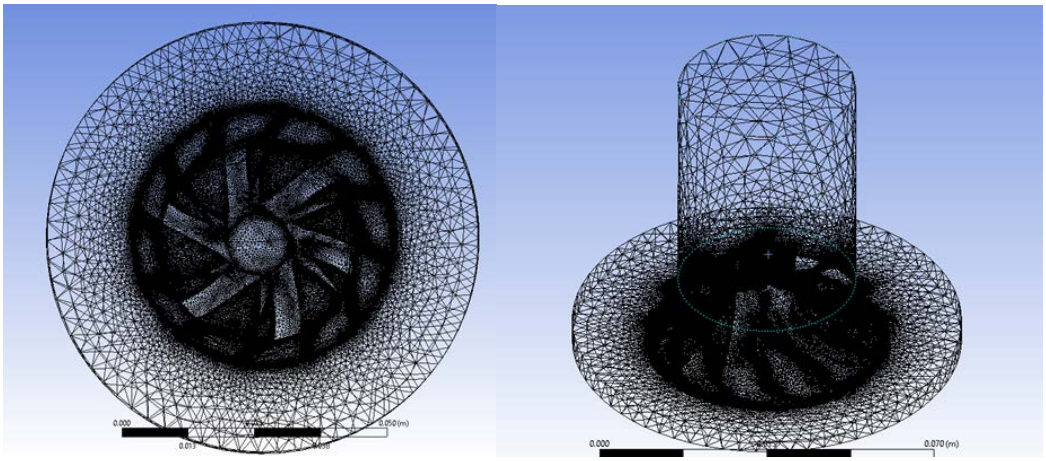

Figure 31. ANSYS Model of Mesh

2. Fluid Flow Setup

Next, the Setup element of the ANSYS Workbench was used to define the conditions of the fluid field model and to set the initial conditions needed for each run of the simulation. Four distinct locations were identified as boundaries. The INLET was designated as the circular surface at the top of the model to allow the fluid to flow down onto the impeller. The OUTLET was designated as the band around the base of the model, to allow flow from the impeller to exit the flow field. The outer casing of the model was designated as the SHROUD and the impeller was designated as the IMPELLER. Figure 32 shows the direction of the flow.

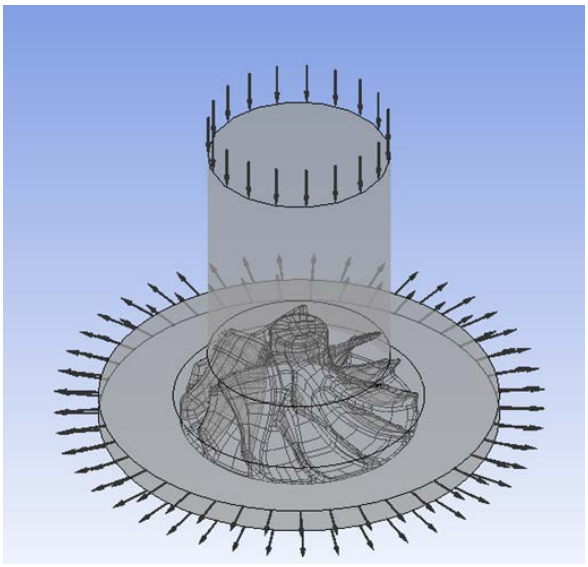

Figure 32. ANSYS Diagram of Fluid Flow through Model

In order to simulate the rotation of the impeller within the fluid flow, the domain was set to rotate, while the SHROUD boundary was designated as a counter rotating wall with a no slip boundary condition. Once a speed was set for the simulation, the relative pressure of the OUTLET was increased from 0 atmospheres (atm) to build the compressor map and force compressor to stall.

3. Solution Element

Once the setup for a run was complete, the Solution element was used to conduct the simulation. For each run, the residuals indicated whether the compressor stalled or not. When the compressor did not stall, the solutions converged and dropped below the set residual threshold as shown on the left of Figure 33. Conversely, if the compressor experienced a stall the solution did not converge, and the residuals did not drop below the threshold, as shown on the right side of Figure 33. After each simulation was conducted, the Results element was used to collect the outcome of the simulation. The data collected from each simulation is shown in Appendix F.

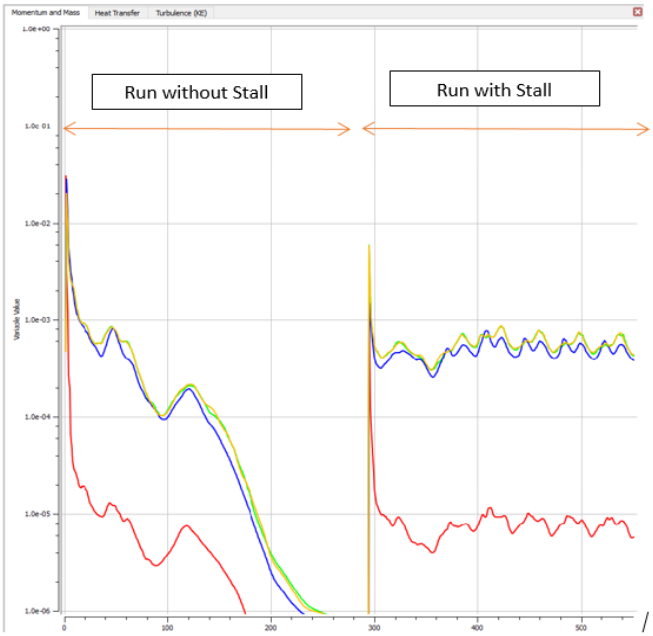

Figure 33. ANSYS Graph of Solution Residuals

4. Model Verification

Before the simulation was conducted with CO_2 as the working fluid, the simulations were conducted using air as the working fluid at 100,000 rotations her minute (RPM). These simulation results were compared to results obtained in previous NPS thesis work conducted by Rivera [11] in 1998. Rivera's thesis conducted experimental runs using the same impeller with air at 100,000 RPM. The pressure ratios and isentropic efficiencies obtained from the CFX model were compared to the results from Rivera, and are shown in Figure 34 and Figure 35.

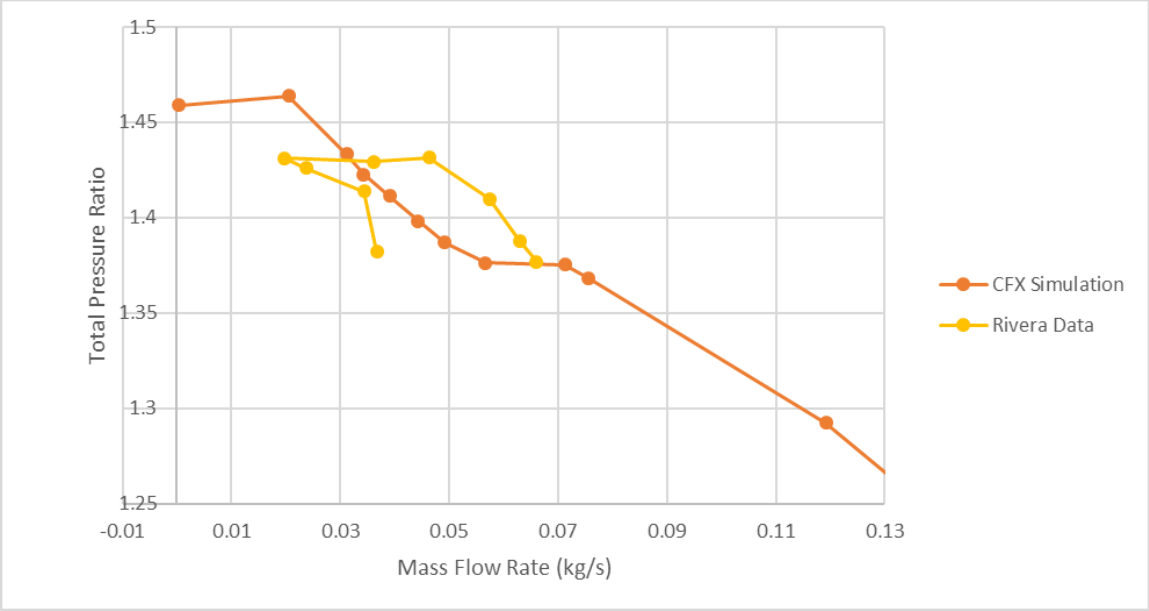

Figure 34. Comparison of Experimental and Simulation Pressure Ratios for Air at 100,000 RPM

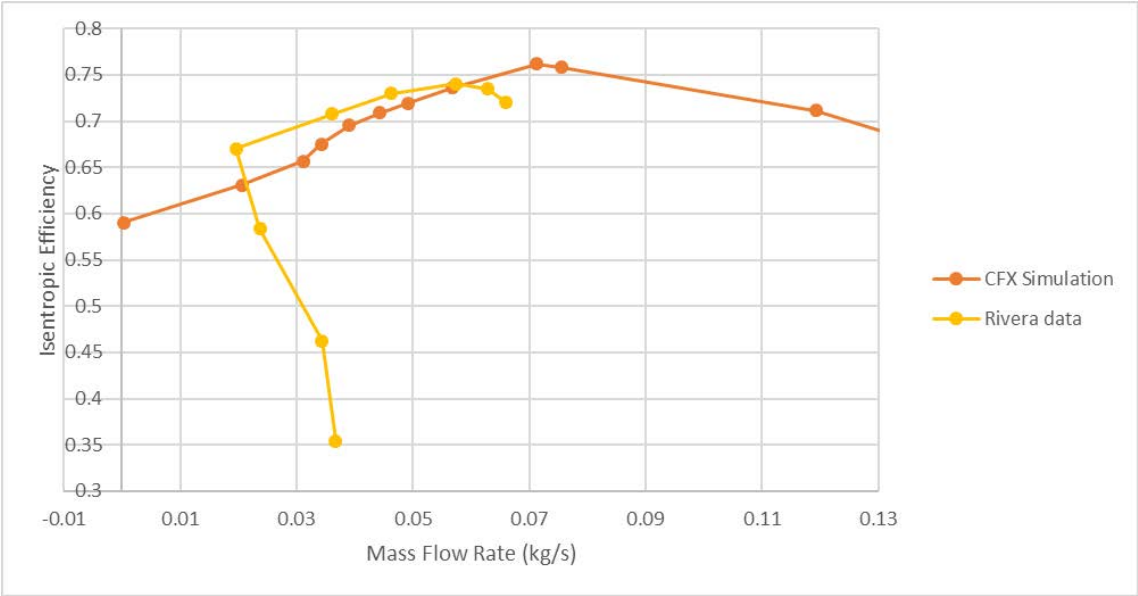

Figure 35. Comparison of Experimental and Simulation Isentropic Efficiencies for Air at 100,000 RPM

The CFX model produced results that were close to the results collected by Rivera. The largest discrepancy occurred in pressure ratio, where the simulated results differed

from the experimental results by 2.7% at a mass flow rate of 0.046 kg/sec. The difference in pressure ratio results was expected because the geometry of the sheath used in experimentation was not the same shape as the sheath used in the simulations, which would result in different back pressures places on the impeller. This analysis verified the CFX model produced results comparable to was could be expected from experimentation.

C. RESULTS OF CO_2 SIMULATIONS

THE CFX model was then used to run simulations using CO_2 at three speeds, 50,000 RPM, 75,000 RPM, and 100,000 RPM. The simulations were run with an initial back pressure of 0 atm and the back pressure was incrementally increased until the CFX model was no longer able to produce a result. The results of the simulations using CO_2 are shown in Figure 36 and Figure 37.

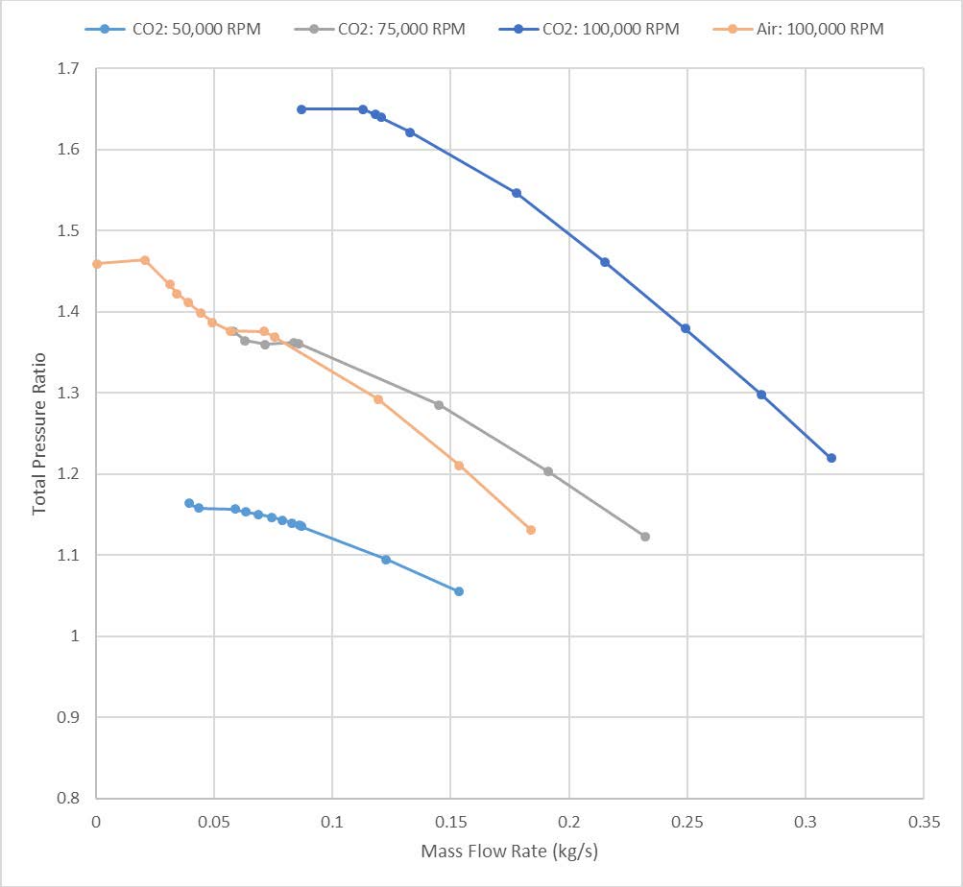

Figure 36. Simulation Pressure Ratios for CO_2

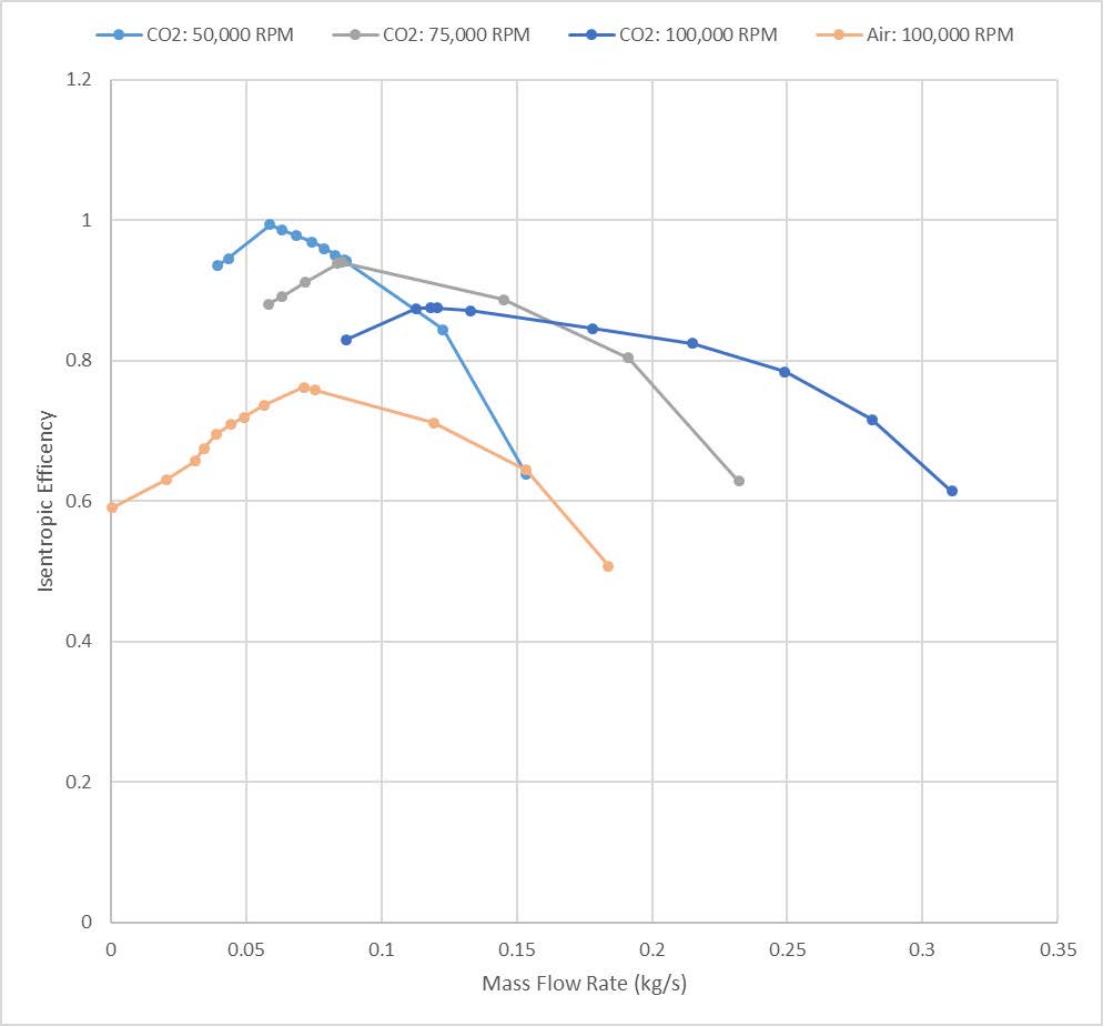

Figure 37. Simulation Isentropic Efficiency for CO_2

The simulations conducted with CO_2 as the working fluid demonstrate CO_2 produces a greater efficiency, mass flow rate, and pressure ratio than using air. The highest pressure ratio and mass flow rates were obtained at 100,000 RPM. For the higher RPM, the isentropic efficiency reached was the lowest. These results demonstrated 100,000 RPM using CO_2 is the ideal configuration for the compressor of the CO_2 loop.

THIS PAGE INTENTIONALLY LEFT BLANK

V. CONCLUSION AND RECOMMENDATIONS FOR FUTURE WORK

A. CONCLUSION

The work outlined in this thesis included the final installation of the Allison T63-A-720 gas turbine, a new data acquisition system for pressure and temperature measurements, new instrumentation, and the establishment of a baseline database for all future activity associated with this engine. Additionally, a prototype heat exchanger design was fabricated and installed onto the engine test rig in order to assess its compatibility with the performance of the engine. This allowed for the study of the effects of the back pressure that the heat exchanger had on the engine and how it will be used for future WHR work. A one-dimensional aero-thermal model of the engine was performed with GasTurb that successfully simulated the off design performance of the engine under all the tests conducted in this project. Finally, validation of the CFX model of the impeller using CO_2 as its fluid medium was confirmed.

B. FUTURE WORK

The back pressure created by the addition of the heat exchanger affected the engine performance at higher N_1 speeds. To reduce this effect, the shape of the upper funnel on the top of the heat exchanger can be modified. Next, the heat exchanger needs to be outfitted with a manifold to run flow through the coils. This manifold needs to include temperature and pressure sensor readings and the ability to manipulate the flow from parallel to series. A preliminary manifold design was included in Polsinelli's [7] thesis. This heat exchanger should then be operated to examine the effects of the flow pattern on the ability to exchange heat.

The back pressure created by the addition of the heat exchanger affected the engine performance at higher N_1 speeds. To reduce this effect, the area ratio of the exhaust nozzle on the top of the heat exchanger needs to be analyzed to minimize the effect of backpressure. Next, the heat exchanger needs to be configured so that CO2 may be fed though it and an initial assessment of performance can be made. This initial configuration

should include a manifold so that flow control, pressure and temperature measurement can be made to aid in the exchanger's performance evaluation. A preliminary manifold design was included in Polsinelli's [7] thesis.

The modelled sheath used for the CO_2 CFX simulations was flat and did not incorporate a scroll. The next step would be to model an updated sheath and run the CFX simulations to analyze the effects of the new shape on backpressure. This analysis can be used to develop the optimal scroll shape for the compressor component of the CO_2 loop.

APPENDIX A. BASELINE DATA FROM SUPERFLOW SYSTEM

Run conducted on 12 October 2018:

Line	TsTim2	EngSpd	N2_RPM	EngTrq	EngPwr	STPPwr	STPTrq
no	second	RPM	RPM	lb-ft	Hp	CHp	Clb-ft
1	0	4020	23436	22.2	17	17.4	22.7
2	-2548.7	3600	20988	135.5	92.9	95.5	139.3
3	-2454.4	4200	24486	116	92.8	95.8	119.8
4	-2372	4800	27984	99.5	90.9	93.9	102.8
5	-2298.2	5390	31423	82.1	84.3	86.8	84.6
6	-2058.4	5410	31540	186.9	192.5	198.5	192.7
7	-1944.3	6010	35038	165.4	189.3	195.3	170.7
8	-1889.4	5990	34921	67.6	77.1	79.4	69.6
9	-1730.2	4800	27984	209.2	191.2	197.3	215.9
10	-1655.9	4200	24486	231.9	185.4	191.4	239.3
11	-1586.9	3700	21571	251.6	177.2	182.9	259.7
12	-1492.2	3600	20988	467.5	320.4	330.7	482.5
13	-1412.5	4200	24486	408.3	326.5	337.6	422.2
14	-1345.4	4800	27984	377.8	345.3	357.1	390.8
15	-1286.4	5400	31482	343.8	353.5	365.5	355.5
16	-1219.5	6000	34980	316.9	362	374.3	327.7

Line	SAEPwr	SAETrq	TsTim2	Fuel A	Air1+2	AirVol	AirCor
no	CHp	Clb-ft	second	lb/hr	scfm	cfm	ratio
1	16.7	21.9	0	71.3	1469	1518.3	0.967
2	91.8	133.9	-2548.7	113.7	2155	2245.3	0.96
3	92.1	115.2	-2454.4	113.4	2131	2241.5	0.951
4	90.3	98.8	-2372	112.9	2132	2242.1	0.951
5	83.5	81.3	-2298.2	111.9	2148	2249.7	0.955
6	190.8	185.3	-2058.4	161.4	2518	2638.1	0.954
7	187.8	164.1	-1944.3	161	2522	2647.9	0.953
8	76.3	66.9	-1889.4	109.6	2172	2271.1	0.956
9	189.7	207.6	-1730.2	161	2524	2649.9	0.953
10	184	230.1	-1655.9	159.2	2534	2659.7	0.953
11	175.9	249.6	-1586.9	157	2537	2662.9	0.953
12	317.9	463.8	-1492.2	258.6	3249	3410.3	0.953
13	324.5	405.8	-1412.5	240.5	3182	3352.8	0.949
14	343.3	375.6	-1345.4	242.4	3182	3353.8	0.949
15	351.3	341.7	-1286.4	241.8	3160	3329.8	0.949
16	359.8	315	-1219.5	242.4	3165	3334.9	0.949

Line	BSFC	BSAC	A/F	FuelSG	AirTmp	Oil In	FuelT
no	lb/hph	lb/hph	Ratio	ratio	degF	degF	degF
1	4.196	395.69	94.3	0.85	70	73	0
2	1.224	106.22	86.77	0.85	74	105	0
3	1.222	105.19	86.04	0.85	79	110	0
4	1.242	107.33	86.45	0.85	79	111	0
5	1.328	116.7	87.87	0.85	77	114	0
6	0.838	59.87	71.42	0.85	77	123	0
7	0.851	61.01	71.73	0.85	78	127	0
8	1.422	128.95	90.71	0.85	76	129	0
9	0.842	60.44	71.78	0.85	78	133	0
10	0.858	62.55	72.86	0.85	78	133	0
11	0.886	65.52	73.97	0.85	78	134	0
12	0.807	46.41	57.51	0.85	78	134	0
13	0.737	44.62	60.57	0.85	80	141	0
14	0.702	42.19	60.1	0.85	80	141	0
15	0.684	40.93	59.84	0.85	80	144	0
16	0.67	40.02	59.78	0.85	80	147	0

Line	AirTmp	Oil In	FuelT	CellT	PwTrl	TC 1	TC 3
no	degF	degF	degF	degF	degF	degF	degF
1	70	73	0	80	1000	80	80
2	74	105	0	100	1070	90	90
3	79	110	0	110	1080	90	90
4	79	111	0	110	1070	90	90
5	77	114	0	110	1070	90	90
6	77	123	0	120	1190	90	90
7	78	127	0	120	1190	100	100
8	76	129	0	120	1030	100	100
9	78	133	0	120	1190	100	100
10	78	133	0	120	1180	100	100
11	78	134	0	120	1160	100	100
12	78	134	0	130	1470	100	100
13	80	141	0	130	1410	100	100
14	80	141	0	140	1420	100	100
15	80	144	0	140	1420	100	100
16	80	147	0	150	1430	100	100

Line	TC 4	TC 5	TC 6	TC 7	Wtr In	WtrOut	OilOut
no	degF	degF	degF	degF	degF	degF	degF
1	80	80	80	80	77	0	0
2	90	90	90	90	75	0	0
3	90	90	90	90	78	0	0
4	90	90	90	90	79	0	0
5	90	90	90	90	80	0	0
6	90	90	90	90	85	0	0
7	100	90	90	90	87	0	0
8	100	100	100	90	85	0	0
9	100	100	100	100	93	0	0
10	100	100	100	100	94	0	0
11	100	100	100	100	97	0	0
12	100	100	100	100	98	0	0
13	100	100	100	100	101	0	0
14	100	100	100	100	102	0	0
15	100	100	100	100	104	0	0
16	100	100	100	100	109	0	0

Line	TsTim2	Oil P	ManPrs	AirTmp	BaroP	VapPrs	AirDen
no	second	psig	inHg	degF	in/Hg	InHg	lb/cFt
1	0	93	0	70	29.91	0.41	0.074
2	-2548.7	90.9	0	74	29.9	0.41	0.073
3	-2454.4	90.4	0	79	29.9	0.41	0.072
4	-2372	91.7	0	79	29.9	0.41	0.072
5	-2298.2	92.1	0	77	29.91	0.41	0.073
6	-2058.4	92.2	0	77	29.9	0.41	0.073
7	-1944.3	93.3	0	78	29.9	0.41	0.072
8	-1889.4	92.6	0	76	29.9	0.41	0.073
9	-1730.2	93.9	0	78	29.9	0.41	0.072
10	-1655.9	94	0	78	29.9	0.41	0.072
11	-1586.9	93.6	0	78	29.9	0.41	0.072
12	-1492.2	95	0	78	29.9	0.41	0.072
13	-1412.5	94.4	0	80	29.9	0.41	0.072
14	-1345.4	94.7	0	80	29.89	0.41	0.072
15	-1286.4	95.9	0	80	29.9	0.41	0.072
16	-1219.5	96.8	0	80	29.9	0.41	0.072

Line no	AirCor ratio	SAECor Factor	STPCor Factor	TsTim2 second	EngSpd RPM	Speed RPM
1	0.967	0.984	1.024	0	4020	4010
2	0.96	0.988	1.028	-2548.7	3600	3600
3	0.951	0.993	1.033	-2454.4	4200	4190
4	0.951	0.993	1.033	-2372	4800	4780
5	0.955	0.991	1.031	-2298.2	5390	5390
6	0.954	0.991	1.031	-2058.4	5410	5400
7	0.953	0.992	1.032	-1944.3	6010	6020
8	0.956	0.99	1.03	-1889.4	5990	5980
9	0.953	0.992	1.032	-1730.2	4800	4810
10	0.953	0.992	1.032	-1655.9	4200	4200
11	0.953	0.992	1.032	-1586.9	3700	3700
12	0.953	0.992	1.032	-1492.2	3600	3600
13	0.949	0.994	1.034	-1412.5	4200	4210
14	0.949	0.994	1.034	-1345.4	4800	4800
15	0.949	0.994	1.034	-1286.4	5400	5390
16	0.949	0.994	1.034	-1219.5	6000	6000

Run conducted on 15 October 2018:

Line	TsTim2	EngSpd	N2_RPM	EngTrq	EngPwr	STPPwr	STPTrq
no	second	RPM	RPM	lb-ft	Hp	CHp	Clb-ft
1	0	4080	23786	23.3	18.1	18.3	23.6
2	148.9	3600	20988	136.9	93.8	95.3	139
3	228.2	4200	24486	118.1	94.4	96	120
4	327.8	4800	27984	101.5	92.8	94.4	103.3
5	413	5400	31482	84.1	86.5	88.1	85.7
6	479.1	6000	34980	65.9	75.3	76.7	67.1
7	571.3	6000	34980	169.5	193.6	197.2	172.6
8	665.6	5400	31482	191.9	197.3	200.6	195.1
9	778.7	4800	27984	216.2	197.6	201	220
10	861.2	4200	24486	239.4	191.4	194.8	243.6
11	949.4	3600	20988	260.7	178.7	182.1	265.7
12	1025.2	3590	20930	462.2	315.9	322	471.1
13	1106.1	4200	24486	403.1	322.4	329.8	412.4
14	1193.9	4800	27984	384.3	351.2	358.8	392.6
15	1255.4	5400	31482	351.4	361.3	369.1	359
16	1329.1	6000	34980	330.3	377.3	385.7	337.6

Line	SAEPwr	SAETrq	TsTim2	Fuel A	Air1+2	AirVol	AirCor
no	CHp	Clb-ft	second	lb/hr	scfm	cfm	ratio
1	17.6	22.7	0	71.4	1506	1539.8	0.978
2	91.6	133.6	148.9	114.1	2178	2238	0.973
3	92.3	115.4	228.2	113.7	2162	2227	0.971
4	90.7	99.3	327.8	113.5	2175	2244.5	0.969
5	84.7	82.4	413	113.7	2163	2240.8	0.965
6	73.7	64.5	479.1	111.5	2175	2248.5	0.967
7	189.6	165.9	571.3	164.3	2538	2624.2	0.967
8	192.8	187.5	665.6	162.2	2560	2636.6	0.971
9	193.3	211.5	778.7	163.1	2556	2638.1	0.969
10	187.2	234.1	861.2	161.7	2566	2647.9	0.969
11	175.1	255.5	949.4	158.2	2557	2648.6	0.965
12	309.6	452.9	1025.2	254.3	3239	3355.4	0.965
13	317	396.5	1106.1	239.6	3177	3315.8	0.958
14	344.9	377.4	1193.9	245.5	3221	3350.1	0.962
15	354.8	345.1	1255.4	244.5	3220	3349.4	0.962
16	370.8	324.6	1329.1	252	3244	3378.7	0.96

Line	BSFC	BSAC	A/F	FuelSG	AirTmp	Oil In	FuelT
no	lb/hph	lb/hph	Ratio	ratio	degF	degF	degF
1	3.945	380.95	96.57	0.85	70	80	0
2	1.216	106.24	87.37	0.85	73	93	0
3	1.204	104.8	87.05	0.85	74	99	0
4	1.224	107.34	87.73	0.85	75	103	0
5	1.315	114.53	87.1	0.85	77	108	0
6	1.481	132.25	89.29	0.85	76	111	0
7	0.848	60.01	70.72	0.85	76	115	0
8	0.822	59.39	72.25	0.85	74	121	0
9	0.825	59.23	71.75	0.85	75	126	0
10	0.845	61.36	72.64	0.85	75	128	0
11	0.885	65.51	73.99	0.85	77	128	0
12	0.805	46.94	58.32	0.85	77	130	0
13	0.743	45.13	60.71	0.85	81	134	0
14	0.699	41.99	60.07	0.85	79	136	0
15	0.677	40.81	60.3	0.85	79	141	0
16	0.668	39.35	58.93	0.85	80	145	0

Line	CellT	PwTrl	TC 1	TC 3	TC 4	TC 5	TC 6
no	degF	degF	degF	degF	degF	degF	degF
1	80	990	80	80	80	80	80
2	90	1060	80	80	80	80	80
3	90	1070	80	80	80	80	80
4	100	1070	80	80	80	80	80
5	100	1070	80	80	80	80	80
6	110	1060	80	80	80	80	80
7	110	1200	80	80	80	80	80
8	120	1200	80	90	80	80	90
9	120	1190	90	90	90	90	90
10	120	1180	90	90	90	90	90
11	130	1160	90	90	90	90	90
12	130	1450	90	90	90	90	90
13	140	1410	90	90	90	90	90
14	150	1420	90	90	90	90	90
15	160	1430	90	90	90	90	90
16	160	1450	90	90	90	90	90

Line	TC 7	Wtr In	WtrOut	OilOut	TsTim2	Oil P	ManPrs
no	degF	degF	degF	degF	second	psig	inHg
1	80	0	0	0	0	89.7	-0.6
2	80	0	0	0	148.9	92.7	-0.6
3	80	0	0	0	228.2	91.5	-0.6
4	80	0	0	0	327.8	91	-0.6
5	80	0	0	0	413	92.3	-0.6
6	80	0	0	0	479.1	92.6	-0.6
7	80	0	0	0	571.3	91.6	-0.6
8	80	0	0	0	665.6	93	-0.6
9	90	0	0	0	778.7	93.6	-0.6
10	90	0	0	0	861.2	93.7	-0.6
11	90	0	0	0	949.4	93.9	-0.6
12	90	0	0	0	1025.2	94.6	-0.5
13	90	0	0	0	1106.1	94.7	-0.6
14	90	0	0	0	1193.9	95	-0.6
15	90	0	0	0	1255.4	95.4	-0.6
16	90	0	0	0	1329.1	96.3	-0.6

Line	AirTmp	BaroP	VapPrs	AirDen	AirCor	SAECor	STPCor
no	degF	in/Hg	InHg	lb/cFt	ratio	Factor	Factor
1	70	30.15	0.32	0.074	0.978	0.973	1.013
2	73	30.16	0.32	0.074	0.973	0.976	1.015
3	74	30.15	0.32	0.074	0.971	0.977	1.016
4	75	30.15	0.32	0.074	0.969	0.978	1.017
5	77	30.15	0.32	0.073	0.965	0.98	1.019
6	76	30.15	0.32	0.074	0.967	0.979	1.018
7	76	30.15	0.32	0.074	0.967	0.979	1.018
8	74	30.15	0.32	0.074	0.971	0.977	1.016
9	75	30.15	0.32	0.074	0.969	0.978	1.017
10	75	30.15	0.32	0.074	0.969	0.978	1.017
11	77	30.15	0.32	0.073	0.965	0.98	1.019
12	77	30.15	0.32	0.073	0.965	0.98	1.019
13	81	30.15	0.32	0.073	0.958	0.984	1.023
14	79	30.14	0.32	0.073	0.962	0.982	1.022
15	79	30.14	0.32	0.073	0.962	0.982	1.022
16	80	30.15	0.32	0.073	0.96	0.983	1.022

Line	TsTim2	EngSpd	Speed
no	second	RPM	RPM
1	0	4080	4080
2	148.9	3600	3610
3	228.2	4200	4200
4	327.8	4800	4820
5	413	5400	5420
6	479.1	6000	6010
7	571.3	6000	6010
8	665.6	5400	5380
9	778.7	4800	4800
10	861.2	4200	4200
11	949.4	3600	3600
12	1025.2	3590	3590
13	1106.1	4200	4200
14	1193.9	4800	4800
15	1255.4	5400	5390
16	1329.1	6000	6010

Run conducted on 01 November 2018:

Line	TsTim2	EngSpd	N2_RPM	EngTrq	EngPwr	STPPwr	STPTrq
no	second	RPM	RPM	lb-ft	Hp	CHp	Clb-ft
1	0	4070	23728	23.4	18.1	18.4	23.7
2	-3461.5	3590	20930	157.4	107.6	109	159.4
3	-3362.6	4200	24486	131.3	105	108	135
4	-3273.1	4800	27984	108.3	99	101.2	110.7
5	-3190.7	5400	31482	97.7	100.5	103.6	100.8
6	-3098.4	6010	35038	70.1	80.2	82.3	71.9
7	-3003.4	6000	34980	162.9	186.1	191.5	167.6
8	-2894.4	5400	31482	162.8	167.4	175.3	170.5
9	-2822.9	4800	27984	205.4	187.7	193.5	211.7
10	-2732.2	4210	24544	212.1	170	177.8	221.8
11	-2640	3600	20988	228.9	156.9	162.8	237.5
12	-2572.8	3600	20988	416.9	285.8	298.8	436
13	-2497.7	4200	24486	390.6	312.4	322.9	403.8
14	-2410.1	4800	27984	328	299.8	319.8	349.9
15	-2299	5410	31540	303.4	312.5	328.8	319.2
16	-2230.3	6000	34980	306	349.6	364	318.6

Line	SAEPwr	SAETrq	TsTim2	Fuel A	Air1+2	AirVol	AirCor
no	CHp	Clb-ft	second	lb/hr	scfm	cfm	ratio
1	17.6	22.8	0	64.2	1519	1551.8	0.979
2	104.8	153.3	-3461.5	107.2	2243	2296.1	0.977
3	103.8	129.8	-3362.6	106.4	2179	2298.2	0.948
4	97.3	106.4	-3273.1	104.5	2232	2327.2	0.959
5	99.6	96.9	-3190.7	105.9	2182	2317.1	0.942
6	79.1	69.2	-3098.4	101.3	2239	2352.7	0.952
7	184.1	161.1	-3003.4	141.7	2507	2648.1	0.947
8	168.5	163.9	-2894.4	135.5	2452	2680.8	0.915
9	186	203.6	-2822.9	140.4	2518	2669.5	0.943
10	170.9	213.2	-2732.2	135.6	2465	2688.9	0.917
11	156.5	228.3	-2640	132.5	2570	2759.5	0.931
12	287.3	419.1	-2572.8	206.8	3098	3380.5	0.917
13	310.4	388.2	-2497.7	204.7	3208	3419.7	0.938
14	307.4	336.4	-2410.1	197.5	3171	3600.8	0.881
15	316.1	306.9	-2299	199.3	3331	3678.7	0.905
16	349.9	306.3	-2230.3	210.2	3393	3669.3	0.925

Line	BSFC	BSAC	A/F	FuelSG	AirTmp	Oil In	FuelT
no	lb/hph	lb/hph	Ratio	ratio	degF	degF	degF
1	3.54	383.48	108.32	0.75	70	72	0
2	0.996	95.45	95.8	0.75	71	85	0
3	1.013	95	93.75	0.75	87	93	0
4	1.056	103.22	97.76	0.75	81	100	0
5	1.054	99.42	94.31	0.75	91	105	0
6	1.263	127.81	101.21	0.75	85	110	0
7	0.761	61.67	80.99	0.75	88	114	0
8	0.81	67.06	82.84	0.75	107	120	0
9	0.748	61.41	82.1	0.75	90	124	0
10	0.798	66.36	83.21	0.75	106	124	0
11	0.844	74.99	88.8	0.75	97	125	0
12	0.724	49.64	68.59	0.75	106	127	0
13	0.655	47.02	71.75	0.75	93	131	0
14	0.659	48.43	73.51	0.75	129	133	0
15	0.638	48.79	76.5	0.75	113	140	0
16	0.601	44.44	73.9	0.75	101	143	0

LineNo	CellT	PwTrl	TC 1	TC 3	TC 4	TC 5	TC 6
	degF	degF	degF	degF	degF	degF	degF
1	80	1010	70	70	70	70	70
2	90	1070	80	70	70	70	80
3	100	1120	80	80	80	80	80
4	120	1120	80	80	80	80	80
5	130	1100	80	80	80	80	80
6	140	1110	80	80	80	80	80
7	150	1200	80	80	80	80	80
8	200	1260	80	80	80	80	80
9	200	1200	90	90	90	90	90
10	220	1220	90	90	90	90	90
11	220	1210	90	90	90	90	90
12	220	1430	90	100	90	90	90
13	220	1410	100	100	100	100	100
14	280	1460	100	100	100	100	100
15	280	1450	100	100	100	100	100
16	270	1450	110	110	110	110	110

LineNo	TC 7	Wtr In	WtrOut	OilOut	TsTim2	Oil P	ManPrs
	degF	degF	degF	degF	second	psig	inHg
1	70	0	0	0	0	91.3	0
2	70	0	0	0	-3461.5	89.4	0
3	80	0	0	0	-3362.6	91.3	0
4	80	0	0	0	-3273.1	91.4	0
5	80	0	0	0	-3190.7	91.5	0
6	80	0	0	0	-3098.4	92.6	0
7	80	0	0	0	-3003.4	90.5	0
8	80	0	0	0	-2894.4	91.7	0
9	90	0	0	0	-2822.9	92	0
10	90	0	0	0	-2732.2	92.4	0
11	90	0	0	0	-2640	92	0
12	100	0	0	0	-2572.8	92.9	0
13	100	0	0	0	-2497.7	93	0
14	100	0	0	0	-2410.1	92.4	0
15	100	0	0	0	-2299	94.3	0
16	110	0	0	0	-2230.3	94.9	0

LineNo	AirTmp	BaroP	VapPrs	AirDen	AirCor	SAECor	STPCor
	degF	in/Hg	InHg	lb/cFt	ratio	Factor	Factor
1	70	30.15	0.3	0.074	0.979	0.973	1.012
2	71	30.15	0.3	0.074	0.977	0.974	1.013
3	87	30.14	0.3	0.072	0.948	0.989	1.028
4	81	30.15	0.3	0.073	0.959	0.983	1.022
5	91	30.15	0.3	0.072	0.942	0.992	1.032
6	85	30.15	0.3	0.072	0.952	0.987	1.026
7	88	30.15	0.3	0.072	0.947	0.989	1.029
8	107	30.14	0.3	0.07	0.915	1.007	1.047
9	90	30.15	0.3	0.072	0.943	0.991	1.031
10	106	30.15	0.3	0.07	0.917	1.005	1.046
11	97	30.15	0.3	0.071	0.931	0.997	1.037
12	106	30.15	0.3	0.07	0.917	1.005	1.046
13	93	30.15	0.3	0.071	0.938	0.994	1.034
14	129	30.15	0.3	0.067	0.881	1.026	1.067
15	113	30.15	0.3	0.069	0.905	1.012	1.052
16	101	30.15	0.3	0.07	0.925	1.001	1.041

LineNo	TsTim2	EngSpd	Speed
	second	RPM	RPM
1	0	4070	4080
2	-3461.5	3590	3590
3	-3362.6	4200	4200
4	-3273.1	4800	4820
5	-3190.7	5400	5400
6	-3098.4	6010	6010
7	-3003.4	6000	6000
8	-2894.4	5400	5400
9	-2822.9	4800	4800
10	-2732.2	4210	4210
11	-2640	3600	3610
12	-2572.8	3600	3600
13	-2497.7	4200	4220
14	-2410.1	4800	4800
15	-2299	5410	5420
16	-2230.3	6000	6000

Run conducted on 08 November 2018:

Line	TsTim2	EngSpd	N2_RPM	EngTrq	EngPwr	STPPwr	STPTrq
no	second	RPM	RPM	lb-ft	Hp	CHp	Clb-ft
1	0	4140	24136	23.9	18.8	18.9	24
2	-1854.4	3600	20988	139.9	95.9	96.3	140.5
3	-1754.3	4200	24486	122.3	97.8	98.3	122.9
4	-1645	4800	27984	103.7	94.8	95.3	104.3
5	-1529.5	5400	31482	87.3	89.8	90.4	87.9
6	-1421.8	6000	34980	69.7	79.6	80.2	70.2
7	-1331	6000	34980	176.7	201.9	203.4	178
8	-1234.3	5400	31482	200.1	205.7	207.2	201.5
9	-1171.7	4790	27925	222.2	202.7	204.3	224
10	-1109.8	4200	24486	244.8	195.8	197.1	246.4
11	-1033.9	3600	20988	268	183.7	185.2	270.1
12	-952.4	3600	20988	469.1	321.5	324.1	472.8
13	-860.2	4200	24486	421.2	336.8	340.4	425.7
14	-780.8	4800	27984	394.3	360.4	363.6	397.8
15	-716.4	5400	31482	365.6	375.9	379.1	368.7
16	-640.2	6000	34980	338.2	386.4	390.3	341.6

Line	SAEPwr	SAETrq	TsTim2	Fuel A	Air1+2	AirVol	AirCor
no	CHp	Clb-ft	second	lb/hr	scfm	cfm	ratio
1	18.2	23	0	64.2	1559	1568.1	0.994
2	92.6	135	-1854.4	0	2227	2248.7	0.99
3	94.5	118.1	-1754.3	0	2221	2246	0.989
4	91.7	100.3	-1645	0	2215	2245.5	0.986
5	86.9	84.5	-1529.5	0	2219	2254.1	0.985
6	77.1	67.5	-1421.8	0	2230	2264.9	0.985
7	195.5	171.2	-1331	0	2596	2641.1	0.983
8	199.2	193.7	-1234.3	0	2609	2649.6	0.985
9	196.4	215.3	-1171.7	0	2605	2650.7	0.983
10	189.4	236.9	-1109.8	0	2618	2657.9	0.985
11	178	259.7	-1033.9	0	2616	2662	0.983
12	311.6	454.5	-952.4	0	3300	3357.8	0.983
13	327.3	409.3	-860.2	0	3271	3347	0.977
14	349.5	382.4	-780.8	0	3309	3373.9	0.981
15	364.4	354.5	-716.4	0	3309	3371.9	0.981
16	375.2	328.4	-640.2	0	3310	3381.5	0.979

LineNo	BSFC	BSAC	A/F	FuelSG	AirTmp	Oil In	FuelT
	lb/hph	lb/hph	Ratio	ratio	degF	degF	degF
1	3.408	378.76	111.15	0.75	64	66	0
2	0	106.31	0	0.75	66	79	0
3	0	103.94	0	0.75	67	91	0
4	0	107	0	0.75	68	99	0
5	0	113.2	0	0.75	69	104	0
6	0	128.22	0	0.75	69	109	0
7	0	58.88	0	0.75	70	112	0
8	0	58.05	0	0.75	69	117	0
9	0	58.85	0	0.75	70	121	0
10	0	61.22	0	0.75	69	121	0
11	0	65.2	0	0.75	70	124	0
12	0	46.98	0	0.75	70	125	0
13	0	44.45	0	0.75	73	128	0
14	0	42.04	0	0.75	71	132	0
15	0	40.3	0	0.75	71	135	0
16	0	39.21	0	0.75	72	139	0

LineNo	CellT	PwTrl	TC 1	TC 3	TC 4	TC 5	TC 6
	degF	degF	degF	degF	degF	degF	degF
1	70	980	70	70	70	70	70
2	70	1050	70	70	70	70	70
3	70	1060	70	70	70	70	70
4	70	1060	70	70	70	70	70
5	80	1050	80	80	80	80	80
6	80	1040	80	80	80	80	80
7	80	1180	80	80	80	80	80
8	80	1190	80	80	80	80	80
9	80	1180	80	80	80	80	80
10	80	1170	80	80	80	80	80
11	80	1160	80	80	80	80	80
12	80	1440	80	80	80	80	80
13	80	1400	90	90	80	90	90
14	90	1420	90	90	90	90	90
15	90	1430	90	90	90	90	90
16	90	1440	90	90	90	90	90

LineNo	TC 7	Wtr In	WtrOut	OilOut	TsTim2	Oil P	ManPrs
	degF	degF	degF	degF	second	psig	inHg
1	70	0	0	0	0	92.3	0
2	70	0	0	0	-1854.4	88.9	0
3	70	0	0	0	-1754.3	91.3	0
4	70	0	0	0	-1645	90.9	0
5	80	0	0	0	-1529.5	90.7	0
6	80	0	0	0	-1421.8	91.8	0
7	80	0	0	0	-1331	92.2	0
8	80	0	0	0	-1234.3	91.1	0
9	80	0	0	0	-1171.7	91.7	0
10	80	0	0	0	-1109.8	92	0
11	80	0	0	0	-1033.9	92	0
12	80	0	0	0	-952.4	93.9	0
13	90	0	0	0	-860.2	93.9	0
14	90	0	0	0	-780.8	94.2	0
15	90	0	0	0	-716.4	94.3	0
16	90	0	0	0	-640.2	94.4	0

LineNo	AirTmp	BaroP	VapPrs	AirDen	AirCor	SAECor	STPCor
	degF	in/Hg	InHg	lb/cFt	ratio	Factor	Factor
1	64	30.11	0.14	0.076	0.994	0.963	1.002
2	66	30.11	0.14	0.075	0.99	0.965	1.004
3	67	30.12	0.14	0.075	0.989	0.966	1.005
4	68	30.11	0.14	0.075	0.986	0.967	1.006
5	69	30.11	0.14	0.075	0.985	0.968	1.007
6	69	30.11	0.14	0.075	0.985	0.968	1.007
7	70	30.12	0.14	0.075	0.983	0.969	1.008
8	69	30.11	0.14	0.075	0.985	0.968	1.007
9	70	30.11	0.14	0.075	0.983	0.969	1.008
10	69	30.12	0.14	0.075	0.985	0.968	1.007
11	70	30.11	0.14	0.075	0.983	0.969	1.008
12	70	30.11	0.14	0.075	0.983	0.969	1.008
13	73	30.11	0.14	0.074	0.977	0.972	1.011
14	71	30.11	0.14	0.075	0.981	0.97	1.009
15	71	30.12	0.14	0.075	0.981	0.97	1.009
16	72	30.1	0.14	0.074	0.979	0.971	1.01

LineNo	TsTim2	EngSpd	Speed
	second	RPM	RPM
1	0	4140	4140
2	-1854.4	3600	3600
3	-1754.3	4200	4190
4	-1645	4800	4800
5	-1529.5	5400	5390
6	-1421.8	6000	6000
7	-1331	6000	6010
8	-1234.3	5400	5400
9	-1171.7	4790	4800
10	-1109.8	4200	4200
11	-1033.9	3600	3610
12	-952.4	3600	3590
13	-860.2	4200	4210
14	-780.8	4800	4800
15	-716.4	5400	5400
16	-640.2	6000	6000

Run conducted on 19 November 2018:

Line	TsTim2	EngSpd	N2_RPM	EngTrq	EngPwr	STPPwr	STPTrq
no	second	RPM	RPM	lb-ft	Hp	CHp	Clb-ft
1	420.7	4090	23845	31.4	24.5	24.7	31.8
2	507.1	3600	20988	148.5	101.8	103	150.2
3	571.2	4210	24544	130.6	104.7	106.1	132.4
4	705.4	4800	27984	113.7	103.9	105.4	115.4
5	795.4	5410	31540	96.2	99.1	100.4	97.5
6	870.8	6000	34980	78	89.1	90.5	79.2
7	955.4	5990	34921	184.9	210.9	214.1	187.7
8	1056.6	5400	31482	205.7	211.5	214.9	209
9	1117.1	4800	27984	228.5	208.8	212.2	232.2
10	1176.9	4210	24544	249.7	200.2	203.6	254
11	1243.2	3600	20988	275	188.5	191.7	279.7
12	1304.4	3600	20988	464.6	318.5	323.9	472.5
13	1416.2	4200	24486	426.9	341.4	347.5	434.6
14	1481.1	4800	27984	398.8	364.5	370.7	405.6
15	1537.7	5400	31482	369.4	379.8	386.3	375.7
16	1592.4	5990	34921	343.2	391.4	398.5	349.4

Line	SAEPwr	SAETrq	TsTim2	Fuel A	Air1+2	AirVol	AirCor
no	CHp	Clb-ft	second	lb/hr	scfm	cfm	ratio
1	23.8	30.5	420.7	62	1536	1559.6	0.985
2	99	144.4	507.1	101.5	2228	2262.7	0.985
3	102	127.3	571.2	100.9	2224	2267.1	0.981
4	101.3	110.9	705.4	100.9	2224	2271.7	0.979
5	96.6	93.7	795.4	100.3	2232	2275.8	0.981
6	87	76.1	870.8	99.5	2229	2281.3	0.977
7	205.8	180.4	955.4	145.6	2600	2659.7	0.978
8	206.6	200.9	1056.6	144.7	2605	2669.3	0.976
9	204	223.2	1117.1	144.1	2609	2673.6	0.976
10	195.7	244.1	1176.9	142.1	2604	2673.9	0.974
11	184.3	268.9	1243.2	140.8	2606	2675.8	0.974
12	311.4	454.3	1304.4	219.6	3253	3340	0.974
13	334.1	417.8	1416.2	214.2	3272	3366.4	0.972
14	356.4	389.9	1481.1	217.9	3292	3380.5	0.974
15	371.4	361.2	1537.7	219.5	3288	3375.7	0.974
16	383.1	335.9	1592.4	222.2	3288	3382.4	0.972

Line	BSFC	BSAC	A/F	FuelSG	AirTmp	Oil In	FuelT
no	lb/hph	lb/hph	Ratio	ratio	degF	degF	degF
1	2.536	287.62	113.44	0.75	64	95	0
2	0.997	100.21	100.5	0.75	64	96	0
3	0.964	97.25	100.91	0.75	66	100	0
4	0.971	97.99	100.92	0.75	67	102	0
5	1.012	103.14	101.9	0.75	66	105	0
6	1.117	114.54	102.58	0.75	68	107	0
7	0.69	56.45	81.75	0.75	68	111	0
8	0.684	56.38	82.4	0.75	69	116	0
9	0.69	57.19	82.88	0.75	69	118	0
10	0.71	59.56	83.89	0.75	70	119	0
11	0.747	63.29	84.73	0.75	70	121	0
12	0.69	46.76	67.81	0.75	70	115	0
13	0.627	43.88	69.94	0.75	71	126	0
14	0.598	41.35	69.17	0.75	70	130	0
15	0.578	39.63	68.57	0.75	70	134	0
16	0.568	38.46	67.74	0.75	71	137	0

Line	CellT	PwTrl	TC 1	TC 3	TC 4	TC 5	TC 6
no	degF	degF	degF	degF	degF	degF	degF
1	70	970	80	80	80	80	80
2	70	1040	80	80	80	80	80
3	80	1050	80	80	80	80	80
4	80	1050	80	80	80	80	80
5	80	1040	80	80	80	80	80
6	80	1030	80	80	80	80	80
7	80	1180	80	80	90	80	80
8	80	1180	90	90	90	90	90
9	80	1170	90	90	90	90	90
10	80	1160	90	90	90	90	90
11	80	1150	90	90	90	90	90
12	80	1410	90	90	90	90	90
13	90	1410	90	90	90	90	90
14	90	1410	90	90	90	90	90
15	90	1420	90	90	90	90	90
16	90	1430	90	90	90	90	90

Line	TC 7	Wtr In	WtrOut	OilOut	TsTim2	Oil P	ManPrs
no	degF	degF	degF	degF	second	psig	inHg
1	80	0	0	0	420.7	88.2	0
2	80	0	0	0	507.1	90	0
3	80	0	0	0	571.2	92.2	0
4	80	0	0	0	705.4	90	0
5	80	0	0	0	795.4	90.7	0
6	80	0	0	0	870.8	92.9	0
7	80	0	0	0	955.4	89.7	0
8	90	0	0	0	1056.6	90.8	0
9	90	0	0	0	1117.1	91.9	0
10	90	0	0	0	1176.9	91.3	0
11	90	0	0	0	1243.2	90.5	0
12	90	0	0	0	1304.4	93.3	0
13	90	0	0	0	1416.2	93.2	0
14	90	0	0	0	1481.1	93.5	0
15	90	0	0	0	1537.7	94	0
16	90	0	0	0	1592.4	94.7	0

Line	AirTmp	BaroP	VapPrs	AirDen	AirCor	SAECor	STPCor
no	degF	in/Hg	InHg	lb/cFt	ratio	Factor	Factor
1	64	29.99	0.29	0.075	0.985	0.972	1.011
2	64	29.98	0.29	0.075	0.985	0.973	1.012
3	66	29.98	0.29	0.075	0.981	0.974	1.014
4	67	29.98	0.29	0.074	0.979	0.975	1.015
5	66	29.98	0.29	0.075	0.981	0.974	1.014
6	68	29.98	0.29	0.074	0.977	0.976	1.015
7	68	29.99	0.29	0.074	0.978	0.976	1.015
8	69	29.99	0.29	0.074	0.976	0.977	1.016
9	69	29.99	0.29	0.074	0.976	0.977	1.016
10	70	29.99	0.29	0.074	0.974	0.978	1.017
11	70	29.99	0.29	0.074	0.974	0.978	1.017
12	70	29.99	0.29	0.074	0.974	0.978	1.017
13	71	29.99	0.29	0.074	0.972	0.979	1.018
14	70	29.99	0.29	0.074	0.974	0.978	1.017
15	70	29.99	0.29	0.074	0.974	0.978	1.017
16	71	29.99	0.29	0.074	0.972	0.979	1.018

Line	TsTim2	EngSpd	Speed
no	second	RPM	RPM
1	420.7	4090	4090
2	507.1	3600	3600
3	571.2	4210	4210
4	705.4	4800	4800
5	795.4	5410	5400
6	870.8	6000	6010
7	955.4	5990	5990
8	1056.6	5400	5410
9	1117.1	4800	4800
10	1176.9	4210	4210
11	1243.2	3600	3610
12	1304.4	3600	3580
13	1416.2	4200	4210
14	1481.1	4800	4810
15	1537.7	5400	5400
16	1592.4	5990	5990

Run conducted on 20 November 2018:

Line	SAEPwr	SAETrq	TsTim2	Fuel A	Air1+2	AirVol	AirCor
no	CHp	Clb-ft	second	lb/hr	scfm	cfm	ratio
1	24.2	30.8	0	65.6	1516	1539.7	0.985
2	99	144.8	1238.8	100.1	2197	2243.6	0.979
3	103	128.8	1361.9	101.9	2201	2249	0.978
4	100.3	109.8	-2118.3	101	2197	2244.2	0.979
5	93.5	90.8	-2014.2	99.9	2182	2241.8	0.973
6	84.6	73.9	-1898.9	98.7	2186	2249.8	0.972
7	182.1	265.7	-1751.6	141	2572	2647.3	0.972
8	193.7	242.3	-1641.8	142.4	2580	2649.7	0.974
9	201.7	220.6	-1574.1	144.1	2566	2641.7	0.971
10	206.5	200.8	-1456.1	145.1	2571	2647.7	0.971
11	205.7	180	-1357.5	145.2	2580	2650.6	0.973
12	270	393.9	-1147.1	190.2	3053	3159.1	0.966
13	298.6	373.4	-967.9	195.9	3107	3221.1	0.964
14	315	306.4	-739.3	193.6	3057	3164.8	0.966
15	318.3	278.7	-665.4	193.4	3047	3148.5	0.968

Line	BSFC	BSAC	A/F	FuelSG	AirTmp	Oil In	FuelT
no	lb/hph	lb/hph	Ratio	ratio	degF	degF	degF
1	2.638	279.13	105.81	0.75	64	71	0
2	0.986	99.08	100.47	0.75	67	96	0
3	0.965	95.44	98.86	0.75	67	105	0
4	0.982	97.8	99.56	0.75	67	109	0
5	1.045	104.49	99.98	0.75	70	113	0
6	1.142	115.84	101.4	0.75	71	116	0
7	0.758	63.31	83.52	0.75	71	119	0
8	0.719	59.62	82.93	0.75	70	121	0
9	0.7	57.05	81.53	0.75	71	123	0
10	0.688	55.85	81.12	0.75	71	128	0
11	0.691	56.18	81.33	0.75	70	131	0
12	0.692	50.82	73.47	0.75	74	136	0
13	0.645	46.8	72.6	0.75	75	142	0
14	0.604	43.63	72.29	0.75	74	150	0
15	0.596	42.99	72.13	0.75	73	152	0

Line	CellT	PwTrI	TC 1	TC 3	TC 4	TC 5	TC 6
no	degF	degF	degF	degF	degF	degF	degF
1	70	1010	80	80	80	80	80
2	80	1040	80	80	80	80	80
3	90	1060	80	80	80	80	80
4	90	1060	80	80	80	80	80
5	110	1060	80	80	80	80	80
6	130	1040	90	90	90	90	90
7	130	1150	90	90	90	90	90
8	130	1170	90	90	90	90	90
9	130	1180	90	90	90	90	90
10	130	1180	90	90	90	90	90
11	120	1180	100	100	90	100	100
12	140	1330	100	100	100	100	100
13	160	1340	100	100	100	100	100
14	160	1350	110	110	110	110	110
15	160	1340	110	110	110	110	110

Line	TC 7	Wtr In	WtrOut	OilOut	TsTim2	Oil P	ManPrs
no	degF	degF	degF	degF	second	psig	inHg
1	80	0	0	0	0	92.6	0
2	80	0	0	0	1238.8	91.9	0
3	80	0	0	0	1361.9	90.3	0
4	80	0	0	0	-2118.3	91.6	0
5	80	0	0	0	-2014.2	91.5	0
6	80	0	0	0	-1898.9	92	0
7	90	0	0	0	-1751.6	90.5	0
8	90	0	0	0	-1641.8	91	0
9	90	0	0	0	-1574.1	91.1	0
10	90	0	0	0	-1456.1	92.7	0
11	90	0	0	0	-1357.5	92.3	0
12	100	0	0	0	-1147.1	93	0
13	100	0	0	0	-967.9	94.5	0
14	110	0	0	0	-739.3	95.3	0
15	110	0	0	0	-665.4	96.4	0

LineNo	AirTmp	BaroP	VapPrs	AirDen	AirCor	SAECor	STPCor
	degF	in/Hg	InHg	lb/cFt	ratio	Factor	Factor
1	64	30.04	0.35	0.075	0.985	0.973	1.012
2	67	30.04	0.35	0.074	0.979	0.975	1.015
3	67	30.02	0.35	0.074	0.978	0.976	1.015
4	67	30.03	0.35	0.074	0.979	0.976	1.015
5	70	30.03	0.35	0.074	0.973	0.978	1.018
6	71	30.04	0.35	0.074	0.972	0.979	1.018
7	71	30.04	0.35	0.074	0.972	0.979	1.018
8	70	30.04	0.35	0.074	0.974	0.978	1.017
9	71	30.03	0.35	0.074	0.971	0.979	1.019
10	71	30.02	0.35	0.074	0.971	0.98	1.019
11	70	30.03	0.35	0.074	0.973	0.978	1.018
12	74	30.04	0.35	0.073	0.966	0.982	1.021
13	75	30.04	0.35	0.073	0.964	0.983	1.022
14	74	30.03	0.35	0.073	0.966	0.982	1.022
15	73	30.03	0.35	0.074	0.968	0.981	1.021

LineNo	TsTim2	EngSpd	Speed
	second	RPM	RPM
1	0	4120	4120
2	1238.8	3590	3590
3	1361.9	4200	4210
4	-2118.3	4800	4820
5	-2014.2	5410	5390
6	-1898.9	6010	5990
7	-1751.6	3600	3600
8	-1641.8	4200	4200
9	-1574.1	4800	4800
10	-1456.1	5400	5390
11	-1357.5	6000	5970
12	-1147.1	3600	3600
13	-967.9	4200	4210
14	-739.3	5400	5400
15	-665.4	6000	6010

THIS PAGE INTENTIONALLY LEFT BLANK

APPENDIX B. BASELINE VIBRATIONS RAW DATA

Run conducted on 15 October 2018:

N1: Idle						
	Channel 1: Radial			Channel 2: Axial		
	Peak to Peak (V)	DCVrms (mV)	DCVrms mean (mV)	Peak to Peak (V)	DCVrms (mV)	DCVrms mean (mV)
Run 1	2.7247	470.546	102.045	1.6929	284.697	80.8399
Run 2	2.6589	539.774	102.061	1.9438	337.995	80.8488
Run 3	3.1969	585.726	102.077	1.7342	348.466	80.8572
Average	2.860166667	532.01533	102.061	1.7903	323.71933	80.84863333

N1: 40,890 RPM						
Nd: 3,600 RPM						
	Channel 1: Radial			Channel 2: Axial		
	Peak to Peak (V)	DCVrms (mV)	DCVrms mean (mV)	Peak to Peak (V)	DCVrms (mV)	DCVrms mean (mV)
Run 1	3.4206	595.345	102.555	3.9251	838.011	81.1031
Run 2	3.606	720.585	102.574	3.4454	716.37	81.124
Run 3	3.7698	647.713	102.592	3.6049	683.308	81.1444
Average	3.5988	654.54767	102.5736667	3.65846667	745.89633	81.12383333
Nd: 4,200 RPM						
	Channel 1: Radial			Channel 2: Axial		
	Peak to Peak (V)	DCVrms (V)	DCVrms mean (mV)	Peak to Peak (V)	DCVrms (mV)	DCVrms mean (mV)
Run 1	5.6204	1.2402	389.235	3.3664	599.766	81.233
Run 2	5.6858	1.30775	102.768	3.3344	723.513	81.2522
Run 3	4.7827	1.05016	102.804	2.3721	464.868	81.2719
Average	5.362966667	1.19937	198.269	3.0243	596.049	81.25236667
Nd: 4,800 RPM						
	Channel 1: Radial			Channel 2: Axial		
	Peak to Peak (V)	DCVrms (V)	DCVrms mean (mV)	Peak to Peak (V)	DCVrms (mV)	DCVrms mean (mV)
Run 1	6.3397	1.33671	103.155	3.6013	826.964	81.4861
Run 2	5.2883	1.16261	103.199	4.1889	1002.94	81.5184
Run 3	6.3743	1.39371	103.245	4.5245	1144.49	81.5512
Average	6.000766667	1.2976767	103.1996667	4.1049	991.46467	81.51856667
Nd: 5,400 RPM						
	Channel 1: Radial			Channel 2: Axial		
	Peak to Peak (V)	DCVrms (mV)	DCVrms mean (mV)	Peak to Peak (V)	DCVrms (mV)	DCVrms mean (mV)
Run 1	4.5147	827.993	103.51	3.6009	716.579	81.579
Run 2	4.7921	762.727	103.532	3.012	558.13	81.7048
Run 3	3.5146	602.951	103.554	2.8749	571.527	81.7216
Average	4.2738	731.22367	103.532	3.1626	615.412	81.66846667
Nd: 6,000 RPM						
	Channel 1: Radial			Channel 2: Axial		
	Peak to Peak (V)	DCVrms (mV)	DCVrms mean (mV)	Peak to Peak (V)	DCVrms (mV)	DCVrms mean (mV)
Run 1	4.4631	897.004	103.673	3.1022	711.741	81.8053
Run 2	4.2907	884.026	103.696	2.6028	558.296	81.8247
Run 3	4.5711	891.233	103.718	3.3662	633.44	81.843
Average	4.441633333	890.75433	103.6956667	3.02373333	634.49233	81.82433333

N1: 46,000 RPM						
Nd: 3,600 RPM						
	Channel 1: Radial			Channel 2: Axial		
	Peak to Peak (V)	DCVrms (mV)	DCVrms mean (mV)	Peak to Peak (V)	DCVrms (mV)	DCVrms mean (mV)
Run 1	4.9029	903.078	105.622	4.4184	978.959	83.2708
Run 2	4.4755	818.689	105.646	4.4417	913.095	83.2949
Run 3	4.4917	945.98	105.673	4.3599	947.993	83.3204
Average	4.62336667	889.249	105.647	4.406666667	946.6823	83.29536667
Nd: 4,200 RPM						
	Channel 1: Radial			Channel 2: Axial		
	Peak to Peak (V)	DCVrms (V)	DCVrms mean (mV)	Peak to Peak (V)	DCVrms (mV)	DCVrms mean (mV)
Run 1	6.3816	1.36154	105.344	3.1644	685.748	83.0639
Run 2	6.3352	1.3121	105.387	2.6572	544.794	83.0843
Run 3	5.9099	1.41346	105.432	3.3576	724.051	83.1045
Average	6.2089	1.3623667	105.3876667	3.059733333	651.531	83.08423333
Nd: 4,800 RPM						
	Channel 1: Radial			Channel 2: Axial		
	Peak to Peak (V)	DCVrms (V)	DCVrms mean (mV)	Peak to Peak (V)	DCVrms (V)	DCVrms mean (mV)
Run 1	7.1481	1.49961	104.999	6.6509	1.56384	82.8592
Run 2	6.7179	1.66448	104.945	6.0094	1.47076	82.8078
Run 3	7.3488	1.73864	105.064	6.5402	1.67784	82.9236
Average	7.0716	1.6342433	105.0026667	6.400166667	1.570813	82.86353333
Nd: 5,400 RPM						
	Channel 1: Radial			Channel 2: Axial		
	Peak to Peak (V)	DCVrms (V)	DCVrms mean (mV)	Peak to Peak (V)	DCVrms (V)	DCVrms mean (mV)
Run 1	6.8771	1.41779	104.349	5.2503	1.08038	82.376
Run 2	6.0483	1.20383	104.385	5.2128	1.23746	82.4058
Run 3	7.1197	1.40329	104.428	4.6783	0.93087	82.4416
Average	6.6817	1.3416367	104.3873333	5.047133333	1.082903	82.4078
Nd: 6,000 RPM						
	Channel 1: Radial			Channel 2: Axial		
	Peak to Peak (V)	DCVrms (V)	DCVrms mean (mV)	Peak to Peak (V)	DCVrms (V)	DCVrms mean (mV)
Run 1	6.8107	1.52713	103.953	5.4903	1.20752	82.0551
Run 2	6.6069	1.32293	103.988	5.1824	1.10266	82.089
Run 3	6.2099	1.13921	104.03	5.4633	1.0353	82.1292
Average	6.5425	1.3298	103.9903	5.3787	1.1152	82.0911

N1: 51,000 RPM						
Nd: 3,600 RPM						
	Channel 1: Radial			Channel 2: Axial		
	Peak to Peak (V)	DCVrms (V)	DCVrms mean (mV)	Peak to Peak (V)	DCVrms (V)	DCVrms mean (mV)
Run 1	6.7625	1.08613	105.847	6.1547	1.38699	83.5515
Run 2	5.2884	1.09246	105.879	5.9073	1.34162	83.5954
Run 3	5.3215	1.13198	105.911	6.3782	1.31438	83.6384
Average	5.7908	1.103523	105.879	6.146733333	1.347663	83.5951
Nd: 4,200 RPM						
	Channel 1: Radial			Channel 2: Axial		
	Peak to Peak (V)	DCVrms (V)	DCVrms mean (mV)	Peak to Peak (V)	DCVrms (mV)	DCVrms mean (mV)
Run 1	5.5608	1.14811	106.108	3.3181	642.461	83.7887
Run 2	5.7601	1.15092	106.142	2.8338	559.126	83.8041
Run 3	7.1185	1.30635	106.177	3.5178	625.926	83.8209
Average	6.146466667	1.201793	106.1423333	3.223233333	609.171	83.80456667
Nd: 4,800 RPM						
	Channel 1: Radial			Channel 2: Axial		
	Peak to Peak (V)	DCVrms (V)	DCVrms mean (mV)	Peak to Peak (V)	DCVrms (V)	DCVrms mean (mV)
Run 1	6.8223	1.43175	106.438	5.3838	1.06991	84.0232
Run 2	5.9293	1.25286	106.478	4.4315	1.01911	84.0545
Run 3	6.2324	1.41331	106.514	4.4305	1.03947	84.081
Average	6.328	1.365973	106.4766667	4.7486	1.04283	84.0529
Nd: 5,400 RPM						
	Channel 1: Radial			Channel 2: Axial		
	Peak to Peak (V)	DCVrms (V)	DCVrms mean (mV)	Peak to Peak (V)	DCVrms (mV)	DCVrms mean (mV)
Run 1	6.6055	1.43928	106.722	4.6819	891.664	84.2086
Run 2	7.9855	1.51694	106.771	4.4561	872.93	84.2386
Run 3	7.3683	1.71097	106.824	5.4842	1020.87	84.2704
Average	7.319766667	1.55573	106.7723333	4.874066667	928.488	84.2392
Nd: 6,000 RPM						
	Channel 1: Radial			Channel 2: Axial		
	Peak to Peak (V)	DCVrms (V)	DCVrms mean (mV)	Peak to Peak (V)	DCVrms (V)	DCVrms mean (mV)
Run 1	8	1.92811	107.178	8	2.12056	84.5706
Run 2	7.8947	1.89413	107.24	8	2.03244	84.6327
Run 3	7.4418	1.79199	107.321	6.5943	1.42229	84.7115
Average	7.7788	1.8714	107.2463	7.5314	1.8584	84.6383

Run conducted on 01 November 2018:

N1: Idle						
	Channel 1: Radial			Channel 2: Axial		
	Peak to Peak (V)	DCVrms (mV)	DCVrms mean (mV)	Peak to Peak (V)	DCVrms (mV)	DCVrms mean (mV)
Run 1	3.113	486.913	612.417	1.6568	268.288	333.889
Run 2	3.594	637.117	613.359	2.1097	368.808	334.098
Run 3	2.6347	487.365	612.317	1.8423	365.559	335.765
Average	3.1139	537.1317	612.6977	1.8696	334.2183	334.584

N1: 40,890 RPM						
Nd: 3,600 RPM						
	Channel 1: Radial			Channel 2: Axial		
	Peak to Peak (V)	DCVrms (mV)	DCVrms mean (mV)	Peak to Peak (V)	DCVrms (mV)	DCVrms mean (mV)
Run 1	4.7399	975.575	755.425	4.0207	903.093	457.546
Run 2	4.6906	996.063	763.537	4.0311	939.411	476.338
Run 3	4.7784	926.61	770.61	4.1493	956.18	493.852
Average	4.7363	966.0827	763.1907	4.067033	932.8947	475.912
Nd: 4,200 RPM						
	Channel 1: Radial			Channel 2: Axial		
	Peak to Peak (V)	DCVrms (V)	DCVrms mean (mV)	Peak to Peak (V)	DCVrms (mV)	DCVrms mean (mV)
Run 1	8	2.34274	962.82	3.9282	971.839	560.92
Run 2	7.5532	1.80272	992.755	3.7024	1025.13	568.106
Run 3	8	2.23278	1018.71	3.9988	939.204	575.154
Average	7.851067	2.12608	991.4283	3.876467	978.7243	568.06
Nd: 4,800 RPM						
	Channel 1: Radial			Channel 2: Axial		
	Peak to Peak (V)	DCVrms (V)	DCVrms mean (V)	Peak to Peak (V)	DCVrms (V)	DCVrms mean (mV)
Run 1	8	1.86228	1.17775	4.9706	1.22373	683.179
Run 2	8	1.86653	1.18941	5.6582	1.59006	695.083
Run 3	7.9239	2.01094	1.20374	5.6911	1.32912	710.084
Average	7.974633	1.91325	1.1903	5.439967	1.38097	696.1153
Nd: 5,400 RPM						
	Channel 1: Radial			Channel 2: Axial		
	Peak to Peak (V)	DCVrms (mV)	DCVrms mean (mV)	Peak to Peak (V)	DCVrms (mV)	DCVrms mean (mV)
Run 1	4.2636	650.957	1224.79	2.9482	554.427	721.493
Run 2	3.5192	622.015	1213.76	3.0726	587.183	718.939
Run 3	4.5891	844.661	1207.29	3.1369	698.785	717.429
Average	4.123967	705.8777	1215.28	3.052567	613.465	719.287
Nd: 6,000 RPM						
	Channel 1: Radial			Channel 2: Axial		
	Peak to Peak (V)	DCVrms (mV)	DCVrms mean (mV)	Peak to Peak (V)	DCVrms (mV)	DCVrms mean (mV)
Run 1	4.3522	843.905	1163.4	2.8406	486.221	698.869
Run 2	5.6953	1150.37	1157.99	2.1911	372.395	695.572
Run 3	4.8842	1050.57	1153.28	2.964	581.016	692.691
Average	4.977233	1014.948	1158.223	2.665233	479.8773	695.7107

N1: 46,000 RPM						
Nd: 3,600 RPM						
	Channel 1: Radial			Channel 2: Axial		
	Peak to Peak (V)	DCVrms (mV)	DCVrms mean (mV)	Peak to Peak (V)	DCVrms (mV)	DCVrms mean (mV)
Run 1	4.5316	1004.43	1197.09	5.0042	1173.62	742.233
Run 2	5.2964	1095.3	1196.31	3.8352	829.116	743.644
Run 3	4.9191	999.583	1195.42	4.2908	964.937	744.742
Average	4.9157	1033.104	1196.273333	4.376733	989.2243	743.5397
Nd: 4,200 RPM						
	Channel 1: Radial			Channel 2: Axial		
	Peak to Peak (V)	DCVrms (V)	DCVrms mean (mV)	Peak to Peak (V)	DCVrms (mV)	DCVrms mean (mV)
Run 1	6.5975	1.77289	1195.15	1.8487	373.385	751.79
Run 2	7.4314	1.83921	1200.27	2.0539	376.698	748.516
Run 3	7.1243	1.80756	1207.46	1.9025	363.861	744.859
Average	7.051067	1.806553	1200.96	1.935033	371.3147	748.3883
Nd: 4,800 RPM						
	Channel 1: Radial			Channel 2: Axial		
	Peak to Peak (V)	DCVrms (V)	DCVrms mean (mV)	Peak to Peak (V)	DCVrms (V)	DCVrms mean (mV)
Run 1	6.5393	1.48597	1145.68	5.0567	1.25024	746.11
Run 2	6.578	1.38008	1149.49	5.6485	1.31624	753.064
Run 3	6.4108	1.40408	1152.15	5.412	1.19584	758.387
Average	6.509367	1.423377	1149.106667	5.3724	1.254107	752.5203
Nd: 5,400 RPM						
	Channel 1: Radial			Channel 2: Axial		
	Peak to Peak (V)	DCVrms (V)	DCVrms mean (mV)	Peak to Peak (V)	DCVrms (V)	DCVrms mean (mV)
Run 1	4.8571	0.974759	1133.9	4.2605	0.913584	726.245
Run 2	4.3897	0.932388	1131.33	4.1619	0.889889	728.134
Run 3	3.8613	0.711535	1128.75	3.8116	0.873292	730.595
Average	4.369367	0.872894	1131.326667	4.078	0.892255	728.3247
Nd: 6,000 RPM						
	Channel 1: Radial			Channel 2: Axial		
	Peak to Peak (V)	DCVrms (V)	DCVrms mean (mV)	Peak to Peak (V)	DCVrms (V)	DCVrms mean (mV)
Run 1	6.2199	1.22756	1151.54	4.6546	0.915633	709.591
Run 2	6.5466	1.38379	1151.56	3.9001	0.881655	711.689
Run 3	5.2181	1.10971	1151.94	4.916	0.947603	713.599
Average	5.9949	1.2404	1151.6800	4.4902	0.9150	711.6263

N1: 51,000 RPM						
Nd: 3,600 RPM						
	Channel 1: Radial			Channel 2: Axial		
	Peak to Peak (V)	DCVrms (V)	DCVrms mean (mV)	Peak to Peak (V)	DCVrms (V)	DCVrms mean (mV)
Run 1	6.0261	1.22026	1200.11	5.3529	1.15692	760.32
Run 2	7.402	1.62994	1202.38	6.7297	1.50274	765.561
Run 3	6.333	1.28736	1204.15	6.1555	1.43811	770.019
Average	6.587033	1.379187	1202.213333	6.079367	1.365923	765.3
Nd: 4,200 RPM						
	Channel 1: Radial			Channel 2: Axial		
	Peak to Peak (V)	DCVrms (V)	DCVrms mean (mV)	Peak to Peak (V)	DCVrms (mV)	DCVrms mean (mV)
Run 1	7.9734	1.45167	1208.52	2.9666	580.03	768.971
Run 2	7.6744	1.77946	1210.13	2.6274	422.094	766.936
Run 3	5.2184	1.22908	1210.71	3.7825	552.863	764.965
Average	6.9554	1.486737	1209.786667	3.1255	518.329	766.9573
Nd: 4,800 RPM						
	Channel 1: Radial			Channel 2: Axial		
	Peak to Peak (V)	DCVrms (V)	DCVrms mean (mV)	Peak to Peak (V)	DCVrms (V)	DCVrms mean (mV)
Run 1	4.7488	0.866411	1208.81	3.8711	0.787441	768.457
Run 2	4.067	0.821607	1206.87	3.8404	0.702878	768.162
Run 3	4.0504	0.816967	1204.14	3.786	0.795451	767.539
Average	4.288733	0.834995	1206.606667	3.8325	0.761923	768.0527
Nd: 5,400 RPM						
	Channel 1: Radial			Channel 2: Axial		
	Peak to Peak (V)	DCVrms (V)	DCVrms mean (mV)	Peak to Peak (V)	DCVrms (mV)	DCVrms mean (mV)
Run 1	7.1445	1.50008	1207.35	5.0139	1044	779.652
Run 2	7.0027	1.68843	1210.55	5.4999	1056.63	781.417
Run 3	7.8736	1.95792	1215.19	5.7793	1209.53	783.765
Average	7.340267	1.715477	1211.03	5.431033	1103.387	781.6113
Nd: 6,000 RPM						
	Channel 1: Radial			Channel 2: Axial		
	Peak to Peak (V)	DCVrms (V)	DCVrms mean (mV)	Peak to Peak (V)	DCVrms (V)	DCVrms mean (mV)
Run 1	8	1.80711	1238.17	6.8748	1.43403	799.989
Run 2	8	1.76282	1244.49	6.1595	1.29385	805.019
Run 3	8	1.78408	1249.31	5.8532	1.28795	808.967
Average	8.0000	1.7847	1243.9900	6.2958	1.3386	804.6583

Run conducted on 08 November 2018:

N1: Idle						
	Channel 1: Radial			Channel 2: Axial		
	Peak to Peak (V)	DCVrms (V)	DCVrms mean (V)	Peak to Peak (V)	DCVrms (V)	DCVrms mean (V)
Run 1	3.055	0.647062	0.120985	1.4933	0.263839	0.072659
Run 2	2.5728	0.53717	0.120993	1.8844	0.299457	0.072662
Run 3	4.4777	0.793525	0.121	2.0777	0.313143	0.072666
Average	3.3685	0.659252	0.120993	1.818467	0.292146	0.072662

N1: 40,890 RPM						
Nd: 3,600 RPM						
	Channel 1: Radial			Channel 2: Axial		
	Peak to Peak (V)	DCVrms (V)	DCVrms mean (V)	Peak to Peak (V)	DCVrms (V)	DCVrms mean (V)
Run 1	3.9219	0.802402	0.121216	3.6867	0.839897	0.072775
Run 2	4.7188	0.935451	0.121226	3.6092	0.771304	0.072786
Run 3	5.2775	0.957708	0.121239	3.7021	0.853145	0.072798
Average	4.6394	0.89852	0.121227	3.666	0.821449	0.072786
Nd: 4,200 RPM						
	Channel 1: Radial			Channel 2: Axial		
	Peak to Peak (V)	DCVrms (V)	DCVrms mean (V)	Peak to Peak (V)	DCVrms (V)	DCVrms mean (V)
Run 1	7.4812	1.76394	0.121353	2.9161	0.648952	0.072868
Run 2	7.0557	1.77165	0.121371	3.4791	0.897341	0.072875
Run 3	6.8832	1.66858	0.121389	3.7166	0.865124	0.072884
Average	7.140033	1.734723	0.121371	3.3706	0.803806	0.072876
Nd: 4,800 RPM						
	Channel 1: Radial			Channel 2: Axial		
	Peak to Peak (V)	DCVrms (V)	DCVrms mean (V)	Peak to Peak (V)	DCVrms (V)	DCVrms mean (V)
Run 1	7.49	1.52554	0.121594	3.6703	0.899886	0.073
Run 2	8	1.30914	0.121613	4.3901	1.0384	0.073013
Run 3	7.2749	1.37977	0.121636	3.9472	0.904924	0.073029
Average	7.5883	1.404817	0.121614	4.002533	0.947737	0.073014
Nd: 5,400 RPM						
	Channel 1: Radial			Channel 2: Axial		
	Peak to Peak (V)	DCVrms (V)	DCVrms mean (V)	Peak to Peak (V)	DCVrms (V)	DCVrms mean (V)
Run 1	4.1152	0.723969	0.121768	2.8902	0.563209	0.073108
Run 2	3.5189	0.795996	0.121778	2.7588	0.494884	0.073116
Run 3	4.8223	0.826156	0.121786	2.8194	0.439184	0.073122
Average	4.152133	0.78204	0.121777	2.8228	0.499092	0.073115
Nd: 6,000 RPM						
	Channel 1: Radial			Channel 2: Axial		
	Peak to Peak (V)	DCVrms (V)	DCVrms mean (V)	Peak to Peak (V)	DCVrms (V)	DCVrms mean (V)
Run 1	4.1393	0.710732	0.121873	2.7713	0.506449	0.073187
Run 2	4.1921	0.764644	0.121881	3.7454	0.791679	0.073194
Run 3	4.1098	0.742187	0.12189	3.2896	0.680635	0.073203
Average	4.147067	0.739188	0.121881	3.268767	0.659588	0.073195

N1: 46,000 RPM						
Nd: 3,600 RPM						
	Channel 1: Radial			Channel 2: Axial		
	Peak to Peak (V)	DCVrms (V)	DCVrms mean (V)	Peak to Peak (V)	DCVrms (V)	DCVrms mean (V)
Run 1	6.0027	1.54701	0.12257	4.6756	0.908865	0.073689
Run 2	5.8255	1.36364	0.122582	3.8983	0.836496	0.073699
Run 3	5.2722	1.19526	0.122595	4.0485	0.83213	0.073709
Average	5.700133	1.368637	0.122582	4.207467	0.859164	0.073699
Nd: 4,200 RPM						
	Channel 1: Radial			Channel 2: Axial		
	Peak to Peak (V)	DCVrms (V)	DCVrms mean (V)	Peak to Peak (V)	DCVrms (V)	DCVrms mean (V)
Run 1	8	2.0211	0.122456	3.1635	0.647446	0.073618
Run 2	7.1993	1.86492	0.122434	2.5191	0.485972	0.073612
Run 3	7.9796	1.93496	0.122481	3.2136	0.580378	0.073625
Average	7.7263	1.940327	0.122457	2.9654	0.571265	0.073619
Nd: 4,800 RPM						
	Channel 1: Radial			Channel 2: Axial		
	Peak to Peak (V)	DCVrms (V)	DCVrms mean (V)	Peak to Peak (V)	DCVrms (V)	DCVrms mean (V)
Run 1	6.6735	1.53845	0.122281	6.0956	1.54905	0.073527
Run 2	8	2.13398	0.122303	6.1141	1.56251	0.073546
Run 3	7.5321	1.8001	0.112326	7.0017	1.59194	0.073567
Average	7.401867	1.824177	0.11897	6.4038	1.567833	0.073547
Nd: 5,400 RPM						
	Channel 1: Radial			Channel 2: Axial		
	Peak to Peak (V)	DCVrms (V)	DCVrms mean (V)	Peak to Peak (V)	DCVrms (V)	DCVrms mean (V)
Run 1	5.6345	1.07953	0.122161	4.4128	1.01795	0.073439
Run 2	5.2115	1.13596	0.122151	4.9276	1.00349	0.073429
Run 3	5.8879	1.24644	0.122175	4.5982	1.00001	0.073451
Average	5.577967	1.153977	0.122162	4.6462	1.00715	0.07344
Nd: 6,000 RPM						
	Channel 1: Radial			Channel 2: Axial		
	Peak to Peak (V)	DCVrms (V)	DCVrms mean (V)	Peak to Peak (V)	DCVrms (V)	DCVrms mean (V)
Run 1	5.2149	0.936007	0.121993	5.3694	1.09604	0.073302
Run 2	5.8958	1.19226	0.122007	4.958	1.05372	0.073317
Run 3	5.5603	1.05129	0.12202	4.188	0.915537	0.073329
Average	5.5570	1.0599	0.1220	4.8385	1.0218	0.0733

N1: 51,000 RPM						
Nd: 3,600 RPM						
	Channel 1: Radial			Channel 2: Axial		
	Peak to Peak (V)	DCVrms (V)	DCVrms mean (V)	Peak to Peak (V)	DCVrms (V)	DCVrms mean (V)
Run 1	6.0691	1.05364	0.122715	6.8473	1.44035	0.073827
Run 2	6.38	1.54323	0.122733	6.4336	1.32629	0.073844
Run 3	7.73	1.63322	0.122749	8	1.67548	0.073861
Average	6.726367	1.41003	0.122732	7.093633	1.480707	0.073844
Nd: 4,200 RPM						
	Channel 1: Radial			Channel 2: Axial		
	Peak to Peak (V)	DCVrms (V)	DCVrms mean (V)	Peak to Peak (V)	DCVrms (V)	DCVrms mean (V)
Run 1	7.9668	1.56291	0.122867	2.7879	0.525163	0.073945
Run 2	6.123	1.06517	0.122887	3.7058	0.668282	0.073953
Run 3	7.7991	1.68306	0.122908	3.1673	0.590651	0.073961
Average	7.2963	1.437047	0.122887	3.220333	0.594699	0.073953
Nd: 4,800 RPM						
	Channel 1: Radial			Channel 2: Axial		
	Peak to Peak (V)	DCVrms (V)	DCVrms mean (V)	Peak to Peak (V)	DCVrms (V)	DCVrms mean (V)
Run 1	5.7692	1.21501	0.123008	4.9538	1.13735	0.074034
Run 2	5.3915	1.21874	0.123018	4.6282	0.932016	0.074043
Run 3	5.2787	1.14971	0.123031	4.2263	0.958061	0.074054
Average	5.4798	1.194487	0.123019	4.602767	1.009142	0.074044
Nd: 5,400 RPM						
	Channel 1: Radial			Channel 2: Axial		
	Peak to Peak (V)	DCVrms (V)	DCVrms mean (V)	Peak to Peak (V)	DCVrms (V)	DCVrms mean (V)
Run 1	6.2076	1.58463	0.123119	4.9253	1.0043	0.074115
Run 2	7.108	1.5851	0.123135	4.5669	0.874298	0.074125
Run 3	5.9987	1.35451	0.123155	4.824	1.0046	0.074137
Average	6.4381	1.50808	0.123136	4.772067	0.961066	0.074126
Nd: 6,000 RPM						
	Channel 1: Radial			Channel 2: Axial		
	Peak to Peak (V)	DCVrms (V)	DCVrms mean (V)	Peak to Peak (V)	DCVrms (V)	DCVrms mean (V)
Run 1	7.4472	1.81259	0.123286	7.2957	1.64156	0.074236
Run 2	8.0147	1.9161	0.123314	7.4756	1.71404	0.074263
Run 3	7.4153	1.4094	0.123335	6.3581	1.34216	0.074284
Average	7.6257	1.7127	0.1233	7.0431	1.5659	0.0743

Run conducted on 19 November 2018:

N1: Idle						
	Channel 1: Radial			Channel 2: Axial		
	Peak to Peak (V)	DCVrms (V)	DCVrms mean (V)	Peak to Peak (V)	DCVrms (V)	DCVrms mean (V)
Run 1	3.1968	0.632239	0.165695	1.5058	0.302292	0.102291
Run 2	2.425	0.470947	0.166284	1.7514	0.357932	0.102567
Run 3	2.0026	0.398409	0.166831	1.3818	0.264027	0.102839
Average	2.541467	0.500532	0.16627	1.546333	0.308084	0.102566

N1: 40,890 RPM						
Nd: 3,600 RPM						
	Channel 1: Radial			Channel 2: Axial		
	Peak to Peak (V)	DCVrms (V)	DCVrms mean (V)	Peak to Peak (V)	DCVrms (V)	DCVrms mean (V)
Run 1	3.8274	0.96551	0.199094	3.0132	0.696248	0.118764
Run 2	3.5174	0.528025	0.199862	2.7582	0.662294	0.119508
Run 3	4.122	0.98967	0.200647	3.076	0.676686	0.120227
Average	3.822267	0.827735	0.199868	2.949133	0.678409	0.1195
Nd: 4,200 RPM						
	Channel 1: Radial			Channel 2: Axial		
	Peak to Peak (V)	DCVrms (V)	DCVrms mean (V)	Peak to Peak (V)	DCVrms (V)	DCVrms mean (V)
Run 1	5.5657	1.24437	0.206347	2.8337	0.544345	0.123306
Run 2	5.4304	1.24964	0.208067	1.9844	0.412578	0.123895
Run 3	5.8034	1.33849	1.23554	2.3922	0.546605	0.473308
Average	5.599833	1.2775	0.549985	2.403433	0.501176	0.24017
Nd: 4,800 RPM						
	Channel 1: Radial			Channel 2: Axial		
	Peak to Peak (V)	DCVrms (V)	DCVrms mean (V)	Peak to Peak (V)	DCVrms (V)	DCVrms mean (V)
Run 1	7.7304	2.0566	1.43755	4.385	1.1384	0.719091
Run 2	8	1.91732	1.45966	3.5412	0.932605	0.742493
Run 3	5.8005	1.36465	1.48238	4.5683	1.05592	0.761863
Average	7.176967	1.779523	1.459863	4.164833	1.042308	0.741149
Nd: 5,400 RPM						
	Channel 1: Radial			Channel 2: Axial		
	Peak to Peak (V)	DCVrms (V)	DCVrms mean (V)	Peak to Peak (V)	DCVrms (V)	DCVrms mean (V)
Run 1	3.901	0.705746	1.29638	2.6042	0.558595	0.689835
Run 2	4.6027	0.837539	1.27245	3.6633	0.744342	0.683308
Run 3	3.8508	0.790214	1.25526	2.2394	0.576237	0.678196
Average	4.118167	0.777833	1.274697	2.835633	0.626391	0.68378
Nd: 6,000 RPM						
	Channel 1: Radial			Channel 2: Axial		
	Peak to Peak (V)	DCVrms (V)	DCVrms mean (V)	Peak to Peak (V)	DCVrms (V)	DCVrms mean (V)
Run 1	4.1103	0.881773	1.1503	3.9797	0.892825	0.691629
Run 2	3.2624	0.798476	1.13814	3.3152	0.853218	0.694757
Run 3	3.758	0.859439	1.12715	2.9232	0.610399	0.698396
Average	3.710233	0.846563	1.13853	3.406033	0.785481	0.694927

N1: 46,000 RPM						
Nd: 3,600 RPM						
	Channel 1: Radial			Channel 2: Axial		
	Peak to Peak (V)	DCVrms (V)	DCVrms mean (V)	Peak to Peak (V)	DCVrms (V)	DCVrms mean (V)
Run 1	5.3961	1.22665	1.22194	3.8174	0.832944	0.880773
Run 2	4.9009	1.17429	1.22254	4.3574	1.03729	0.881791
Run 3	5.4616	1.16857	1.22279	4.4383	0.980163	0.88275
Average	5.252867	1.189837	1.222423	4.204367	0.950132	0.881771
Nd: 4,200 RPM						
	Channel 1: Radial			Channel 2: Axial		
	Peak to Peak (V)	DCVrms (V)	DCVrms mean (V)	Peak to Peak (V)	DCVrms (V)	DCVrms mean (V)
Run 1	4.8182	1.07717	1.2263	2.3944	0.543673	0.890909
Run 2	6.8199	1.68155	1.22883	2.1091	0.471222	0.885776
Run 3	5.3574	1.31311	1.2319	2.5855	0.518637	0.880198
Average	5.665167	1.357277	1.22901	2.363	0.511177	0.885628
Nd: 4,800 RPM						
	Channel 1: Radial			Channel 2: Axial		
	Peak to Peak (V)	DCVrms (V)	DCVrms mean (V)	Peak to Peak (V)	DCVrms (V)	DCVrms mean (V)
Run 1	6.2652	1.34106	1.18679	5.8856	1.43096	0.886765
Run 2	6.5901	1.56903	1.19471	5.3642	1.45163	0.895701
Run 3	6.4341	1.71434	1.20221	5.6583	1.41945	0.904339
Average	6.4298	1.541477	1.19457	5.636033	1.434013	0.895602
Nd: 5,400 RPM						
	Channel 1: Radial			Channel 2: Axial		
	Peak to Peak (V)	DCVrms (V)	DCVrms mean (V)	Peak to Peak (V)	DCVrms (V)	DCVrms mean (V)
Run 1	6.2374	1.21944	1.13183	5.3921	1.15542	0.850438
Run 2	7.1091	1.43978	1.13333	4.7506	0.963322	0.853369
Run 3	5.319	1.16693	1.13453	4.8176	1.04943	0.855711
Average	6.221833	1.275383	1.13323	4.986767	1.056057	0.853173
Nd: 6,000 RPM						
	Channel 1: Radial			Channel 2: Axial		
	Peak to Peak (V)	DCVrms (V)	DCVrms mean (V)	Peak to Peak (V)	DCVrms (V)	DCVrms mean (V)
Run 1	5.3066	1.17034	1.10698	4.1535	0.945147	0.824922
Run 2	5.9381	1.28978	1.10737	6.2312	1.4149	0.816152
Run 3	3.842	0.814376	1.10921	5.251	1.13826	0.799089
Average	5.0289	1.0915	1.1079	5.2119	1.1661	0.8134

N1: 51,000 RPM						
Nd: 3,600 RPM						
	Channel 1: Radial			Channel 2: Axial		
	Peak to Peak (V)	DCVrms (V)	DCVrms mean (V)	Peak to Peak (V)	DCVrms (V)	DCVrms mean (V)
Run 1	6.684	1.71263	1.23338	7.2993	1.69305	0.903268
Run 2	7.0634	1.76923	1.23758	6.4445	1.58116	0.909796
Run 3	5.8341	1.51822	1.24127	7.1991	1.6788	0.916733
Average	6.527167	1.666693	1.23741	6.980967	1.651003	0.909932
Nd: 4,200 RPM						
	Channel 1: Radial			Channel 2: Axial		
	Peak to Peak (V)	DCVrms (V)	DCVrms mean (V)	Peak to Peak (V)	DCVrms (V)	DCVrms mean (V)
Run 1	6.3105	1.33587	1.25872	2.5647	0.612268	0.891826
Run 2	6.9164	1.49721	1.26127	2.405	0.546937	0.888026
Run 3	7.416	1.76906	1.26351	3.4499	0.717812	0.884884
Average	6.880967	1.534047	1.261167	2.806533	0.625672	0.888245
Nd: 4,800 RPM						
	Channel 1: Radial			Channel 2: Axial		
	Peak to Peak (V)	DCVrms (V)	DCVrms mean (V)	Peak to Peak (V)	DCVrms (V)	DCVrms mean (V)
Run 1	5.2406	1.29521	1.26318	3.6108	0.839918	0.889935
Run 2	5.3941	1.19605	1.26288	3.2786	0.805201	0.890903
Run 3	4.4554	1.10894	1.26232	4.0368	0.915721	0.891887
Average	5.030033	1.200067	1.262793	3.642067	0.853613	0.890908
Nd: 5,400 RPM						
	Channel 1: Radial			Channel 2: Axial		
	Peak to Peak (V)	DCVrms (V)	DCVrms mean (V)	Peak to Peak (V)	DCVrms (V)	DCVrms mean (V)
Run 1	7.5244	1.85007	1.27424	4.6908	1.00736	0.896531
Run 2	7.8656	1.96956	1.27933	5.4995	1.11736	0.898464
Run 3	6.5306	1.5395	1.28291	5.5161	1.08218	0.899917
Average	7.306867	1.786377	1.278827	5.235467	1.068967	0.898304
Nd: 6,000 RPM						
	Channel 1: Radial			Channel 2: Axial		
	Peak to Peak (V)	DCVrms (V)	DCVrms mean (V)	Peak to Peak (V)	DCVrms (V)	DCVrms mean (V)
Run 1	8	2.32164	1.30056	8.0039	1.93256	0.923041
Run 2	7.5923	1.84425	1.3057	5.4719	1.3871	0.932352
Run 3	7.505	1.95646	1.31136	6.9179	1.61433	0.941832
Average	7.6991	2.0408	1.3059	6.7979	1.6447	0.9324

Run conducted 20 November 2018:

N1: Idle						
	Channel 1: Radial			Channel 2: Axial		
	Peak to Peak (V)	DCVrms (V)	DCVrms mean (V)	Peak to Peak (V)	DCVrms (V)	DCVrms mean (V)
Run 1	2.5483	0.652019	0.124111	1.9394	0.370786	0.085446
Run 2	2.5744	0.567752	0.124163	1.7493	0.347607	0.08547
Run 3	4.5333	0.860916	0.12421	1.4067	0.288795	0.085493
Average	3.218667	0.693562	0.124161	1.698467	0.335729	0.08547

N1: 40,890 RPM						
Nd: 3,600 RPM						
	Channel 1: Radial			Channel 2: Axial		
	Peak to Peak (V)	DCVrms (V)	DCVrms mean (V)	Peak to Peak (V)	DCVrms (V)	DCVrms mean (V)
Run 1	4.3767	1.03911	0.125796	3.406	0.756687	0.086203
Run 2	3.2801	0.625124	0.125862	2.668	0.582463	0.086256
Run 3	3.2861	0.715309	0.125915	3.7968	0.836286	0.086299
Average	3.647633	0.793181	0.125858	3.290267	0.725145	0.086253
Nd: 4,200 RPM						
	Channel 1: Radial			Channel 2: Axial		
	Peak to Peak (V)	DCVrms (V)	DCVrms mean (V)	Peak to Peak (V)	DCVrms (V)	DCVrms mean (V)
Run 1	5.6701	1.30898	0.126748	2.483	0.498955	0.086842
Run 2	5.6546	1.27495	0.126847	2.8508	0.632367	0.086882
Run 3	5.766	1.32256	0.126949	2.4987	0.627085	0.086919
Average	5.6969	1.302163	0.126848	2.610833	0.586136	0.086881
Nd: 4,800 RPM						
	Channel 1: Radial			Channel 2: Axial		
	Peak to Peak (V)	DCVrms (V)	DCVrms mean (V)	Peak to Peak (V)	DCVrms (V)	DCVrms mean (V)
Run 1	6.5805	1.4375	0.128266	3.6767	0.897073	0.087481
Run 2	4.8858	1.06833	0.128374	3.3619	0.753449	0.087542
Run 3	5.8155	1.49026	0.128485	3.3577	0.825602	0.087604
Average	5.7606	1.33203	0.128375	3.465433	0.825375	0.087542
Nd: 5,400 RPM						
	Channel 1: Radial			Channel 2: Axial		
	Peak to Peak (V)	DCVrms (V)	DCVrms mean (V)	Peak to Peak (V)	DCVrms (V)	DCVrms mean (V)
Run 1	3.1099	0.617396	0.129301	3.1234	0.564226	0.08809
Run 2	4.4911	0.893981	0.129351	3.256	0.626312	0.088132
Run 3	4.4169	0.81396	0.1294	3.3062	0.702797	0.088171
Average	4.005967	0.775112	0.129351	3.228533	0.631112	0.088131
Nd: 6,000 RPM						
	Channel 1: Radial			Channel 2: Axial		
	Peak to Peak (V)	DCVrms (V)	DCVrms mean (V)	Peak to Peak (V)	DCVrms (V)	DCVrms mean (V)
Run 1	4.0164	0.890323	0.130025	3.9799	0.767607	0.088663
Run 2	4.3904	1.03852	0.130076	2.82	0.644475	0.088717
Run 3	3.5087	0.696107	0.130127	3.1957	0.728101	0.088769
Average	3.971833	0.874983	0.130076	3.331867	0.713394	0.088716

N1: 46,000 RPM						
Nd: 3,600 RPM						
	Channel 1: Radial			Channel 2: Axial		
	Peak to Peak (V)	DCVrms (V)	DCVrms mean (V)	Peak to Peak (V)	DCVrms (V)	DCVrms mean (V)
Run 1	5.3731	1.22899	0.131379	4.1838	0.942424	0.089627
Run 2	4.0811	1.06484	0.13149	3.8368	0.875038	0.089708
Run 3	5.7219	1.33075	0.131582	4.4863	0.945639	0.089777
Average	5.0587	1.208193	0.131484	4.168967	0.921034	0.089704
Nd: 4,200 RPM						
	Channel 1: Radial			Channel 2: Axial		
	Peak to Peak (V)	DCVrms (V)	DCVrms mean (V)	Peak to Peak (V)	DCVrms (V)	DCVrms mean (V)
Run 1	4.9882	1.13201	0.132493	2.7546	0.495557	0.090321
Run 2	5.1024	1.18235	0.13258	3.0035	0.53662	0.090352
Run 3	5.3586	1.2571	0.132679	2.8169	0.506089	0.090386
Average	5.149733	1.190487	0.132584	2.858333	0.512755	0.090353
Nd: 4,800 RPM						
	Channel 1: Radial			Channel 2: Axial		
	Peak to Peak (V)	DCVrms (V)	DCVrms mean (V)	Peak to Peak (V)	DCVrms (V)	DCVrms mean (V)
Run 1	7.9094	0.189284	0.13325	5.8817	1.51992	0.090777
Run 2	6.0999	1.53169	0.133441	4.1154	1.13983	0.090879
Run 3	7.101	1.71198	0.133561	5.3018	1.27891	0.090982
Average	7.036767	1.144318	0.133417	5.099633	1.312887	0.090879
Nd: 5,400 RPM						
	Channel 1: Radial			Channel 2: Axial		
	Peak to Peak (V)	DCVrms (V)	DCVrms mean (V)	Peak to Peak (V)	DCVrms (V)	DCVrms mean (V)
Run 1	6.0993	1.42542	0.134714	4.7591	1.11919	0.091891
Run 2	5.8698	1.13767	0.134814	4.7079	1.01587	0.091974
Run 3	5.9071	1.35391	0.134899	5.6237	1.08624	0.092046
Average	5.958733	1.305667	0.134809	5.030233	1.073767	0.09197
Nd: 6,000 RPM						
	Channel 1: Radial			Channel 2: Axial		
	Peak to Peak (V)	DCVrms (V)	DCVrms mean (V)	Peak to Peak (V)	DCVrms (V)	DCVrms mean (V)
Run 1	5.579	1.22238	0.135774	5.5744	1.33417	0.092794
Run 2	4.4922	0.898471	0.135906	5.4203	1.14198	0.092953
Run 3	4.0947	0.81087	0.135991	5.6733	1.25329	0.093056
Average	4.7220	0.9772	0.1359	5.5560	1.2431	0.0929

N1: 51,000 RPM						
Nd: 3,600 RPM						
	Channel 1: Radial			Channel 2: Axial		
	Peak to Peak (V)	DCVrms (V)	DCVrms mean (V)	Peak to Peak (V)	DCVrms (V)	DCVrms mean (V)
Run 1	5.8682	1.81178	0.138221	6.3325	1.60375	0.094984
Run 2	4.3304	0.865908	0.138334	5.3258	1.25374	0.095102
Run 3	6.0422	0.692692	0.138462	5.5887	1.35311	0.095233
Average	5.4136	1.12346	0.138339	5.749	1.403533	0.095106
Nd: 4,200 RPM						
	Channel 1: Radial			Channel 2: Axial		
	Peak to Peak (V)	DCVrms (V)	DCVrms mean (V)	Peak to Peak (V)	DCVrms (V)	DCVrms mean (V)
Run 1	4.9254	1.0696	0.140223	2.7105	0.473559	0.096756
Run 2	5.0813	1.07484	0.140311	2.0162	0.378281	0.096793
Run 3	4.9811	1.02602	0.140397	2.4689	0.5231	0.096828
Average	4.995933	1.05682	0.14031	2.398533	0.458313	0.096792
Nd: 4,800 RPM						
	Channel 1: Radial			Channel 2: Axial		
	Peak to Peak (V)	DCVrms (V)	DCVrms mean (V)	Peak to Peak (V)	DCVrms (V)	DCVrms mean (V)
Run 1	4.9002	1.1426	0.141709	4.1306	0.825047	0.09761
Run 2	5.4052	1.37658	0.141809	3.5239	0.765368	0.097683
Run 3	5.69	1.16208	0.142014	4.058	0.794157	0.097831
Average	5.3318	1.227087	0.141844	3.904167	0.794857	0.097708
Nd: 5,400 RPM						
	Channel 1: Radial			Channel 2: Axial		
	Peak to Peak (V)	DCVrms (V)	DCVrms mean (V)	Peak to Peak (V)	DCVrms (V)	DCVrms mean (V)
Run 1	7.2003	1.85787	0.14307	6.5122	1.46867	0.098505
Run 2	7.3512	1.69621	0.143208	5.8943	1.29754	0.098591
Run 3	7.0918	1.96908	0.143425	5.5916	1.17677	0.098726
Average	7.214433	1.841053	0.143234	5.999367	1.314327	0.098607
Nd: 6,000 RPM						
	Channel 1: Radial			Channel 2: Axial		
	Peak to Peak (V)	DCVrms (V)	DCVrms mean (V)	Peak to Peak (V)	DCVrms (V)	DCVrms mean (V)
Run 1	7.8317	1.7444	0.144326	8	2.12368	0.099501
Run 2	7.6749	1.85882	0.144455	7.6296	1.69573	0.099642
Run 3	7.877	1.58517	0.144583	8	2.000133	0.099777
Average	7.7945	1.7295	0.1445	7.8765	1.9398	0.0996

APPENDIX C. REFURBISHMENT BASELINE RAW DATA

Performance Spreadsheet T63-A-720:

Engine Model	T63-A-720	Compressor SN	CAC-AC-18790	Accel: OK				Cruise B	Cruise A	Normal Cruise	takeoff	
Serial Number	AE-406244	Gearbox SN	CAG-AG-406244	BV Chk: OK		SPEC GPTOT		0	0	1360	1490	
Work Order	33733	Turbine SN	CAT-AT-18605	AI Chk: OK		Pred SHP @ SPEC MGT		0	0	375	454	
Run Number	1	Fuel Control SN	324455H	Preserved: OK		SPEC SHAFT PWR		185	278	370	420	
Run Date	3/21/2018	Governor SN	HR46645	Comment: OK		% DELTA FROM SPEC PWR		0	0	1.3	8.1	
Customer	Naval Academy	Fuel Temp	72	# Starts: 1		Predicted SFC		0.847	0.632	0.632	0.612	
Operator	Chris Carino	SG at Fuel Temp	0.81	Coastdn: 23.1		SPEC SFC		0.827	0.651	0.651	0.65	
Assistant	Nate Farnsworth	LHV (BTU/LB)	18523	Orifice: 4		% DELTA FROM SPEC SFC		2.5	-2	-3	-5.9	
Oil Flow in CCs:	0	Engine TT	1764									
Run Comments												
Functional test of engine plus 5 points for power												
Date		3/21/2018	3/21/2018	3/21/2018	3/21/2018	3/21/2018	3/21/2018	3/21/2018	3/21/2018	3/21/2018	3/21/2018	3/21/2018
time		9:26:30 AM	9:34:09 AM	9:40:17 AM	9:42:26 AM	9:45:22 AM	9:47:45 AM	9:50:01 AM	9:50:47 AM	9:51:05 AM	9:51:45 AM	9:56:12 AM
setting		Ground Idle	Run In	1st PPT	2nd PPT	3rd PPT	4th PPT	5th PPT	AintilceOff	AntilceOn	GvnrDroop	Shutdown
Run Time	HH:MM:SS	0:03:31	0:11:11	0:17:18	0:19:28	0:22:23	0:24:46	0:27:03	0:27:48	0:28:06	0:28:46	0:33:13
N1 RPM	RPM	32628	51947	48499	49434	50381	51267	51984	49009	48875	44710	31863
N1 PCT	%	64	101.9	95.1	96.9	98.8	100.5	101.9	96.1	95.8	87.7	62.5
Peak N1	rpm	32822	51947	51996	51996	51996	51996	52056	52056	52056	52056	52056
N1 RPM Corrected	RPM	0	51344	47902	48860	49796	50589	51296	48360	48251	44109	0
N2 RPM	RPM	26933	33274	33322	33274	33242	33227	33258	33258	33227	33892	23588
N2 PCT	%	80.9	100	100.1	100	99.9	99.8	99.9	99.9	99.8	1018	70.9
Max. N2	rpm	28312	33496	33496	33496	33496	33496	33496	33496	33496	34051	34051
Min. N2	rpm	-16	32101	32101	32101	32101	32101	32101	32101	32101	32101	23588
Dyno RPM	RPM	4868	6018	6032	6014	6011	6013	6013	6016	6010	6131	4253
Dyno Torque	lbs-ft	15	352.5	243	276	307.5	331.5	352.5	259.5	252	135	27
Dyno HP	HP	0	403.6	278.6	316	351.7	379	403.4	297	288.1	157.4	0
HP Corrected	HP	0	415.9	286.7	325.2	362	390.7	415.4	305.5	296.5	166	0
Dyno Tout Temp.	F	77	110	98	103	110	115	119	107	106	89	77
Engine Torquemeter	PSIG	4.6	96.6	67.5	76.1	84.1	91.3	96.3	71.5	69.6	38	6.7
GPTOT	F	956	1476	1280	1331	1379	1432	1471	1300	1338	1114	949
Peak T5	F	1322	1481	1481	1481	1481	1481	1481	1481	1481	1481	1481
GPTOT Corrected	F	0	1435	1237	1291	1339	1385	1424	1254	1292	1052	0
Wf Observed	PPH	66.8	248.5	188.7	206.7	220	235.7	247.5	194.2	195.4	136.6	63.8
Wf Corrected	PPH	0	258.9	196.2	215.4	229.1	244.9	257.2	201.8	203.3	140.2	0
Fuel Temp	F	77	69	69	70	69	69	69	69	69	70	75
SFC Corrected	LBS/HP/HR	0	0.6224	0.6844	0.6624	0.6327	0.6268	0.6192	0.6606	0.6856	0.8444	0
Main Oil Pressure	psig	119	119	119	119	119	120	125	125	126	125	91
Anti Ice Line	F	85	97	101	103	103	102	103	104	171	187	109
Baro	" HGA	28.54	28.54	28.54	28.54	28.54	28.54	28.54	28.54	28.54	28.54	28.54
CIP	" HGA	28.54	28.52	28.52	28.52	28.52	28.52	28.52	28.52	28.52	28.52	28.52
CIT	F	71	71.3	72	71.3	71.3	73	73	73	72.5	73.3	76.5
CDP	"Hg	44.5	175.9	145.6	153.7	161.8	169.9	173.9	149.6	145.6	113.2	42.5
CDP normalized	psia	0	106.4	90.9	95.1	99.2	103.3	105.4	93	90.9	75.2	0
CDT	F	284.5	595.9	536.1	552.7	571.2	587.1	599.5	550.7	551.2	473.1	282.1
CDT Normalized	F	0	563	503	521	539	551	563	516	517	447	0
Exhaust Static Prs	" HGA	28.56	28.11	28.24	28.15	28.11	28.19	28.13	28.21	28.21	28.42	28.56
Scavenge Oil Pressure	psig	22.6	28.3	26.6	27.3	27.2	27.9	30.4	28	28.6	26.7	18.3
Oil in Temp	F	107	179	177	177	176	176	176	177	177	176	177
Oil Out Temp	F	131	245	237	239	243	245	247	245	243	235	201
Comp Seal Vent Press	"Hg	2.2	8	6.3	6.9	7.1	7.1	6.9	5.9	5.7	4.3	1.8
Airflow Correced	PPM	0	4.02	3.63	3.71	3.83	3.95	3.97	3.69	3.57	3.14	0
Gear Box ST Prs	" H2O	2.7	12.5	9.3	10.8	12.1	12.9	12.8	10.9	9.7	6.9	3.3
Turbine Vibration	IPS	0.1	0.21	0.21	0.21	0.21	0.21	0.21	0.21	0.21	0.21	0.09
Gearbox Vibration	IPS	0.06	0.11	0.14	0.11	0.11	0.14	0.11	0.11	0.17	0.11	0.06
Reduction Gearbox Vibration	IPS	0.08	0.08	0.08	0.08	0.08	0.08	0.08	0.08	0.08	0.08	0.08
Compressor Vibration	IPS	0.12	0.28	0.32	0.38	0.32	0.26	0.3	0.28	0.3	0.28	0.08
Accel Time	Seconds	0	0	0	0	0	0	0	0	0	0	0
Decel Time	Seconds	0	0	0	0	0	0	0	0	0	0	0
N1 Coast Down Time	Seconds	0	0	0	0	0	0	0	0	0	0	0
N2 Coast Down Time	Seconds	0	0	0	0	0	0	0	0	0	0	0
Comments 1		Test Accepted										
Comments 2												
Comments 3												

Corrected SHP vs Temperature T63-A-720:

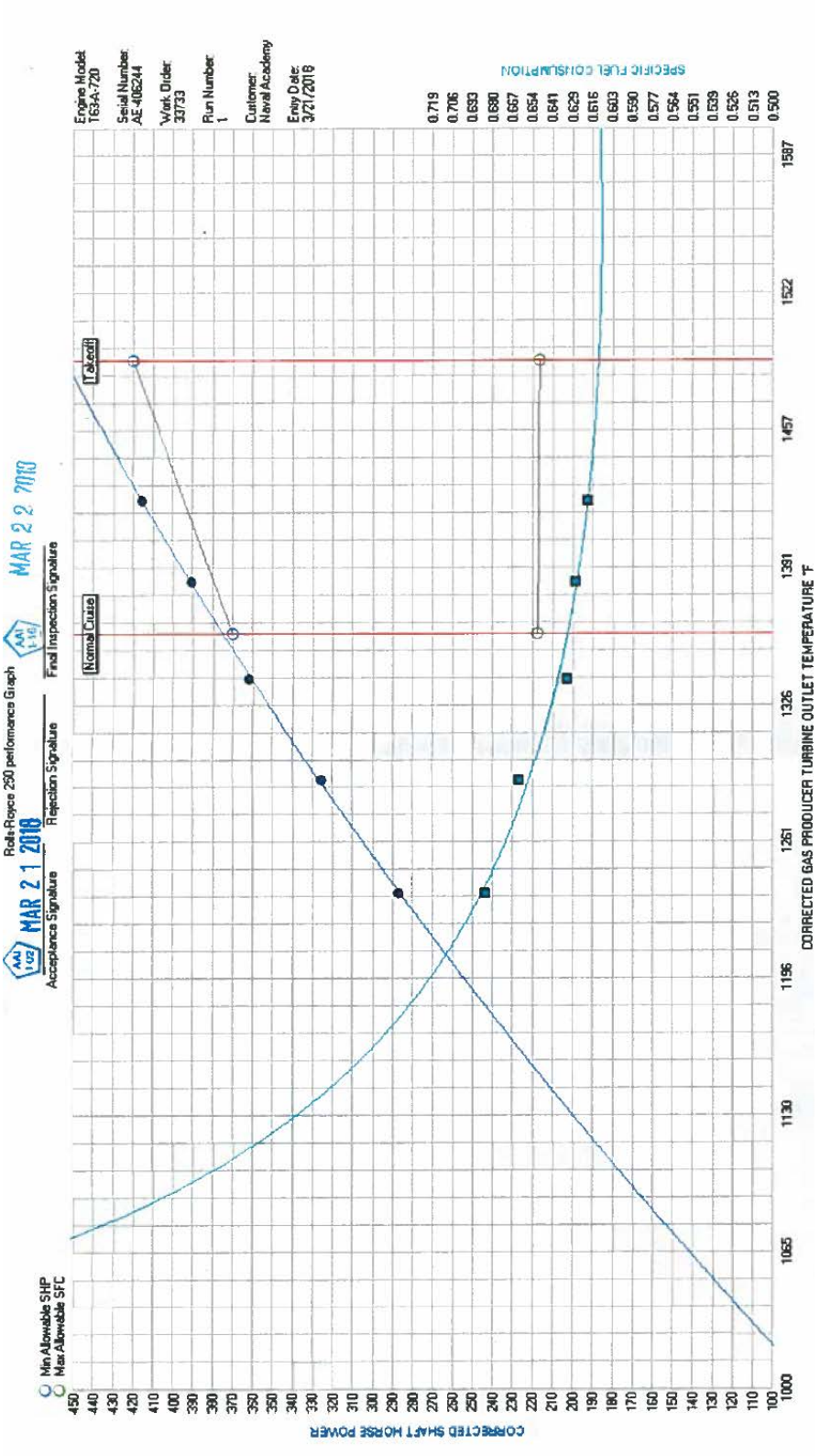

APPENDIX D. RAW MATLAB DATA

Run conducted on 01 November 2018:

PRESSURE																
Port	1	2	3	4	5	6	7	8	9	10	11	12	13	14	15	16
1.01	-999999	-999999	-999999	-999999	-999999	-999999	-999999	-999999	-999999	-999999	-999999	-999999	-999999	-999999	-999999	-999999
1.02	-279.7	-533.05	-503.76	-511.14	-504.59	-508.64	-628.03	-614.7	-660.77	-620.63	-638.48	-885.75	-905.88	-909.4	-910.64	-953.96
1.09	194.21	97.54	311.67	440.76	572.16	421.49	695.18	524.53	180.85	134.79	-6.49	22.2	103.49	79.98	170.35	373.29
1.10	-54.08	536.02	300.93	127.9	33.31	-61.64	285.33	309.07	607.72	638.1	-164.48	-897.56	-1086.9	-565.89	573.09	1055.56
2.01	-3505.97	-7247.3	-6924.42	-6438.62	-6747.92	-6214.13	-8288.89	-7829.94	-8067.58	-7959.87	-7666.18	-11220.44	-10716.77	-10743.23	-10587.31	-11479.86
2.02	-276.95	-532.02	-504.44	-511.01	-503.97	-508.12	-627.84	-614.2	-661.7	-620.15	-638.5	-885.13	-904.23	-908.64	-908.07	-953.5
2.09	198.29	105.32	314.87	450.05	567.71	430.93	687.59	547.54	182.29	132.88	-2.07	38.96	111.49	94.39	179.44	382.83
2.10	-50.62	538.63	301.23	126.32	34.41	-58.11	283.09	313.82	603.69	644.94	-161.65	-885.5	-1102.05	-545.44	566.77	1080.34
3.01	-3481.36	-7242.44	-6928.7	-6448.64	-6754.82	-6221.84	-8292.71	-7840.85	-8063.8	-7966.59	-7658.2	-11222.7	-10719.96	-10742.63	-10588.98	-11502.38
3.02	-264.62	-505.89	-490.32	-498.11	-494.21	-498.11	-618.74	-610.96	-661.55	-618.74	-645.98	-887.25	-902.81	-902.81	-922.27	-972.86
3.03	158172.28	328294.32	325838.42	306921	323766.99	298305.55	430489.4	410179.6	423254.56	417609.2	393277.89	568068.94	545752.32	551397.8	547513.81	581642.2
3.04	153095.48	316919.9	315166.43	297324.64	313248.13	289207.34	417075.28	397268.17	410118.42	404615.71	381557.66	553199.97	531433.75	536795.74	533269.38	565834.06
3.09	227.28	123.27	327.43	473.8	585.52	442.99	685.67	558.55	188.75	138.67	-7.7	26.97	115.56	92.45	207.95	392.9
3.10	-70.34	529.92	296.46	107.47	18.53	-88.85	266.8	314.98	607.72	644.78	-166.59	-925.49	-1136.5	-588.61	548.41	1082.03

TEMPERATURE																
Probe	1	2	3	4	5	6	7	8	9	10	11	12	13	14	15	16
1	297.53	294.39	298.23	309.37	299.1	313.5	298.58	311.19	304.63	306.51	321.45	305.54	316.17	314.9	321.27	305
2	299.53	294.94	299.77	308.5	300.35	313.26	299.89	310.46	303.05	306.67	313.36	305.69	309.35	313.62	312.95	304.5
3	416.56	486.41	491.88	503.97	492.48	506.14	532.45	545.04	540.72	540.22	552.64	589.55	602.11	600.54	605.53	590.19
4	418.35	487.99	493.32	504.33	494.06	506.86	533.8	543.45	539.08	539.9	548.65	588.26	597.51	596.51	599.98	590.14
5	821.96	847.92	862.57	885.43	860.86	882.76	915.98	941.7	923.48	922.98	935.33	1045.66	1045.44	1052.75	1062.56	1058.39
6	764.91	746.44	761.74	779.58	765.76	788.6	789.19	816.03	793.72	803.41	815.24	878.95	878.03	891.38	892.23	974.19
7	766.01	751.44	763.76	779.1	764.51	787.34	786.57	815.09	796.9	806.39	822.05	886.38	885.86	894.23	892.98	874.88
8	753.64	753.78	778.74	791.23	769.93	795.77	794.37	828.33	801.83	808.37	817.85	900.59	890.62	899.99	897.23	888.45
9	760.24	750.4	774.76	788.28	2563.62	2563.68	2563.73	2563.79	2563.83	2563.86	2563.9	2563.93	2563.97	2564	2564.05	2564.08

Run conducted on 08 November 2018:

			10" H2O			
N1	Nd	Timestamp	Comp inlet static	Comp inlet total	left stack	right stack
idle	idle	Pdata_20181108_1023_48	-999999	-264.49	210.29	-39.77
40890	3600	Pdata_20181108_1026_49	-999999	-478.73	118.74	415.77
40890	4200	Pdata_20181108_1028_24	-999999	-478.86	357.35	213.82
40890	4800	Pdata_20181108_1030_12	-999999	-480.24	490.31	144.63
40890	5400	Pdata_20181108_1032_07	-999999	-482.08	386.68	16.3
40890	6000	Pdata_20181108_1033_56	-999999	-487.35	484.3	-39.28
46000	6000	Pdata_20181108_1035_26	-999999	-635.62	751.53	339.72
46000	5400	Pdata_20181108_1037_03	-999999	-642.24	494.02	469.71
46000	4800	Pdata_20181108_1038_05	-999999	-635.48	272.17	813.5
46000	4200	Pdata_20181108_1039_10	-999999	-635.39	65.74	420.13
46000	3600	Pdata_20181108_1040_23	-999999	-635.77	90.41	-355.85
51000	3600	Pdata_20181108_1041_47	-999999	-942.14	82.72	-1107.58
51000	4200	Pdata_20181108_1043_17	-999999	-929.84	101.85	-1206.28
51000	4800	Pdata_20181108_1044_36	-999999	-937.99	176.73	-921.02
51000	5400	Pdata_20181108_1045_41	-999999	-937.07	37.29	-218.64
51000	6000	Pdata_20181108_1046_55	-999999	-942.42	331.66	961.63

			2.5 PSI			
N1	Nd	Timestamp	Comp inlet static	Comp inlet total	left stack	right stack
idle	idle	Pdata_20181108_1023_48	-3653.29	-260.13	220.28	-35.44
40890	3600	Pdata_20181108_1026_49	-6951.83	-473.68	126.37	419.01
40890	4200	Pdata_20181108_1028_24	-6893.02	-475.89	360.9	217.32
40890	4800	Pdata_20181108_1030_12	-6805.3	-476.78	498.99	145.94
40890	5400	Pdata_20181108_1032_07	-6788.32	-479.09	393.1	19.28
40890	6000	Pdata_20181108_1033_56	-6806.55	-483.37	488.29	-35.44
46000	6000	Pdata_20181108_1035_26	-8952.32	-632.81	754.74	340.17
46000	5400	Pdata_20181108_1037_03	-8978.26	-641.31	494.71	480.95
46000	4800	Pdata_20181108_1038_05	-8925.53	-632.99	273.33	796.45
46000	4200	Pdata_20181108_1039_10	-8901.21	-632.05	74.13	425.68
46000	3600	Pdata_20181108_1040_23	-8946.43	-633.23	88.21	-350.98
51000	3600	Pdata_20181108_1041_47	-13240.14	-940.09	84.09	-1140.5
51000	4200	Pdata_20181108_1043_17	-12658.34	-926.48	104.36	-1191.58
51000	4800	Pdata_20181108_1044_36	-12626.19	-936.09	187.52	-919.01
51000	5400	Pdata_20181108_1045_41	-12550.04	-933.95	51.14	-207.48
51000	6000	Pdata_20181108_1046_55	-12508.18	-939.35	339.68	990.75

			100 PSI					
N1	Nd	Timestamp	Comp inlet static	Comp inlet total	comp outlet left	comp outlet right	left stack	right stack
idle	idle	Pdata_20181108_1023_48	-3617.45	-241.27	164129.12	160697.26	254.24	-37.02
40890	3600	Pdata_20181108_1026_49	-6924.93	-451.41	308797.74	301084.34	154.09	429.87
40890	4200	Pdata_20181108_1028_24	-6875.79	-459.19	309610.48	301859.41	389.06	218.64
40890	4800	Pdata_20181108_1030_12	-6785.07	-455.3	307847.73	300075.27	539.3	148.23
40890	5400	Pdata_20181108_1032_07	-6769.95	-466.98	308698.67	301023.04	419.88	25.94
40890	6000	Pdata_20181108_1033_56	-6792.63	-474.76	307939.44	300251.9	512.33	-48.13
46000	6000	Pdata_20181108_1035_26	-8947.22	-618.74	446788.59	435273.8	781.98	333.52
46000	5400	Pdata_20181108_1037_03	-8981.24	-622.63	450909.18	439099.68	504.63	474.33
46000	4800	Pdata_20181108_1038_05	-8924.53	-618.74	448408.65	436815.22	304.32	774.5
46000	4200	Pdata_20181108_1039_10	-8898.07	-622.63	445141.98	433344.99	92.46	407.63
46000	3600	Pdata_20181108_1040_23	-8924.53	-622.63	442893.06	431354.79	111.71	-362.79
51000	3600	Pdata_20181108_1041_47	-13237.48	-933.95	613836.01	597109.84	96.3	-1136.5
51000	4200	Pdata_20181108_1043_17	-12655.36	-922.27	602387.43	585641.14	111.71	-1232.75
51000	4800	Pdata_20181108_1044_36	-12625.12	-922.27	608003.13	591503.43	196.45	-958.81
51000	5400	Pdata_20181108_1045_41	-12557.07	-933.95	609360.32	593013.89	61.64	-229.52
51000	6000	Pdata_20181108_1046_55	-12515.49	-926.16	611460.96	595092.61	342.83	952.36

			Temperature								
N1	Nd	Timestamp	Comp. Inlet 1	Comp. inlet 2	comp. outlet left	comp. out right	T5	Left Stack 1	Left Stack 2	Right Stack 1	Right Stack 2
idle	idle	Tdata_20181108_1023_48	290.81	291.3	407.69	409.22	802.29	745.97	747.38	735.11	741.92
40890	3600	Tdata_20181108_1026_49	291.42	292.63	475.05	476.72	836.01	741.1	745.32	745.07	741.58
40890	4200	Tdata_20181108_1028_24	291.51	293.29	476.28	478.17	839.78	743.34	743.63	754.93	750.55
40890	4800	Tdata_20181108_1030_12	293.32	293.82	477.57	478.21	839.64	747.88	744.93	748.96	749.32
40890	5400	Tdata_20181108_1032_07	293.14	294.09	478.12	479.49	838.43	750.22	748.52	749.88	753.06
40890	6000	Tdata_20181108_1033_56	292.49	293.89	477.41	478.42	829.79	747.24	747.01	747.91	750.17
46000	6000	Tdata_20181108_1035_26	291.95	293.03	528.39	528.94	907.76	777.46	773.52	779.69	2561.74
46000	5400	Tdata_20181108_1037_03	291.68	292.32	529.13	529.7	912.31	839.98	777.56	785.54	2561.83
46000	4800	Tdata_20181108_1038_05	291.44	292.68	528.51	529.1	907.48	1009.4	777.31	781.47	2561.88
46000	4200	Tdata_20181108_1039_10	292.41	293.87	529.39	530.03	902	832.34	779.22	778.86	2561.93
46000	3600	Tdata_20181108_1040_23	292.95	294.02	529.44	529.46	894.05	795.25	776.89	780.29	2561.99
51000	3600	Tdata_20181108_1041_47	292.46	292.85	580.63	582.09	1049.93	866.71	877.32	900.86	2562.06
51000	4200	Tdata_20181108_1043_17	292.44	293.07	577.35	579.05	1026.38	881.92	858.97	873.69	2562.14
51000	4800	Tdata_20181108_1044_36	292.53	293.24	579.43	581.3	1038.7	870	863.93	878.57	2562.2
51000	5400	Tdata_20181108_1045_41	292.85	293.47	580.33	581.66	1047.58	906.27	862.51	879.44	2562.25
51000	6000	Tdata_20181108_1046_55	292.84	292.91	580.26	582.01	1053.3	1388.51	858.94	881.87	2562.3

Run conducted on 19 November 2018:

			10" H2O											
N1	Nd	Timestamp	Comp inlet static	Comp inlet total	Right stack 2	right stack 3	left stack 1	right stack 1	risght stack 4	right stack 5	left stack 2	left stack 3	left stack 4	left stack 5
idle	idle	Pdata_20181119_1012_02	-999999	-256.06	177.62	79.38	232.34	-39.45	-235.36	29.55	-10.28	1.93	-65.55	-19.54
40890	3600	Pdata_20181119_1018_41	-999999	-483.78	73.6	-14.98	120.83	479.44	-480.08	39.88	150.31	64.87	-264.7	22.57
40890	4200	Pdata_20181119_1019_43	-999999	-480.33	198.79	32.43	351.72	218.38	-574.26	55.67	138.5	65.74	-229.65	11.22
40890	4800	Pdata_20181119_1021_59	-999999	-483.22	189.95	51.02	475.56	157.41	-604.84	69.71	146.06	68.95	-208.47	1.73
40890	5400	Pdata_20181119_1023_28	-999999	-485.81	289.33	126.08	412.06	29.43	-498.37	78.78	83.07	38.98	-166.64	-10.25
40890	6000	Pdata_20181119_1024_43	-999999	-488.58	411.3	197.99	503.71	-31.75	-457.54	96.29	43.3	21.37	-150.65	-17.54
46000	6000	Pdata_20181119_1026_07	-999999	-632.99	275.63	56.55	710.22	331.69	-948.1	122.28	252.46	129.29	-373.96	20.01
46000	5400	Pdata_20181119_1027_50	-999999	-637.06	321.33	40.61	455.38	496.65	-928.04	109.93	202.78	98.91	-438.77	37.49
46000	4800	Pdata_20181119_1028_51	-999999	-639.01	121.92	-15.83	279.21	830.34	-785.66	78.92	257.49	134.24	-443.33	54.76
46000	4200	Pdata_20181119_1029_50	-999999	-632.72	135.96	5.49	54.7	454.04	-740.32	72.6	267.45	149.6	-526.41	65.05
46000	3600	Pdata_20181119_1030_56	-999999	-636.23	212.41	63.42	78.47	-344.67	-627.79	66.81	143.06	120.94	-600.68	75.22
51000	3600	Pdata_20181119_1031_58	-999999	-916.26	343.88	137.28	47.79	-1115.81	-527.87	76.01	171.59	175.58	-1473.78	158.4
51000	4200	Pdata_20181119_1033_50	-999999	-917.17	437.92	190.72	72.44	-1171.01	-777.67	100.53	308.58	182	-1093.62	140.92
51000	4800	Pdata_20181119_1034_55	-999999	-934.54	395.84	141.04	204.43	-916	-896.81	111.43	306.64	220.73	-966.77	132.45
51000	5400	Pdata_20181119_1035_50	-999999	-928.79	286.77	56.71	68.59	-249.37	-1096.77	131.65	460.46	254.51	-921.47	127.09
51000	6000	Pdata_20181119_1036_45	-999999	-931.95	277.76	19.77	354.81	846.28	-1200.16	139.13	497.52	254.63	-792.13	111.78

			2.5 PSID											
N1	Nd	Timestamp	Comp inlet static	Comp inlet total	Right stack 2	right stack 3	left stack 1	right stack 1	risght stack 4	right stack 5	left stack 2	left stack 3	left stack 4	left stack 5
idle	idle	Pdata_20181119_1012_02	-3527.2	-252.38	179.09	81.36	240.74	-31.28	-234.7	36.34	-8.94	4.06	-61.1	-16.56
40890	3600	Pdata_20181119_1018_41	-7099.72	-478.78	76.17	-10.53	147.59	466.22	-477.51	49.18	153.29	68.78	-260.14	28.5
40890	4200	Pdata_20181119_1019_43	-6999.06	-475.38	201.47	36.09	363.91	224.32	-570.09	67.98	141.11	70.81	-223.65	17.16
40890	4800	Pdata_20181119_1021_59	-6999.59	-477.08	193.39	57.08	498.64	166.97	-601.22	80.22	149.13	74.54	-200.52	7.77
40890	5400	Pdata_20181119_1023_28	-7000.68	-479.66	291.95	128.29	421.31	32.5	-493.48	91.16	85.86	42.35	-160.18	-4.87
40890	6000	Pdata_20181119_1024_43	-6992.45	-483.94	413.83	199.81	508.34	-24.27	-449.36	104	46.34	27.44	-143.27	-11.04
46000	6000	Pdata_20181119_1026_07	-9148.9	-629.07	278.58	58.4	718.95	347.99	-945.28	135.33	255.78	134.17	-369.59	27.85
46000	5400	Pdata_20181119_1027_50	-9133.23	-631.8	327.08	45.93	492.18	494.58	-931.48	123.43	206.77	107.06	-423.58	45.66
46000	4800	Pdata_20181119_1028_51	-9114.3	-632.48	126.54	-10.53	324	813.57	-787.74	93.35	261.43	142.3	-438.7	62.5
46000	4200	Pdata_20181119_1029_50	-9063.28	-628.74	138.05	11.15	78.86	443.91	-738.22	83.33	270.34	158.56	-521.33	72.54
46000	3600	Pdata_20181119_1030_56	-9069.35	-631.46	217.33	67.91	90.58	-332.14	-625.92	78.94	146.46	127.73	-597.77	83.56
51000	3600	Pdata_20181119_1031_58	-13277.82	-909.61	346.98	142.38	68.4	-1038.34	-522.99	87.72	172.31	179.91	-1473.44	167.43
51000	4200	Pdata_20181119_1033_50	-12785.67	-908.89	443.36	196.18	111.8	-1200.81	-776.37	114.65	312.51	184.99	-1086.23	148.65
51000	4800	Pdata_20181119_1034_55	-12866.96	-926.61	400.77	146.32	235.96	-899.01	-891.69	123.73	309.47	232.38	-962.84	140.54
51000	5400	Pdata_20181119_1035_50	-12692.84	-920.15	293.81	65.29	106.42	-182.36	-1091.73	140.97	464.82	261.19	-915.08	134.4
51000	6000	Pdata_20181119_1036_45	-12648.35	-923.89	278.89	22.63	390.2	889.29	-1199.74	150.37	500.76	255.8	-790.2	117.55

			100 PSID												
N1	Nd	Timestamp	Comp inlet static	Comp inlet total	comp outlet	comp outlet	Right stack 2	right stack 3	left stack 1	right stack 1	risght stack 4	right stack 5	left stack 2	left stack 3	left stack 4	left stack 5
idle	idle	Pdata_20181119_1012_02	-3544.94	-256.84	149690.25	153581.5	153.32	98.41	223.42	-59.23	-250.33	0	-39.41	-15.17	-108.59	-45.48
40890	3600	Pdata_20181119_1018_41	-7105.45	-513.67	299728.81	302919.26	46	-7.56	146.38	437.27	-500.65	7.35	142.06	22.77	-310.27	0
40890	4200	Pdata_20181119_1019_43	-7006.73	-521.46	297342.39	300425.2	168.65	30.29	362.1	185.26	-578.88	36.74	110.49	30.36	-279.24	-7.58
40890	4800	Pdata_20181119_1021_59	-6992.99	-505.79	298044.82	301230.51	153.38	60.56	477.66	155.59	-594.53	58.77	134.12	68.32	-217.26	-15.16
40890	5400	Pdata_20181119_1023_28	-7008.11	-505.72	297918.53	301008.22	253.07	158.96	423.61	29.64	-492.83	73.46	63.12	37.95	-186.22	-30.32
40890	6000	Pdata_20181119_1024_43	-7008.11	-505.72	295655.69	299105.06	391.04	227.09	523.73	-22.21	-438.07	95.5	15.79	15.19	-162.94	-37.9
46000	6000	Pdata_20181119_1026_07	-9185.38	-669.11	431662.64	433827.49	275.97	68.12	747.05	333.4	-946.55	117.53	228.88	129.05	-387.96	0
46000	5400	Pdata_20181119_1027_50	-9170.26	-630.42	434231.91	435652.83	306.64	75.69	492.93	481.74	-915.26	102.85	165.71	91.09	-457.8	22.75
46000	4800	Pdata_20181119_1028_51	-9146.38	-630.42	434712.21	435606.88	99.66	7.57	300.47	807.85	-790.09	66.12	236.73	136.63	-473.32	37.92
46000	4200	Pdata_20181119_1029_50	-9100.42	-630.42	430984.19	431795.99	122.66	37.85	77.04	407.63	-743.16	73.46	252.5	144.22	-550.91	37.91
46000	3600	Pdata_20181119_1030_56	-9106.78	-638.2	429634.79	430991.38	206.99	83.26	107.86	-347.95	-633.64	44.08	126.28	113.87	-636.26	53.07
51000	3600	Pdata_20181119_1031_58	-13296.25	-918.39	595645.8	585334.34	345.02	151.41	77.04	-1058.7	-524.12	66.12	142.07	159.42	-1489.78	136.49
51000	4200	Pdata_20181119_1033_50	-12783.93	-918.39	597431.19	580297.65	421.79	204.45	92.45	-1199.44	-782.27	80.81	315.62	151.87	-1109.58	121.32
51000	4800	Pdata_20181119_1034_55	-12851.97	-933.95	608204.1	589852.5	383.44	143.88	223.42	-895.88	-891.79	102.85	292.02	205.03	-993.19	113.74
51000	5400	Pdata_20181119_1035_50	-12685.65	-933.95	607784.94	590397.16	268.41	60.58	92.45	-207.31	-1095.18	117.54	434.09	220.21	-954.39	113.75
51000	6000	Pdata_20181119_1036_45	-12632.73	-941.74	609432	591662.95	253.07	22.72	377.51	852.32	-1189.05	124.88	465.66	220.21	-822.48	75.83

			Temperature													
N1	Nd	Timestamp	Comp. Inlet 1	Comp. inlet 2	comp. outlet left	comp. out right	T5	Left Stack 1	Left Stack 2	Right Stack 1	Right Stack 2	Left Stack 3	Left Stack 4	Left Stack 5	Right Stack 3	Right Stack 4	Right Stack 5
idle	idle	Tdata_20181119_1012_02	290.86	2561.87	406.05	407.17	795.75	750.18	2561.87	734.89	741.36	729.61	724.73	710.96	731.48	727.31	720.21
40890	3600	Tdata_20181119_1018_41	291.02	2562.13	474.06	477.23	832.21	737.1	2562.13	743.04	739.39	729.7	726.6	716.67	743.89	739.32	728.78
40890	4200	Tdata_20181119_1019_43	290.97	2562.16	474.53	477.8	835.91	740.54	2562.16	750.68	2562.16	728.2	726.02	714.62	746.38	743.24	732.39
40890	4800	Tdata_20181119_1021_59	291.36	2562.24	475.04	478.78	835.15	741.78	2562.24	746.74	2562.24	729.88	727.8	713	740.85	739.53	731.29
40890	5400	Tdata_20181119_1023_28	290.8	2562.29	475.29	479.22	833.13	744.95	2562.29	745.77	2562.29	731.9	728.74	717.54	741.34	738.81	734.2
40890	6000	Tdata_20181119_1024_43	291.73	2562.33	475.39	478.97	826.87	743.45	2562.33	746.2	2562.33	727.64	724.32	715.1	742.2	739.18	736.77
46000	6000	Tdata_20181119_1026_07	292.4	2562.38	527.04	527.32	904.36	775.99	2562.38	778.49	2562.38	764.14	762.15	747.1	774.4	772.77	764.73
46000	5400	Tdata_20181119_1027_50	292.4	2562.42	528.37	528.97	905.64	827.03	2562.42	782.1	2562.42	761.75	759.83	748.39	780.63	777.31	765.87
46000	4800	Tdata_20181119_1028_51	292.36	2562.45	527.88	528.79	902.06	1010.89	2562.45	776.84	2562.45	763.91	761.82	752.62	778.2	774.17	765.12
46000	4200	Tdata_20181119_1029_50	293.42	2562.49	528.96	528.93	896.2	1174.1	2562.49	774.59	2562.49	767.73	764.97	755.16	774.51	770.24	761.54
46000	3600	Tdata_20181119_1030_56	293.32	2562.52	528.93	527.92	892	768.83	2562.52	779.7	2562.52	770.28	767.14	758.4	775.02	771.2	760.58
51000	3600	Tdata_20181119_1031_58	292.15	2562.56	573.12	574.2	1032.15	854.68	2562.56	883.8	2562.56	863.67	862.45	852.17	875.06	867.64	859.4
51000	4200	Tdata_20181119_1033_50	292.47	2562.61	575.46	575.34	1020.37	852.4	2562.61	871.79	2562.61	853.01	849.4	839.92	866.41	862.26	849.8
51000	4800	Tdata_20181119_1034_55	292.83	2562.64	578.44	579.83	1036.62	856.82	2562.64	874.82	2562.64	852.24	848.16	838.05	871.15	866.4	852.11
51000	5400	Tdata_20181119_1035_50	292.44	2562.67	577.58	578.45	1041.01	877.56	2562.67	874.43	2562.67	849.13	845.91	834.89	875.44	870	858.2
51000	6000	Tdata_20181119_1036_45	292.82	2562.69	578.18	580	1048.49	892.32	2562.69	878.05	2562.69	845.41	843.42	832.4	880.34	874.97	863.12

Run conducted on 20 November 2018:

			10" H2O											
N1	Nd	Timestamp	Comp inlet static	Comp inlet total	Right stack 2	right stack 3	left stack 1	right stack 1	risght stack 4	right stack 5	left stack 2	left stack 3	left stack 4	left stack 5
idle	idle	Pdata_20181120_1151_21	-999999	-258.34	729.62	666.16	730.37	-65.99	706.24	723.35	62.63	6.77	-91.92	-15.81
40890	3600	Pdata_20181120_1155_58	-999999	-481.82	706.77	648.85	793.88	482.16	795.1	794.44	307.09	125.47	-372.64	31.23
40890	4200	Pdata_20181120_1158_01	-999999	-481.75	660.08	665.65	916.54	237.98	844.86	850.59	360.54	145.14	-315.87	35.06
40890	4800	Pdata_20181120_1200_03	-999999	-481.07	716.11	733.26	915.21	-29.72	928.31	933.58	303.98	141.93	-299.49	36.69
40890	5400	Pdata_20181120_1201_45	-999999	-480.84	1424.02	1322.7	1427.65	-19.54	1429.43	1451.93	166.49	98.13	-262.42	1.43
40890	6000	Pdata_20181120_1203_41	-999999	-487.06	1686.85	1544.47	1727.43	-96.01	1671.26	1673.94	135.9	55.96	-213.54	-10.25
46000	3600	Pdata_20181120_1206_12	-999999	-635.8	1122.48	1017.04	1051.77	-537.77	1196.39	1160.21	343.99	180.6	-776.33	67.46
46000	4200	Pdata_20181120_1207_57	-999999	-637.65	1158.74	1057.57	1179.52	-137.07	1273.96	1244.95	429.14	212.63	-688.64	63.47
46000	4800	Pdata_20181120_1209_09	-999999	-640.97	1200.63	1118.51	1413.8	579.97	1403.32	1378.17	511.49	238.09	-630.41	59.36
46000	5400	Pdata_20181120_1211_05	-999999	-638.04	1160.02	1149.18	1690.12	511.13	1485.93	1468.29	557.36	247.43	-557.99	58.17
46000	6000	Pdata_20181120_1212_42	-999999	-638.62	1129.28	1178.23	1757.05	138.7	1540.73	1520.4	503.71	234.17	-497.7	67.03
51000	3600	Pdata_20181120_1216_13	-999999	-837.45	1499.98	1343.09	1308.13	-948.68	1523.39	1495.03	233.01	204.04	-1292.52	127.64
51000	4200	Pdata_20181120_1219_13	-999999	-856.94	1661.3	1490.07	1520.94	-1052.45	1727.63	1665.9	376.25	246.46	-1170.3	115.05
51000	4800	Pdata_20181120_1221_19	-999999	-833.54	1598.49	1464.71	1493.47	-724.1	1757.06	1700.02	659.71	318.61	-1004.53	108.68
51000	5400	Pdata_20181120_1222_56	-999999	-841.63	1661.69	1515.85	1780.35	-188.3	1887.37	1832.7	634.85	352.65	-1973.53	91.45
51000	6000	Pdata_20181120_1224_13	-999999	-830.69	1709.85	1595.56	2215.93	741.3	2012.19	1969.6	693.55	362.84	-866.13	81.79

			2.5 PSID											
N1	Nd	Timestamp	Comp inlet static	Comp inlet total	Right stack 2	right stack 3	left stack 1	right stack 1	risght stack 4	right stack 5	left stack 2	left stack 3	left stack 4	left stack 5
idle	idle	Pdata_20181120_1151_21	-3557.02	-253.15	732.46	669.74	741.2	-63.85	708.54	730.22	64.13	8.47	-88.62	-12.02
40890	3600	Pdata_20181120_1155_58	-7032.18	-479.12	708.52	651.45	801.61	485.21	797.45	800.46	308.19	128	-370.12	34.31
40890	4200	Pdata_20181120_1158_01	-6979.26	-478.11	661.85	669.04	936.53	235.18	846.9	857.56	361.93	147.63	-312.45	38.19
40890	4800	Pdata_20181120_1200_03	-6903.86	-475.93	718.43	735.94	927.34	-28.41	930.67	938.71	305.5	143.56	-297.04	39.81
40890	5400	Pdata_20181120_1201_45	-6824.66	-480.21	1418.06	1314.88	1413.5	-19.15	1424.92	1449.08	168.32	99.56	-261.17	4.21
40890	6000	Pdata_20181120_1203_41	-6849.05	-483.54	1688.66	1546.75	1722.29	-89.36	1672.72	1678.7	138.02	57.56	-210.99	-7.47
46000	3600	Pdata_20181120_1206_12	-9007.72	-632.9	1125.05	1021.59	1058.28	-538.74	1197.65	1164.63	346.09	185.57	-771.86	74.75
46000	4200	Pdata_20181120_1207_57	-8971.04	-634.43	1160.94	1061.27	1178.71	-118.11	1275.89	1247.98	430.21	212.63	-686.86	67.95
46000	4800	Pdata_20181120_1209_09	-8995.88	-638.83	1201.98	1120.63	1409	605.95	1404.55	1382.15	513.05	241.41	-627.57	63.75
46000	5400	Pdata_20181120_1211_05	-8908.04	-634.94	1162.83	1151.13	1734.01	520.54	1487.18	1470.28	558.68	248.18	-552.5	62.78
46000	6000	Pdata_20181120_1212_42	-8904.54	-635.11	1130.47	1181.31	1747.63	146.22	1541.52	1524.35	505.48	235.01	-493.87	71.19
51000	3600	Pdata_20181120_1216_13	-11434.8	-832.87	1500.76	1344.3	1297.58	-934.81	1525.85	1495.55	234.49	203.16	-1291.61	130.4
51000	4200	Pdata_20181120_1219_13	-11474.9	-852.57	1662.64	1490.89	1515.25	-1020.35	1730.63	1668.36	377.25	245.1	-1169.06	118.78
51000	4800	Pdata_20181120_1221_19	-11080.4	-828.79	1600.05	1465.97	1496.74	-730.23	1759.35	1705.41	661.75	317.93	-1001.73	112.28
51000	5400	Pdata_20181120_1222_56	-11083.5	-837.95	1663.05	1516.8	1788.06	-181.6	1889.62	1836.79	637.45	354.11	-1974.6	98.03
51000	6000	Pdata_20181120_1224_13	-10970.6	-826.3	1711.03	1599.12	2214.54	716.45	2014.68	1973.6	695.4	366.92	-859.86	88

			100 PSID												
N1	Nd	Timestamp	Comp inlet static	Comp inlet total	comp outlet left	comp outlet right	Right stack 2	right stack 3	left stack 1	right stack 1	risght stack 4	right stack 5	left stack 2	left stack 3	left stack 4	left stack 5
idle	idle	Pdata_20181120_1151_21	-3530.5	-241.27	162831.1	157450.4	736.19	681.49	762.71	-81.44	720.57	734.35	55.24	0	-85.35	-37.89
40890	3600	Pdata_20181120_1155_58	-7023.2	-466.97	314273.7	303701.6	713.18	658.77	839.75	474.33	814.56	807.78	307.8	121.49	-364.68	7.58
40890	4200	Pdata_20181120_1158_01	-6962.72	-466.97	314937.6	304177.4	667.17	689.06	963.02	200.1	869.39	859.18	347.26	136.68	-310.37	30.33
40890	4800	Pdata_20181120_1200_03	-6909.8	-466.97	312594.9	302174.6	728.52	749.64	955.32	-51.83	947.71	954.65	284.13	136.68	-302.61	30.33
40890	5400	Pdata_20181120_1201_45	-6819.08	-466.97	308359.6	297946.3	1441.71	1347.84	1463.79	-51.83	1464.65	1461.35	149.96	75.93	-271.57	-7.58
40890	6000	Pdata_20181120_1203_41	-6849.32	-466.97	308527.5	298023.1	1687.11	1575	1764.25	-118.46	1691.79	1689	94.71	37.97	-225.02	-37.89
46000	3600	Pdata_20181120_1206_12	-8996.34	-630.41	443160	428619.5	1134.96	1037.37	1101.69	-584.91	1206.18	1174.96	331.4	151.87	-768.16	53.08
46000	4200	Pdata_20181120_1207_57	-8981.21	-622.63	445431.9	431556.5	1165.63	1075.24	1194.14	-162.89	1300.17	1241.05	426.09	212.56	-690.57	37.91
46000	4800	Pdata_20181120_1209_09	-9017.83	-622.63	450905.6	436610.8	1196.31	1135.81	1402.15	600.32	1417.65	1387.92	512.92	265.68	-644.02	53.08
46000	5400	Pdata_20181120_1211_05	-8933.49	-622.63	448984.5	434802.2	1165.63	1166.09	1741.12	548.44	1495.97	1476.04	560.36	265.67	-558.66	37.91
46000	6000	Pdata_20181120_1212_42	-8925.94	-638.2	448306	434081.5	1134.96	1203.96	1795.05	148.22	1558.63	1512.75	481.43	242.9	-496.59	45.49
51000	3600	Pdata_20181120_1216_13	-11449.5	-817.2	550890.1	535997.9	1503.04	1362.97	1294.28	-925.49	1527.29	1498.06	236.68	220.13	-1303.55	106.16
51000	4200	Pdata_20181120_1219_13	-11481.3	-848.33	562510.3	547505.9	1664.08	1514.4	1517.69	-1043.95	1746.59	1674.29	363.04	250.49	-1179.4	106.16
51000	4800	Pdata_20181120_1221_19	-11060.2	-824.99	552979.6	538750.3	1595.06	1521.43	1517.69	-762.6	1770.08	1696.32	662.7	318.8	-1008.7	98.57
51000	5400	Pdata_20181120_1222_56	-11075.3	-840.55	555770.3	541103.9	1648.73	1566.85	1802.73	-192.5	1903.23	1835.84	623.48	356.76	-1986.36	83.41
51000	6000	Pdata_20181120_1224_13	-10969.4	-817.2	552148.6	537684.8	1702.41	1642.54	2226.45	681.83	2012.87	1968.01	686.61	371.94	-861.27	75.82

Temperature															
N1	Nd	Timestamp	Comp. Inlet 1	Comp. inlet 2	comp. outlet left	comp. out right	T5	Left Stack 1	Left Stack 2	Right Stack 1	Right Stack 2	Left Stack 3	Left Stack 4	Left Stack 5	Right Stack 3
idle	idle	Tdata_20181120_1151_21	290.89	291.25	407.15	407.74	814.03	757.58	2563.95	747.87	755.07	743.83	737.09	716.48	741.47
40890	3600	Tdata_20181120_1155_58	291.14	291.8	475.59	477.36	835.95	741.28	2563.94	741.99	739.17	737.73	734.41	721.89	743.38
40890	4200	Tdata_20181120_1158_01	291.34	292.22	476.7	478.49	840.1	741.18	2563.95	747.62	2563.95	734.31	732.1	722.21	748.65
40890	4800	Tdata_20181120_1200_03	292.47	293.41	477.67	478.38	840.79	742.32	2563.98	752.06	2563.98	734.17	732.16	724.46	748.74
40890	5400	Tdata_20181120_1201_45	293.92	294.56	478.26	478.22	839.67	748.98	2564	755.17	2564	739.34	736.53	725.06	750.09
40890	6000	Tdata_20181120_1203_41	293.89	294.07	477.92	478.29	832.95	747.01	2564	755.15	2564	738.65	735.09	721.59	749.01
46000	3600	Tdata_20181120_1206_12	293.34	293.93	528.71	527.91	893.86	772.68	2564.01	778.78	2564.01	776.16	772.03	761.38	774.33
46000	4200	Tdata_20181120_1207_57	293.73	293.91	529.97	529.37	902.09	778.61	2564.02	779.02	2564.02	775.87	772.35	761.01	778.09
46000	4800	Tdata_20181120_1209_09	293.06	294.1	530.78	530.58	910.13	780.85	2564.03	782.56	2564.03	774.46	772.06	760.65	784.01
46000	5400	Tdata_20181120_1211_05	293.36	293.19	530.26	529.61	911.65	805.86	2564.03	784.74	2564.03	768.46	766.77	755.66	784.56
46000	6000	Tdata_20181120_1212_42	292.92	293.36	530	529.26	909.85	790.77	2564.04	784.06	2564.04	769.34	767.07	760.76	781.11
51000	3600	Tdata_20181120_1216_13	295.17	295.34	567.55	566.25	987.19	895.54	2564.05	851.33	2564.05	844.49	841.29	830.88	843.51
51000	4200	Tdata_20181120_1219_13	296.14	295.41	571.29	569.45	999.35	956.66	2564.04	852.33	2564.04	842.95	838.5	826.54	847.26
51000	4800	Tdata_20181120_1221_19	296.31	295.28	568.46	566.35	995.34	922.56	2564.06	844.27	2564.06	834.85	831.03	818.07	842.52
51000	5400	Tdata_20181120_1222_56	295.33	295.19	567.79	566.64	1002.88	1022.42	2564.06	846.56	2564.06	830.31	827.43	814.17	847.63
51000	6000	Tdata_20181120_1224_13	294.44	294.49	564.67	563.78	997.52	1064.5	2564.07	843.84	2564.07	823.09	821.3	808.09	845.63

APPENDIX E. ANSYS WORKBENCH SETUP

Mesh element:

Details of "Geometry"

Definition	
Source	E:\Buck\CFD Project\CFD_term_project_files\dp0\CFX\DM\CFX...
Type	SpaceClaim
Length Unit	Meters
Bounding Box	
Length X	8.1472e-002 m
Length Y	6.483e-002 m
Length Z	8.1472e-002 m
Properties	
Volume	8.3621e-005 m^3
Scale Fact...	1.
Statistics	
Bodies	1
Active Bod...	1
Nodes	845683
Elements	2096576
Mesh Metric	None
Basic Geometry Options	
Solid Bodies	Yes
Surface Bo...	Yes
Line Bodies	Yes
Parameters	Independent
Parameter ...	
Attributes	Yes
Attribute K...	
Named Sel...	Yes
Named Sel...	
Material Pr...	Yes
Advanced Geometry Options	
Use Associ...	Yes
Coordinat...	Yes
Coordinat...	
Reader Mo...	No
Use Instan...	Yes
Smart CAD...	Yes
Compare P...	No
Analysis Ty...	3-D
Mixed Imp...	None
Decompos...	Yes
Enclosure ...	No

Details of "Mesh"	
Display	
Display Style	Body Color
Defaults	
Physics Preference	CFD
Solver Preference	CFX
Relevance	0
Element Order	Linear
Sizing	
Size Function	Proximity and Curvature
Relevance Center	Coarse
Max Face Size	Default (6.5896e-003 m)
Mesh Defeaturing	Yes
Defeature Size	Default (3.2948e-005 m)
Transition	Slow
Growth Rate	Default (1.20)
Span Angle Center	Fine
Min Size	Default (6.5896e-005 m)
Max Tet Size	Default (1.3179e-002 m)
Curvature Nor...	36.0 °
Proximity Min ...	Default (6.5896e-005 m)
Num Cells Acr...	1
Proximity Size Fu...	Faces and Edges
Bounding Box Di...	0.13220 m
Minimum Edge L...	6.5767e-006 m
Quality	
Check Mesh Qua...	Yes, Errors
Target Skewn...	Default (0.900000)
Smoothing	Medium
Mesh Metric	None
Inflation	
Use Automatic In...	All Faces in Chosen Named Selection
Named Selection	IMPELLER
Inflation Option	Smooth Transition
Transition Ratio	0.77
Maximum Lay...	20
Growth Rate	1.1
Inflation Algorit...	Pre
View Advanced ...	No
Advanced	
Number of CPUs ...	Program Controlled
Straight Sided El...	
Number of Retries	0
Rigid Body Beha...	Dimensionally Reduced
Mesh Morphing	Disabled
Triangle Surface ...	Program Controlled
Topology Checki...	No
Pinch Tolerance	Default (5.9306e-005 m)
Generate Pinch o...	No
Statistics	
Nodes	845683
Elements	2096576

Setup element:

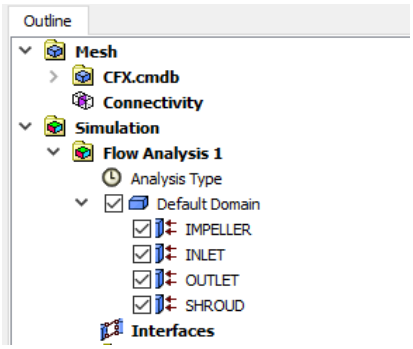

Default Domain:

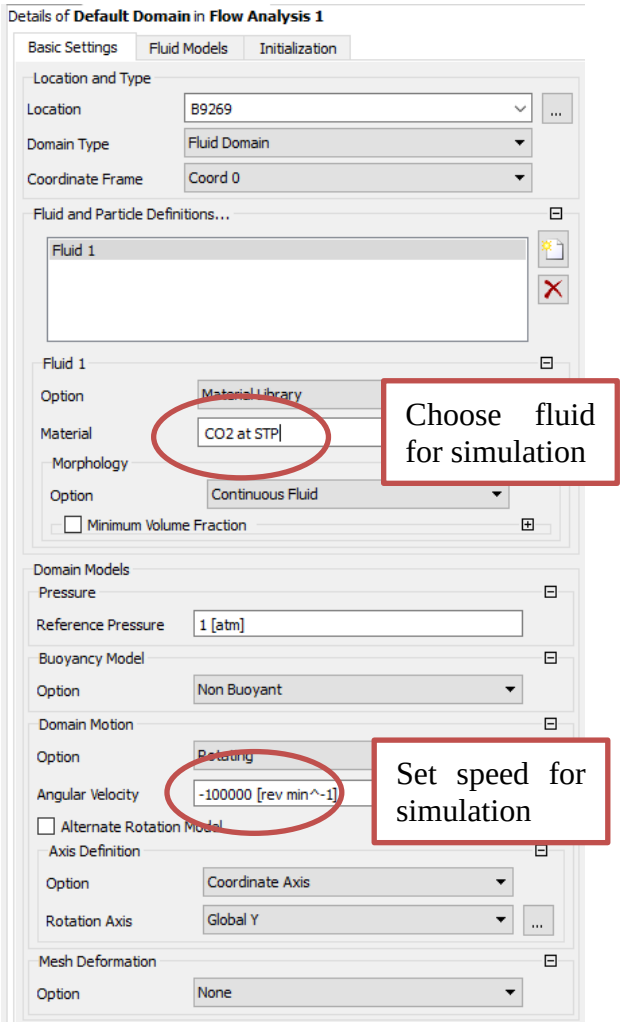

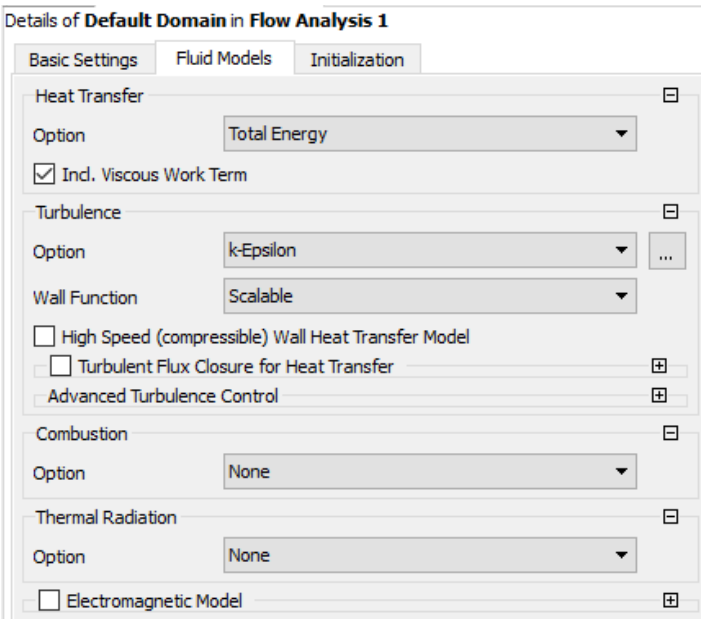

IMPELLER:

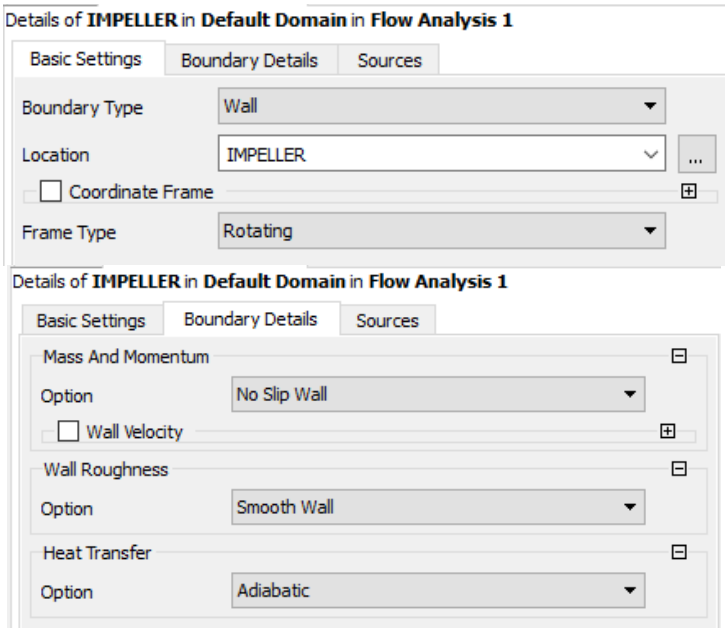

INLET:

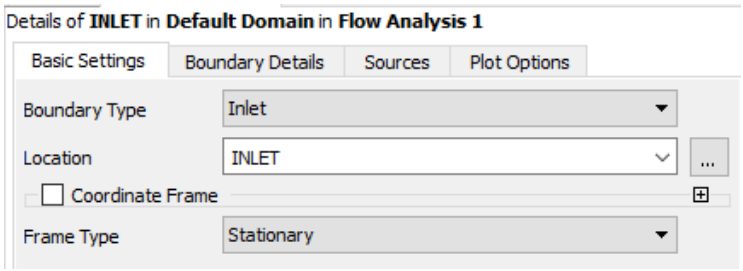

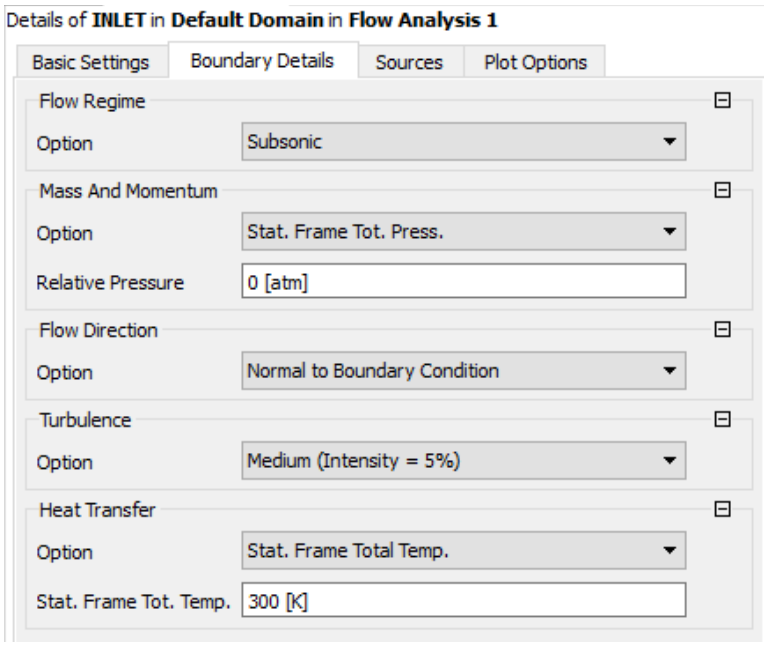
Details of INLET in Default Domain in Flow Analysis 1
Basic Settings
Boundary Details
Sources
Plot Options
Flow Regime
Option
Subsonic
Mass And Momentum
Option
Stat. Frame Tot. Press.
Relative Pressure
0 [atm]
Flow Direction
Option
Normal to Boundary Condition
Turbulence
Option
Medium (Intensity = 5%)
Heat Transfer
Option
Stat. Frame Total Temp.
Stat. Frame Tot. Temp.
300 [K]

OUTLET:

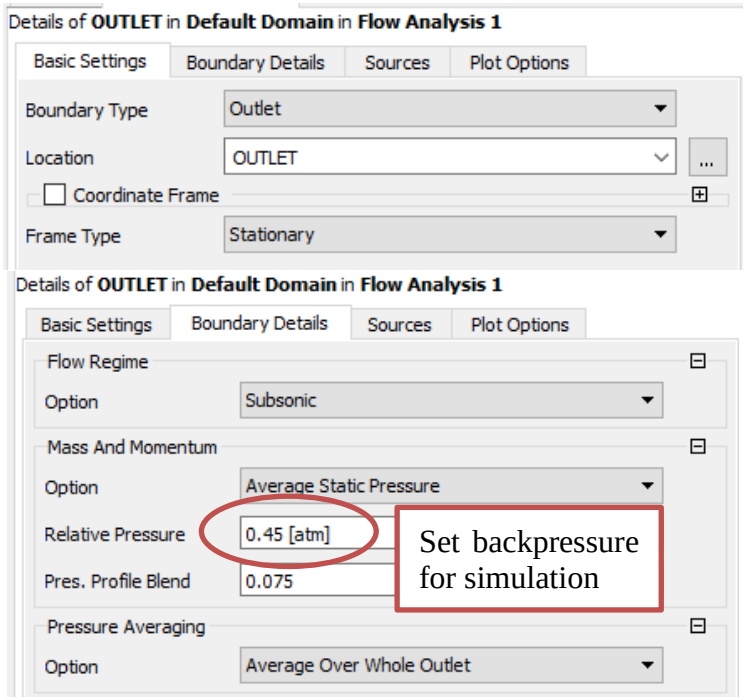
Details of OUTLET in Default Domain in Flow Analysis 1
Basic Settings
Boundary Details
Sources
Plot Options
Boundary Type
Outlet
Location
OUTLET
Coordinate Frame
Frame Type
Stationary
Details of OUTLET in Default Domain in Flow Analysis 1
Basic Settings
Boundary Details
Sources
Plot Options
Flow Regime
Option
Subsonic
Mass And Momentum
Option
Average Static Pressure
Relative Pressure
0.45 [atm]
Pres. Profile Blend
0.075
Set backpressure for simulation
Pressure Averaging
Option
Average Over Whole Outlet

SHROUD:

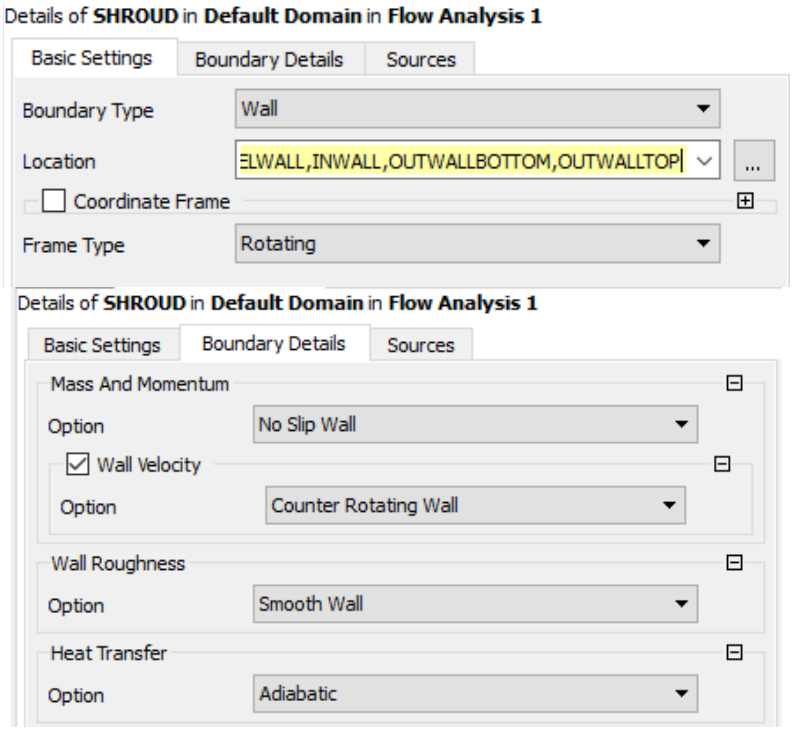
Details of SHROUD in Default Domain in Flow Analysis 1
Basic Settings
Boundary Details
Sources
Boundary Type
Wall
Location
ELWALL,INWALL,OUTWALLBOTTOM,OUTWALLTOP
...
Coordinate Frame
Frame Type
Rotating
Details of SHROUD in Default Domain in Flow Analysis 1
Basic Settings
Boundary Details
Sources
Mass And Momentum
Option
No Slip Wall
Wall Velocity
Option
Counter Rotating Wall
Wall Roughness
Option
Smooth Wall
Heat Transfer
Option
Adiabatic

APPENDIX F. RAW DATA FROM CFX SIMULATIONS

Air at 100,000 RPM						
outlet static back pressure	mass flow rate in	masss flow rate out	total pressure ratio	total temp ratio	isentropic efficency total to total	isentropic efficency total to static
0	0.18388	-0.18388	1.131243737	1.070665029	0.507489	0.0292503
0.1	0.153645	-0.153645	1.210421949	1.087036411	0.644312	0.337779
0.2	0.119252	-0.119252	1.292370254	1.106844334	0.711606	0.51492
0.3	0.075561	-0.075561	1.368250493	1.123642974	0.757955	0.639624
0.31	0.0712426	-0.0712426	1.375443837	1.12515928	0.761873	0.650555
0.32	0.0566945	-0.0566946	1.376354737	1.129800391	0.736228	0.64464
0.33	0.0491943	-0.0491952	1.386856734	1.136192545	0.719216	0.6316
0.34	0.0442836	-0.0442852	1.398348176	1.141778042	0.709111	0.622894
0.35	0.0390819	-0.0390792	1.411257696	1.148728449	0.695426	0.609443
0.36	0.0342886	-0.042884	1.422513798	1.156937874	0.675026	0.592309
0.37	0.0311622	-0.0311622	1.43324106	1.164996289	0.656461	0.577367
0.4	0.0205609	-0.0205329	1.463762906	1.182353614	0.630678	0.557778
0.45	0.000288428	-0.000405124	1.459062419	1.193070068	0.590367	0.554868

CO2 at 50,000 RPM						
outlet static back pressure	mass flow rate in (kg/s)	masss flow rate out (kg/s)	total pressure ratio	total temp ratio	isentropic efficency total to total	isentropic efficency total to static
0	0.153567	-0.153567	1.054642167	1.020846186	0.637428	
0.05	0.122759	-0.122759	1.094246649	1.026775878	0.844002	0.478608
0.1	0.0868333	-0.0868333	1.135533748	1.034025447	0.941628	0.718775
0.101	0.0860454	-0.0860454	1.136339895	1.034162965	0.943157	0.722566
0.105	0.0828941	-0.0828941	1.139501689	1.034672539	0.94983	0.738223
0.11	0.0788221	-0.0788221	1.1432863	1.035223951	0.959094	0.758884
0.115	0.0742957	-0.0742957	1.146848111	1.035697671	0.968726	0.780477
0.12	0.0687032	-0.0687032	1.150052295	1.036099419	0.977792	0.802902
0.125	0.0631891	-0.0631891	1.153302277	1.036519512	0.986401	0.824379
0.13	0.0588486	-0.0588486	1.156865784	1.037046381	0.993786	0.842921
0.135	0.0434044	-0.0434051	1.158129123	1.039253544	0.945062	0.823325
0.14	0.0392519	-0.0392526	1.163864007	1.041051679	0.934651	0.814686

CO2 at 75,000 RPM						
outlet static back pressure	mass flow rate in	masss flow rate out	total pressure ratio	total temp ratio	isentropic efficency total to total	isentropic efficency total to static
0	0.232131	-0.232131	1.12319147	1.046562408	0.628074	0.0361833
0.1	0.191345	-0.191344	1.202678942	1.058307005	0.8036	0.435221
0.2	0.145137	-0.145137	1.285214563	1.072431578	0.886889	0.655861
0.3	0.0855054	-0.0855054	1.360647679	1.084497871	0.939745	0.807369
0.302	0.0837161	-0.0837161	1.361696006	1.084834595	0.938447	0.808845
0.305	0.071636	-0.0716387	1.35972541	1.086964723	0.911001	0.795543
0.31	0.063033	-0.0630333	1.364205314	1.089955445	0.890508	0.787548
0.32	0.0581442	-0.0581445	1.375682235	1.093549557	0.88032	0.771949

CO2 at 100,000 RPM						
outlet static back pressure	mass flow rate in	masss flow rate out	total pressure ratio	total temp ratio	isentropic efficency total to total	isentropic efficency total to static
0	0.310751	-0.310751	1.219538621	1.082226565	0.613886	0.0363863
0.1	0.281217	-0.281217	1.298286684	1.093510962	0.715577	0.285128
0.2	0.249191	-0.249191	1.379217842	1.10593548	0.783903	0.460256
0.3	0.215108	-0.215108	1.461506502	1.119740596	0.82452	0.580579
0.4	0.178009	-0.178009	1.54600374	1.134962607	0.845835	0.660349
0.5	0.132813	-0.132813	1.621016253	1.146243472	0.870697	0.735999
0.525	0.120485	-0.120485	1.639527136	1.149217262	0.874659	0.751423
0.53	0.118162	-0.118162	1.64308491	1.149821108	0.875193	0.75432
0.54	0.112925	-0.112925	1.649366237	1.151203155	0.874279	0.759041
0.55	0.0870077	-0.0870051	1.64947299	1.159327022	0.829816	0.731022

LIST OF REFERENCES

[1] Environmental and Energy Study Institute, "DoD's Energy Efficiency and Renewable Energy Initiatives," Environmental and Energy Study Institute, Washington, DC, 2011.

[2] Schwartz, Moshe, Blakeley, Katherine, and O'Rourke, Ronald. "Department of Defense Energy Initiatives: Background and Issues for Congress," CRS Report for Congress, R42558. Congressional Research Service, Washington, DC 2012.

[3] Lundquist, Edward., 2011, "Navy Removes Waste Heat Boilers, Steam Systems and Piping from Cruisers," from http://articles.maritimepropulsion.com/article/Navy-removes-waste-heat-boilers-steam-systems-and-piping-from-cruisers94802.aspx.

[4] Beale, Mark. "Turning Vanes in Exhaust Duct Flow: Study for Energy Efficiency, Optimization and Pressure Drop Mitigation," M.S. thesis, Mech. Eng. Dept., Naval Postgraduate School, Monterey, CA. 2014.

[5] Bohning, Ryan. "Optimal Placement of Non-Intrusive Waste Heat Recovery Devices in Exhaust Ducts," M.S. thesis, Mech. Eng. Dept., Naval Postgraduate School, Monterey, CA. 2015.

[6] VanDenBerg, Aaron. "Energy Efficient Waste Heat Recovery from an Engine Exhaust System," M.S. thesis, Mech. Eng. Dept., Naval Postgraduate School, Monterey, CA. 2016.

[7] Polsinelli, Samuel. "Waste Heat Recovery Carbon Dioxide Heat Exchanger for Gas Turbine Engines," M.S. thesis, Mech. Eng. Dept., Naval Postgraduate School, Monterey, CA. 2018.

[8] Rolls-Royce, 2009, "A Look Back at the Development of the Model 250 Turbine Engine," from https://www.scribd.com/document/241498784/Model250?doc_id=241498784&download=true&order=451289537

[9] Wong, Sam. 2012, "APEC Capacity Building in the APEC Region," from https://hub.globalccsinstitute.com/publications/building-capacity-co2-capture-and-storage-apec-region-training-manual-policy-makers-and-practitioners/module-4-co2-compression-and-transportation-storage-site

[10] Wadas, Brian. 2010, “GE Oil & Gas: Innovation Now,” from http://dc.engconfintl.org/cgi/viewcontent.cgi?article=1035&context=co2_summit

[11] Rivera, Gilbert. “Turbochargers to Small Turbojet Engines for Uninhabited Aerial Vehicles,” M.S. thesis, Mech Eng Dept., Naval Postgraduate School, Monterey, CA. 1998.

INITIAL DISTRIBUTION LIST

1. Defense Technical Information Center
   Ft. Belvoir, Virginia

2. Dudley Knox Library
   Naval Postgraduate School
   Monterey, California